





# 1 Deliverable administrative information

Deliverable number	D2.6
Deliverable title	Integrated EV Mobility and Energy Planning Tools
Dissemination level	Public
Submission deadline	30/09/2024
Version number	V1.0
Authors	Authors tool A (City of Utrecht & Utrecht University): Transformer Load Capacity Tool for Integrated EV mobility and energy scenario planning.  Gertjan Geurts (City of Utrecht)  Nico Brinkel (University of Utrecht)  Authors tool B (CERTH):  CERTH'S Energy Planning Tool in-house-developed and INTEMA.grid simulator  Chairopoulos Nikolaos Charalampos (CERTH)  Giourka Paraskevi (CERTH)  Nikolopoulos Nikolaos (CERTH)  Petridis Stefanos (CERTH)  Rotas Renos (CERTH)  Salanova Grau Josep Maria (CERTH)  Tamvakos Athanasios (CERTH)  Touliou Katerina (CERTH)  Grigoropoulos Konstantinos (CERTH)  Gkaidatzis Paschalis (CERTH)



	<ul><li>Bintoudi Angelina (CERTH)</li><li>Ioannidis Dimosthenis (CERTH)</li></ul>
Internal reviewers	Nico Brinkel (Utrecht University) Gertjan Geurts (City of Utrecht) Gkaidatzis Paschalis (CERTH) Grigoropoulos Konstantinos (CERTH) Rotas Renos (CERTH) Kevin Haesevoets (Enervalis) Frank Geerts (ElaadNL) Marisca Zweinstra (ElaadNL) Yannick Huc (Trialog)
Document approval	City of Utrecht Utrecht University CERTH

## 1.1 Legal Disclaimer

SCALE is funded by the European Union's Horizon Europe Research and Innovation programme under Grant Agreement No 101056874. The views represented in this document only reflect the views of the authors and not the views of the European Commission. The dissemination of this document reflects only the author's view and the European Commission is not responsible for any use that may be made of the information it contains.



## 2 SCALE Introduction

SCALE (Smart Charging Alignment for Europe) is a three-year Horizon Europe project that explores and tests smart charging solutions for electric vehicles. It aims to advance smart charging and Vehicle-2-Grid (V2G) ecosystems to shape a new energy system wherein the flexibility of EV batteries' is harnessed. The project will test and validate a variety of smart charging and V2X solutions and services in 13 use cases in real-life demonstrations in 7 European contexts: Oslo (NO), Rotterdam/Utrecht (NL), Eindhoven (NL), Toulouse (FR), Greater Munich Area (GER), Budapest/Debrecen (HU) and Gothenburg (SE). Going further, project results, best practices, and lessons learned will be shared across EU cities, regions, and relevant e-mobility stakeholders. SCALE aims to create a system blueprint for user-centric smart charging and V2X for European cities and regions.

SCALE's consortium comprises 29 cutting-edge European e-mobility actors covering the entire smart charging and V2X value chain (equipment and charging manufacturers, flexibility service providers, research and knowledge partners, public authorities, consumer associations, etc.) It is led by ElaadNL, one of the world's leading knowledge and innovation centres in smart charging and charging infrastructure.



## 3 Deliverable executive summary

SCALE (Smart Charging Alignment for Europe) is a three-year Horizon Europe project that aims at preparing EU cities for mass deployment of electric vehicles and the accompanying smart charging infrastructure.

In the SCALE proposal, we committed to delivering tools aimed at supporting cities and regions in their energy transition efforts. In Task 2.6, two tools were developed by two teams. The City of Utrecht collaborated with Utrecht University in developing a tool aiming to guide cities in making policy choices to facilitate the ongoing energy transition, while CERTH developed a tool that solves the problem of finding charging infrastructure optimal position in a distribution grid ensuring its reliability and stability, also using data from the Utrecht Use Case. The teams exchanged knowledge, shared data, and kept each other informed of progress. Both teams developed a tool with a different purpose. The tool from Utrecht focused on scenario planning for policy choices by cities, regions, and grid operators. This helps cities and regions plan for integrated shared and private EV mobility, as well as EV charging infrastructure rollout, including congestion forecasting and management in various environments and scenarios, and enabling interaction with additional energy networks.

The CERTH tool is designed for cities/regions, OEMs, grid-operators, end-users, DSOs and manufacturers, offering functionalities tailored to these audience, including:

- Solving the optimal EVCI location problem using specialised Optimal Power Flow (OPF) algorithms
- Integrating mobility behaviour patterns
- Stress testing the proposed topology through dynamic component-based modelling

CERTH has developed the EV Mobility and Energy Planning Tool and adapted its in-house INTEMA grid simulator to identify the optimal locations and sizes (Nominal Apparent Power, Nominal Active Power) for V2G and V2X EV chargers within a Distribution Electric Network. The tool's main objective is to minimize both overall network power losses and network congestion while ensuring energy supply to meet mobility needs and the technical feasibility of integrating chargers into the power system.

## 3.1 Key words

Electric vehicles, smart charging, V2G, V2X, bidirectional charging, optimal power flow, dynamic grid simulation, congestion, congestion forecast, energy planning, transformer capacity scenario planning, integrated planning, energy network planning, policy making, flexibility.



# 4 SCALE partners

#### List of participating cities:

- Oslo (NO)
- Rotterdam & Utrecht (NL)
- Eindhoven (NL)
- Toulouse (FR)
- Greater Munich Area (GER)
- Budapest & Debrecen (HU)
- Gothenburg (SE)

#### List of partners:

- (Coordinator) STICHTING ELAAD NL
- POLIS PROMOTION OF OPERATIONAL LINKS WITH INTEGRATED SERVICES, ASSOCIATION INTERNATIONALE POLIS BE
- GoodMoovs NL
- Rupprecht Consult Forschung & Beratung GmbH RC DE
- Trialog FR
- WE DRIVE SOLAR NL BV NL
- UNIVERSITEIT UTRECHT NL
- LEW Verteilnetz GmbH DE
- BAYERN INNOVATIV BAYERISCHE GESELLSCHAFT FUR INNOVATION UND WISSENSTRANSFER MBH DE
- ABB BV NL
- Enervalis BE
- GEMEENTE UTRECHT NL
- Equigy B.V. NL
- Meshcrafts As (Current) NO
- Research Institutes of Sweden AB SE
- ETHNIKO KENTRO EREVNAS KAI TECHNOLOGIKIS ANAPTYXIS (CERTH) GR
- FIER Automotive FIER NL
- Emobility Solutions Kft. HU
- Serviced Office Belbuda Kft HU
- Enedis FR
- L'ASSOCIATION EUROPEENNE DE LA MOBILITE ELECTRIQUE (AVERE) BE
- Norsk elbilforening NO
- VDL ENABLING TRANSPORT SOLUTIONS BV NL
- Urban Electric Mobility Initiative UEMI DE



- Renault FR
- Chalmers University SE
- Polestar SE
- Hyundai NL NL

#### Social Links:



twitter.com/scaleproject\_



www.linkedin.com/company/ scale-project-smart-charging-alignment-for-europe



www.youtube.com/channel/UC1HVFu5uJPCNSV96b3I\_rcg

For further information please visit WWW.SCALE-HORIZON.EU



# 5 Elaboration on the report

In the SCALE proposal, we committed to delivering tools aimed at supporting cities and regions in their energy transition efforts. In Task 2.6, two tools were developed by two teams. The City of Utrecht collaborated with Utrecht University in developing a tool aiming to guide cities in making policy choices to facilitate the ongoing energy transition, while the CERTH team adapted its in-house-developed tool, also using data from the Utrecht Use Case. The teams exchanged knowledge, shared data, and kept each other informed of progress. Both teams developed a tool with a different purpose. The tool from the City of Utrecht and Utrecht University is titled as the *Transformer Load Capacity Tool for Integrated EV mobility and Energy Scenario planning* tool and focused on scenario planning for policy choices by cities, regions, and grid operators. This helps cities and regions plan for integrated shared and private EV mobility, as well as EV charging infrastructure rollout, including congestion forecasting and management in various environments and scenarios, and enabling interaction with additional energy networks. The CERTH tool is designed for cities/regions, OEMs, grid-operators, end-users, DSOs and manufacturers, offering functionalities tailored to these audience, including:

- Solving the optimal EVCI location problem using specialised Optimal Power Flow (OPF) algorithms
- Integrating mobility behaviour patterns
- Stress testing the proposed topology through dynamic component-based modelling

The tools have been developed with replicability and scalability of the developed suite of tools in mind. This replicability and scalability for other cities and relevant stakeholders of the consortium, will be further assessed during the Joint Procurement Programme (SCALE Task 5.4), V2X-alliance meetings and during the upcoming consortium meeting in Budapest. This to ensure large-scale adoptability by European actors. This report and these tools are input to create implementation scenarios (towards 2030 & beyond) for policy development for WP5.

To make a clear distinction between the tools, which serve different purposes, each tool has been described in a different section:

**Section 9** has been written by the City of Utrecht & Utrecht University and is about the Transformer Load Capacity Tool for Integrated EV mobility and Energy Scenario planning.

**Section 10** has been written by CERTH and is about CERTH's EV Mobility and Energy Planning Tool and dynamic simulations.

This report is accompanied by two videos that provide a demo with explanation of the developed tools.



# **6** Table of contents

1	DELIVERABLE ADMINISTRATIVE INFORMATION		
1.1	Legal Disclaimer	2	
2	SCALE INTRODUCTION	3	
3	REPORT EXECUTIVE SUMMARY	4	
3.1	Key words	4	
4	SCALE PARTNERS	5	
5	ELABORATION ON THE REPORT	7	
6	TABLE OF CONTENTS	8	
7	LIST OF ABBREVIATIONS AND ACRONYMS	10	
8	PURPOSE OF THE DELIVERABLE	11	
8.1	Attainment of the objectives and explanation of deviations	11	
8.2	Intended audience	11	
9	TOOL A – TOOL DEVELOPED BY CITY OF UTRECHT & UTRECHT UNIVERSIT	ГΥ	
9.1	Introduction	12	
9.2	Tool selection	15	
9.3	Tool installation and setup	16	
9.4	Structure of the tool	17	
9.5	Modelling framework of the tool	22	
9.6	Case study introduction	25	
9.7	Scenario assessment	26	
9.8	Conclusions and next steps	<b>29</b>	



10	TOOL B – TOOL DEVELOPED BY CERTH	32
10.1	Overview of the tool	32
10.2	Different scenarios based on the transport model	36
10.3	EV charging infrastructure rollout optimisation methodology	37
10.4	V2G dynamic models	46
10.5	Conclusions of Tool B	65
11	REFERENCES	66
12	ANNEX	68
12.1	List of figures	68
12.2	List of tables	71
12.3	Li-ion battery cell dynamic model	71
12.4	EV powertrain dynamic model for verification	74
12.5	Detailed results of the verification of battery models	82



# 7 List of abbreviations and acronyms

Acronym	Meaning
BESS	Battery Energy Storage System
BMS	Battery Management System
DCFC	DC fast charger
DER	Distributed Energy Resources
DSO	Distribution System Operator
ЕСМ	Equivalent Circuit Model
ESS	Energy Storage System
EV	Electric Vehicle
EVCI	Electric Vehicle Charging Infrastructure
LFP	Lithium-iron Phosphate
LMO	Lithium-manganese Oxide
LV	Low Voltage
NCA	Lithium-nickel Cobalt Aluminium Oxide
NMC	Lithium-nickel Manganese Cobalt Oxide
OEM	Original Equipment Manufacturer
OPF	Optimal Power Flow
PV	Photovoltaic
RES	Renewable Energy Sources
SoC	State-of-Charge
UFLS	Under-frequency Load Shedding
V2G	Vehicle-to-Grid
V2X	Vehicle-to-Everything



# 8 Purpose of the deliverable

## 8.1 Attainment of the objectives and explanation of deviations

The objectives related to this deliverable have been achieved in full and as scheduled.

#### 8.2 Intended audience

This report presents background information on the two tools developed in Task 2.6 of the SCALE project. This report is accompanied by two videos that provide a demo with explanation of the developed tools.

The intended audience for this deliverable includes European cities and regions, as well as grid operators, OEMs, end-users, DSOs and manufacturers in those regions. It aims to assist them in planning for the integrated deployment of shared and private EV mobility and EV charging infrastructure, including congestion forecasting and management in various environments, while facilitating interaction with additional energy networks.



# 9 Tool A – Tool developed by City of Utrecht & Utrecht University

As described above, two tools have been developed in this Task. Each tool has different functionality and is therefore treated in a different section. Also, a video is created for each tool, showing visually and verbally what the tools do and how they can be used by the target audience(s). First, the tool developed by the City of Utrecht and Utrecht University will be discussed. This chapter will mostly focus on how the tool can be implemented, on how it can be used and on how it functions.

# Transformer Load Capacity Tool for Integrated EV mobility and Energy Scenario planning

A demo video of this tool has been submitted together with this report, which provides a detailed explanation of the functioning of the tool. The video is titled "SCALE D2.6 - Demo tool A – Utrecht and Utrecht University – SCALE.mp4".

#### 9.1 Introduction

The City of Utrecht and Utrecht University have developed an open-source tool to assist cities in planning for the integration of shared and private EV mobility, as well as the rollout of EV charging infrastructure. This tool, which is open-access and can be potentially implemented in any city, was developed based on Utrecht's own needs for this and offers capabilities such as congestion forecasting and management across different environments, while enabling interaction with additional energy networks. The objective of this task within SCALE was to develop and implement the tool in Utrecht, with the broader vision that it could also benefit other European cities progressing through similar phases of the energy transition. Key areas of focus include the growing adoption of EV mobility, electrification resulting from the transition from gas to electric heating (via heat pumps), and the associated risks of grid congestion. The tool was designed to be scalable to other cities and regions in Europe, and insights from the research in SCALE Task 1.3 were incorporated into its development.

#### 9.1.1 The problem of grid congestion in cities

The ongoing energy and mobility transitions increasingly put pressure on cities, due to the problem of grid congestion. Cities aim to become sustainable cities while also facing challenges to accommodate a growing population.

One of the cities facing this challenge is the city of Utrecht in the Netherlands. During the course of the SCALE project, grid congestion has become a major issue in Utrecht. The city is working towards a clean energy system by facilitating the adoption of renewable energy technologies, by stimulating building adaptations (through energy savings and insulation), by pursuing district-based alternatives to natural gas, and by strengthening the electricity grid. This ensures that Utrecht remains a pleasant and healthy city for everyone, both now and in the future.

The transition away from fossil fuels in sectors like transportation and home heating is happening faster than the infrastructure involved can be adapted and expanded. As a result, bottlenecks have emerged in the electricity grid, leading to grid congestion. To address this, the City of Utrecht has developed the Electricity Infrastructure and Grid Congestion Implementation Program, and the Dutch government has introduced additional measures for the provinces of Flevoland, Gelderland, and Utrecht (FGU).



In tackling grid congestion, the future energy system serves as the city's guiding principle. Key characteristics of this system include being (nearly) fossil-free, accessible, efficient, smart, grid-conscious, and locally focused. The City of Utrecht prefers to implement measures that bring the future energy system closer, such as smart charging of electric vehicles, grid-efficient installations, and grid-conscious construction. The urgency of this problem is becoming very high, as grid congestion has now become a crisis in the city of Utrecht, the province of Utrecht, and large parts of the Netherlands. There is a substantial waiting list for large consumer connections to the grid, which can no longer be granted. Consequently, the city's businesses and residents are being affected by this.

The city is currently experiencing these problems while it is only at the beginning of the ongoing energy transition. Figure 1, and Figure 2 show that the city needs to integrate a large number of charging stations in the coming years to keep up with the expected growth of the EV fleet in the city. Therefore, there is an urgent need to ensure that EV charging is done smartly, outside of peak grid hours as much as possible. Additionally, the city must continue to fully expand the bidirectional charging network to create the conditions for establishing a virtual power plant from the combined battery capacity of bidirectional EVs (V2G). This will allow the city to balance the grid during moments of congestion, leveraging the grid's smallest connections.

A key point of focus is the funding of the municipal approach to grid congestion. Utrecht is being hit exceptionally hard, as the highest building demand coincides with the most severe grid congestion. The better Utrecht understands the problem across different scenarios, the more informed policy decisions can be made.

The tool developed in this SCALE Task 2.6 supports this effort. By developing this tool, the city can make better-informed policy decisions to support the ongoing electricity transition. Also, by developing this tool, it supports other cities that will inevitably experience these problems in coming years in making the right policy decisions from an early stage.

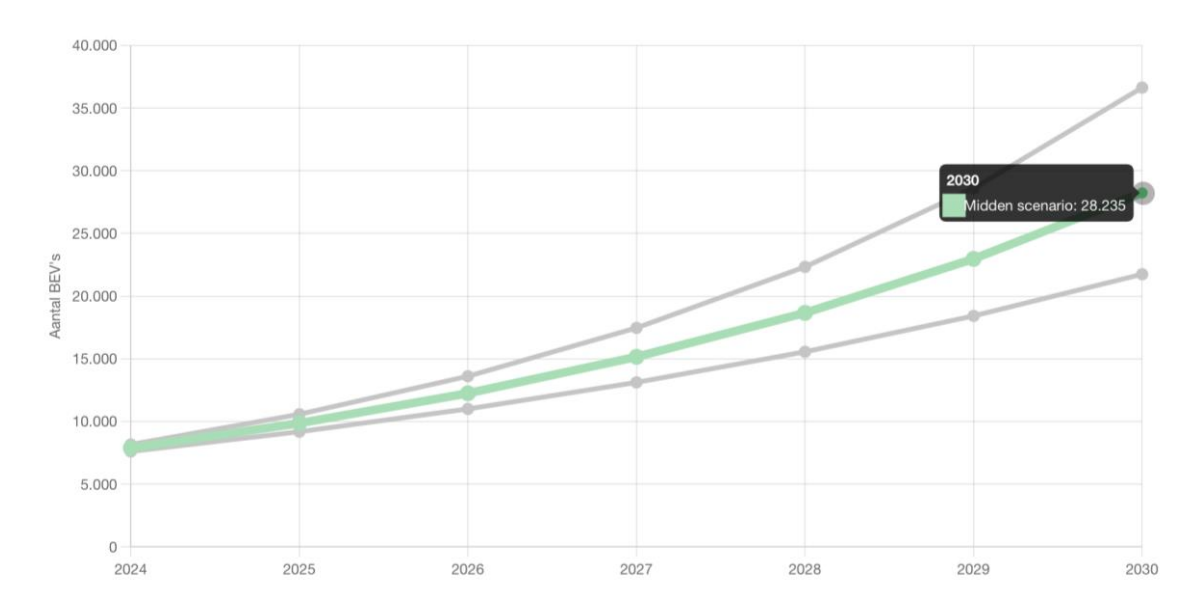


Figure 1: Forecast for the growth of EVs in the City of Utrecht. 'Midden scenario' is Dutch for Mid-Scenario. Others are the high scenario and low scenario. Source: ElaadNL.



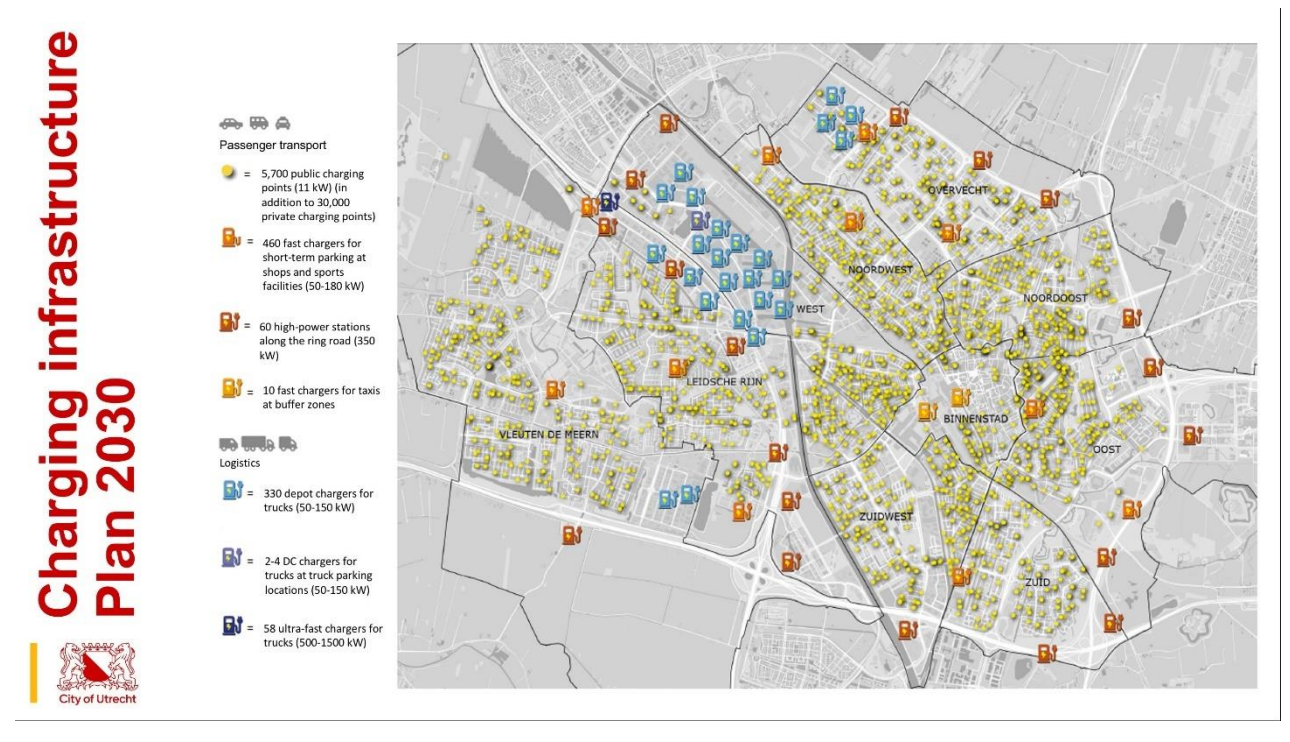


Figure 2: Expected rollout for charging infrastructure for the city of Utrecht by 2030. Source: City of Utrecht.



#### 9.2 Tool selection

This section describes the preparatory steps followed in creating the tool. It will outline the requirements of the tool and will also describe the results of the market scan that was performed of the available tools in the market. One of these tools was subsequently selected and served as a base model. This base model has been further developed in this task.

The needs and challenges in integrated planning for smart charging and V2X services were outlined in Task 1.3 and described in the Task 1.3 report (D1.3). These were used as input for Task 2.6: an integrated EV Mobility and Energy Planning Tool for the City of Utrecht.

This tool aims to address the needs and challenges found in the SCALE research and enable smart data sharing between stakeholders, such as urban planners, policymakers, and DSOs. The research showed that cities and regions in more advanced phases of EV charging have a need for this. More and more European cities and regions are entering that phase in the near future. An important recommendation from the Task 1.3 report is to assess two key issues before starting to build such a tool:

- 1. Which cities and regions are already using or developing such tools?
- 2. Which digital tools have already been developed and are in use for integrated E-Mobility and Energy network planning?

This should be tested against the city needs and challenges identified in the Task 1.3 report. In the research for that report, it was already found that the city of Amsterdam was developing a digital tool that dealt with the scope of Task 2.6. In addition, different other tools were identified in the market scan performed for Task 2.6. This served as the starting point for the assessment of tools for integrated EV Mobility and Energy Planning in the initial phase of execution. The results of this comprehensive assessment are included in the spreadsheet titled "SCALE D2.6 - Tools assessment Utrecht and UU SCALE Task 2.6.xlsx", which has been submitted as a project deliverable for this task.

Out of all the tools in the assessment, three candidate tools were identified as having significant potential to meet the identified requirements for the tool. These tools were:

- 1. Phase-2-Phase tool
- 2. Zenmo Zero tool
- 3. Amsterdam partnered collaboration tool Grid operator Liander/ Municipality of Amsterdam

We did a deep dive into these tools and requested demos for these candidate tools and held video calls with the product developers and users. Based on all the input, it was found that the Zenmo Zero tool best suited our needs. Key reasons for this included:

- As mentioned, it helps cities plan for integrated shared and private EV mobility and EV charging
  infrastructure rollout, including congestion forecasting and management in different environments,
  enabling interaction with additional energy networks.
- The tool was customisable to be able to study specific scenarios for specific locations.
- It allowed for the integration of data from the Utrecht use case, which Utrecht University has been analysing for years.
- It could import transformer load data from the local grid operator in Utrecht.
- The tool can easily be scaled to other locations and to broader areas.
- Development and implementation fit within the schedule.



- Development and implementation fit within the budget.
- Open source.
- User-friendly interface (UI), suitable for the less technical target audience of city planners and policymakers.
- Based on agent-based modelling, which enables the generation of a diverse range of scenarios.

To summarize, the tool could function as a very good fit to build upon. In this section, we provide a detailed explanation of the tool and our results. The attached screencast video also offers an in-depth overview of the tool and its functionalities. And explains in detail how we met the goal of SCALE Task 2.6.

## 9.3 Tool installation and setup

In this task, a tool has been developed for conducting in-depth grid load analyses for any city district. This section explains how to configure the tool for a specific city district on a high level. A more detailed manual for setting up this tool can be found in the documentation of the used model: <a href="https://zerodocs.zenmo.com/">https://zerodocs.zenmo.com/</a>.

The first step involves downloading the required software tools for setting up the tool for a specific city district. The tool makes use of open-source models developed by the company Zenmo Simulations<sup>1</sup>, which are accessible through Github<sup>2</sup>. One needs to download the free Anylogic Simulation Modeling software tool<sup>3</sup> to apply these open-source models to a specific case study. After setting up the tool for a specific city district, the model can be uploaded online and can be used without downloading the Anylogic Simulation Modeling software tool.

Different data inputs are required to set up the tool for a specific city district. First, data about all residential objects (households, companies, schools, etc.) within the specified district need to be imported into the tool. This data should be formatted as an Excel file and include the following details:

- The address of each residential object;
- The function of each residential object (household/company/school, etc.)
- The area of each residential object (in m²);
- The year of construction for each residential object;
- The geographical coordinates (longitude and latitude) of each residential object;
- The energy label of each residential object;
- Geometric data for each residential object, provided as a multipolygon outlining the building's contour;
- The transformer station each residential object is connected to;
- The annual electricity consumption (in kWh) and gas consumption (in m³) for each residential object;
- The installed photovoltaic capacity (in kWp);

<sup>&</sup>lt;sup>1</sup> https://zenmo.com/

<sup>&</sup>lt;sup>2</sup> https://github.com/Zenmo/zero\_results\_UI, https://github.com/Zenmo/zero\_engine and https://github.com/Zenmo/zero\_Interface-Loader

<sup>&</sup>lt;sup>3</sup> https://www.anylogic.com/



The current heating system used by each residential object.

In different countries, including the Netherlands, the information outlined in the first seven points is released as open data by public institutions<sup>4</sup>. Open-source tools such as QGIS<sup>5</sup> can be used to format this data into the right Excel structure. Information about the transformer station to which a property is connected is often not publicly available, as this is commercial information to the grid operator, but can be provided by the grid operator. In case this is not possible, this can be estimated from the locations of the different transformer stations, using tools such as QGIS. The annual electricity/gas consumption profiles for each household are usually not available on the individual household/company level, as this is privacy-sensitive information. Aggregated consumption data, such as the average consumption level for a street or zip code area, is often available and could be used for estimating the electricity and gas consumption of an individual grid connection<sup>6</sup>. Similarly, the installed photovoltaic capacity and current heating system of a household/company is often not publicly available. These can be estimated through reports from grid operators, satellite images (for photovoltaic systems) or aggregated data on the adoption of photovoltaic systems and different heating technologies.

Secondly, one needs to import data on the location and capacity of transformer stations to configure the tool. The location of transformer stations is published by grid operators in different countries<sup>7</sup> and can otherwise be retrieved from satellite images. The capacity of these stations can be obtained from grid operators, if these are not publicly available, and can otherwise be estimated based on information on most commonly installed capacities of transformer stations<sup>8</sup>.

A third required input for the tool is weather data, presenting hourly temperature, insolation and wind speed data. This data is used to model heat losses from buildings and to model the generation from photovoltaic systems.

Lastly, the tool requires EV charging session data and potential locations for EV charging stations as data input. The charging session data should outline the arrival time, departure time, charging demand (kWh), charging station and maximum charging power of each charging session. One can use open datasets for this, such as the open charging session dataset from ElaadNL<sup>9</sup>, or use location-specific, non-public EV charging session data. Potential locations for EV charging stations in a city district can be identified using tools such as QGIS or Google Maps.

#### 9.4 Structure of the tool

Once the tool is initialized, it can be utilized to conduct in-depth grid load analyses for a specific city district. The tool is organized into various panes, each serving a specific function in the analysis process. This section

 $<sup>^4</sup>$  e.g.  $\underline{\text{https://www.pdok.nl/}}$  and  $\underline{\text{https://www.vlaanderen.be/digitaal-vlaanderen/onze-oplossingen/gebouwen-en-adressenregister}}$ 

<sup>&</sup>lt;sup>5</sup> https://www.ggis.org/

<sup>6</sup> https://www.stedin.net/zakelijk/open-data/verbruiksgegevens

<sup>&</sup>lt;sup>7</sup> https://www.stedin.net/zakelijk/open-data/liggingsdata-kabels-en-leidingen

<sup>&</sup>lt;sup>8</sup> This is, for instance, outlined in: Phase to Phase. (2012). Netten voor distributie van elektriciteit

<sup>9</sup> https://platform.elaad.io/download-data/



will explain the tool's structure by detailing the purpose and available options for each pane. These panes are also shown in the demonstration video accompanied with this report.

#### 9.4.1 Scenario pane

The left part of the tool is the scenario pane, as displayed in Figure 3. Using this pane, a user of the tool can change the adoption rates of specific technologies, as well as the application and usage of these technologies and the electricity consumption and insulation levels of buildings. In this way, a wide array of scenarios can be studied by grid operators, municipalities and other users of this tool, making them better informed about the potential future directions for a city district and the range in outcomes with different policy measures. This section will outline the different functions that are considered in the scenario pane of the tool.



Figure 3: The considered city planning tool, with the scenario pane highlighted using a red frame

At the top of the scenario pane, the user can select different pre-defined scenarios. These scenarios outline the extreme scenarios that are foreseen, enabling users to quickly assess the potential impacts of different variables on the grid load. A user also has the option to create a custom scenario. In this option, the user can manually change the settings for each of the considered functions that are considered in the tool.

When manually adjusting the settings, the user has the option to change functions using two panes: i) the electricity pane and ii) the heating pane. In the electricity pane, the user can manually set values for the following functions:

- The share of buildings equipped with a photovoltaic system;
- The share of buildings with a photovoltaic system that is equipped with a battery system;
- The share of households that use electric stoves for cooking;
- The growth/reduction in electricity consumption by residential objects;
- The ownership rate of EVs, expressed in EVs per household;
- The charging strategy employed for EV charging;
- The installed capacity of a neighbourhood battery, in kW.



The heating pane can be used to manually set values for an additional set of functions:

- The share of residential objects equipped with a gas burner;
- The share of residential objects equipped with an all-electric heat pump;
- Whether a high-temperature heating district is available in the considered area;
- The share of residential objects equipped with an airconditioning unit;
- A possible reduction in the insulation values of residential objects.

After changing the settings for each of these functions, the tool will automatically calculate how this will affect the grid flows in the considered city district, using the modelling approach outlined in Section 229.5.

#### 9.4.2 Mapping pane

The mapping pane can be found in the middle part of the tool, as highlighted in Figure 4.



Figure 4: The considered city planning tool, with the mapping pane highlighted using a red frame

The top part of the mapping pane shows a map of the considered city district. The user can use this map to specifically select different objects within the considered district, such as transformer stations, individual buildings or charging stations. After selecting an object, the consumption and generation profiles for the selected object will appear in the results pane.

At the bottom of the mapping pane, a legend displays all the items present on the map. Additionally, it allows the user to modify the colors of the objects on the map based on the following factors:

- Annual electricity consumption of the buildings;
- Annual photovoltaic generation of the buildings;
- The transformer station each building is connected to;
- The purpose or function of the building.



#### 9.4.3 Simulation pane

The right pane in the tool presents the results of the model simulations, as highlighted in Figure 5.

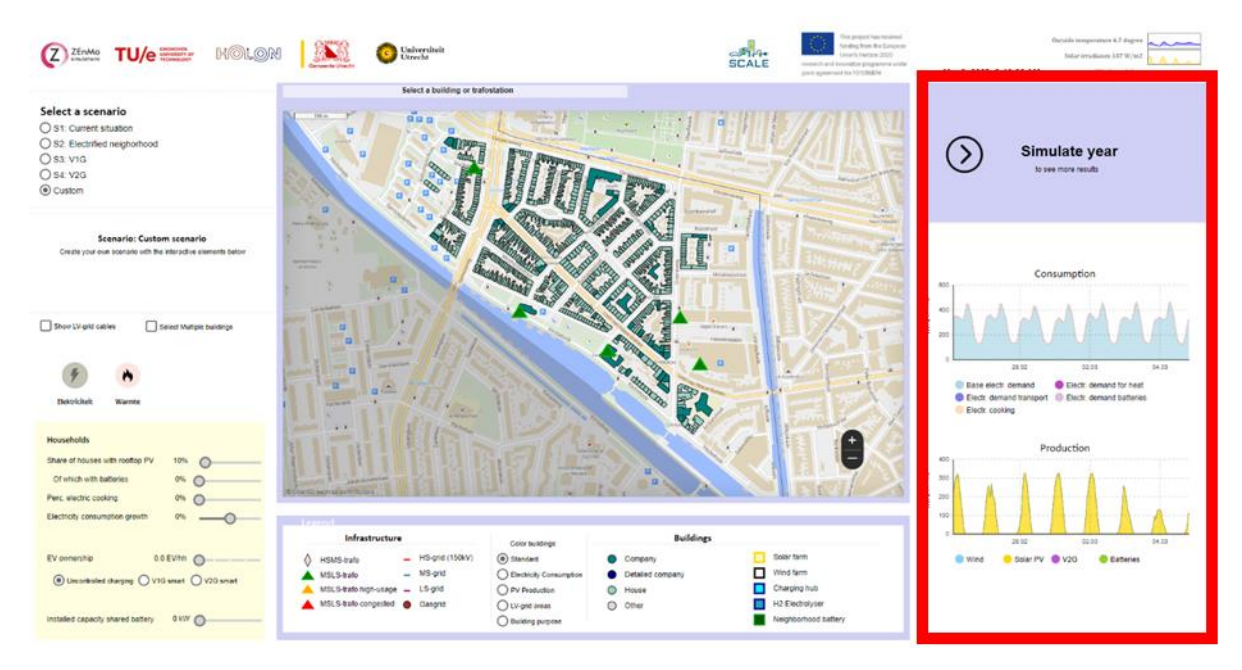


Figure 5: The considered city planning tool, with the simulation pane highlighted using a red frame

When running a simulation, the simulation pane displays two figures. The top figure shows the electricity consumption profile for the selected object in the mapping pane, while the bottom figure shows the electricity generation profile for this selected object.

At the top of the simulation pane, the user has the option to switch from live simulation to yearly simulation. After clicking this option, the user can choose between different figures which provide insight into the grid flows on an annual timescale. For instance, the user can gain insight into load duration curves for a specific object, such as a transformer station (see Figure 6). In addition, the user can gain insight into the annual generation, consumption and self-consumption (see Figure 6).





Figure 6: Examples of figures for the yearly simulation function of the tool. The left graph shows a load duration curve for a specific object. The right graph shows the annual consumption/generation volumes of a specific object.

Lastly, when performing live simulations, a user can gain detailed insight into the electricity consumption and generation profiles of individual households. Selecting a household in the mapping pane triggers a detailed simulation pane (see Figure 7), which pops up by clicking a button on the top-right. This detailed simulation pane shows the electricity consumption and generation profiles, the heat flows and the temperatures within the selected household and can be used to understand the dynamics within the model.

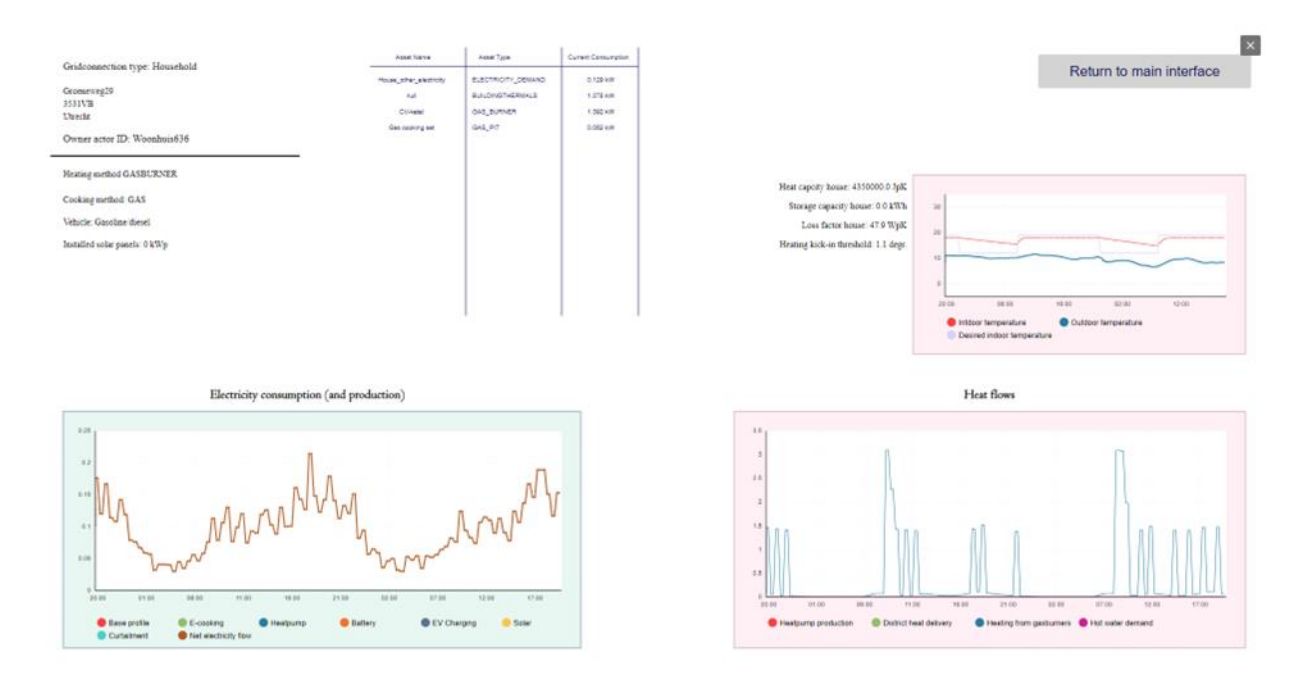


Figure 7: Detailed simulation pane for one individual household.



## 9.5 Modelling framework of the tool

This tool employs an agent-based modelling approach to simulate the grid load of the selected city district, taking into account the various functions that users can activate in the scenario pane. In an agent-based modelling approach, the electricity consumption/generation patterns of individual agents in the model are modelled. Examples of agents are households, companies and EV charging stations. Each agent has its own characteristics and preferences and acts based on these preferences, resulting in each individual agent having its own electricity consumption patterns. Examples of such characteristics and preferences are the thermostat settings, the insulation levels, area and the annual baseload electricity demand of a residential object. The main advantage of using agent-based modelling over other modelling approaches, such as optimization, is its ability to capture the diverse behaviours and interactions of individual agents, which better reflects the variability and unpredictability of real-world behaviour and results in more realistic simulations. Also, the agent-based approach allows for studying an unlimited number of scenarios, as it will be modelled for each individual agent how it will react to a changing situation, whereas with optimization, only a limited number of scenarios can be studied, due to the high computational burden that is associated with this modelling approach.

This work used the existing Zenmo Zero model as a baseline model (see Section 9.2) and in this Task, this model has been further developed by the City of Utrecht and Utrecht University, in collaboration with the company Zenmo, in order to make the model more realistic and to increase the model's functionalities.

This section provides a generic description of how the consumption and generation profiles are determined for the main components of the model. More detailed documentation can be found in the documentation of this tool: <a href="https://zerodocs.zenmo.com/">https://zerodocs.zenmo.com/</a>.

#### 9.5.1 Base consumption profiles of households, companies and other residential objects

The base consumption profiles of households, companies and other residential objects are based on the function of the object, its annual electricity consumption, the considered reduction/growth factor in electricity consumption and the standard consumption profile for each type of residential object. The tool also considers the heterogeneity among grid connections by considering a randomization factor in the baseload profile.

#### 9.5.2 Heat pump profiles

If heat pumps are activated in the scenario pane of the tool, heat pumps are randomly assigned to individual property objects. A standard 3 kW capacity for heat pumps has been assumed in the model. For each individual property object, a temperature model runs in the background of the tool. This temperature model models the heat losses of property objects, based on randomly-assigned insulation values of the property and outside temperatures, and activates the heat pump if the inside temperature drops below the thermostat setting of the property object. The thermostat preferences of a property object are based on a random value, extracted from the known distribution of household preferences.

#### 9.5.3 PV generation profiles

When enabling the installation of PV systems in the scenario pane of the tool, these systems are randomly assigned to property objects within the city district. The installed capacity for each PV system at a property is randomly selected, following a uniform distribution between 2 and 6 kWp. The PV generation profiles are then modelled based on the installed system capacity and solar insolation weather data, which serves as an input to the model (refer to Section 9.3).



#### 9.5.4 Battery profiles

Users can enable two types of battery systems in the scenario pane of the tool: a community battery and a battery linked to a PV system. When activating a community battery, the defined capacity of the battery is used to manage grid congestion and optimize energy usage by balancing supply and demand. The charging behaviour of the batteries considers several factors, including the forecasted local solar generation for the next 18 hours and the potential grid feed-in limitations.

When users enable the adoption of batteries linked to PV systems, property objects with PV systems are randomly assigned a battery system. This battery charges when the PV generation levels exceed the consumption level of a household, and discharges at peak moments when the consumption levels are higher.

#### 9.5.5 Airconditioning and cooking profiles

The activation of airconditioning units at property objects that have been assigned one is based on the same temperature model used for heat pump activation. If the inside temperature exceeds a certain threshold, which is different for different property objects, an airconditioning unit is activated until the temperature drops below this setpoint.

A standard electric cooking profile is considered for the property objects that have been assigned electric cooking.

#### 9.5.6 EV charging profiles

The user can vary the adoption rate of EVs in the considered city district. This tool represents the EV adoption rate as an EV ownership rate, defined as the number of EVs per household, rather than a percentage. This approach is taken because car ownership rates can differ significantly across various districts, making it a more relevant metric for comparison and analysis. By focusing on the number of EVs per household, users can gain a clearer understanding of how EV integration might unfold in different contexts.

Based on the considered EV ownership rate, EV charging stations will be placed in each considered low-voltage grid. The number of charging stations in each low-voltage grid is based on the number of households in the respective grid, the expected charging demand per EV owner and the average annual charging demand per charging station. In this work the average charging demand per EV owner was estimated based on the average annual mileage of one car of 12,000 km<sup>10</sup> and an average driving efficiency of 0.191 kWh/km<sup>11</sup>. The location of the charging stations on the map is based on the input file with potential charging station locations (see Section 9.3). Each charging station is assigned the charging sessions associated with a randomly selected charging station in the used charging session data. Using these charging sessions, the charging profiles of a charging station are modelled.

This tool can analyse the grid impact of different EV charging strategies. The first considered charging strategy is uncontrolled charging, which serves as a reference charging strategy. In this strategy, EVs begin

<sup>&</sup>lt;sup>10</sup> Statistics Netherlands. <a href="https://www.cbs.nl/nl-nl/visualisaties/verkeer-en-vervoer/verkeer/verkeersprestaties-">https://www.cbs.nl/nl-nl/visualisaties/verkeer-en-vervoer/verkeer/verkeersprestaties-</a>

personenautos#:~:text=Het%20gemiddeld%20jaarkilometrage%20nam%20toe,in%202019%2C%20voor%20de%20coronapandemie.

<sup>&</sup>lt;sup>11</sup> Based on <a href="https://ev-database.org/cheatsheet/energy-consumption-electric-car">https://ev-database.org/cheatsheet/energy-consumption-electric-car</a>



charging as soon as they are plugged in, without any coordination or scheduling, until their charging demand is met.

The second considered charging strategy is smart charging without V2G functions. In this strategy, charging schedules are optimized to meet a specific goal, while assuring that the charging demand is met before the EV departs the charging station. EVs are not able to discharge in this scenario.

Smart charging can be employed for a wide range of objectives, each with different charging schedules and a different grid impact. In this tool, smart charging is employed according to the principles of Grid Aware Charging ('netbewust laden') 12. This is a national smart charging system developed by grid operators, charging station operators and governments in the Netherlands aiming to ensure that grid congestion caused by EV charging is minimized. In this system, grid operators forecast the load of all grid assets except EV charging stations in their grid for every 15-minute timestep, and based on these forecasts and the grid capacity, a specific capacity is available for all charging stations within one low-voltage grid. The charging station operator must keep the total charging power of these charging stations below this available capacity at all timesteps and have to pay a fine if the charging power exceeds the available capacity. However, the model ensures that the charging demand of an EV is met at the moment the vehicle departs the charging station. Figure 8 presents a visual explanation of how this system works. It is possible to adjust the tool to model other smart charging systems.

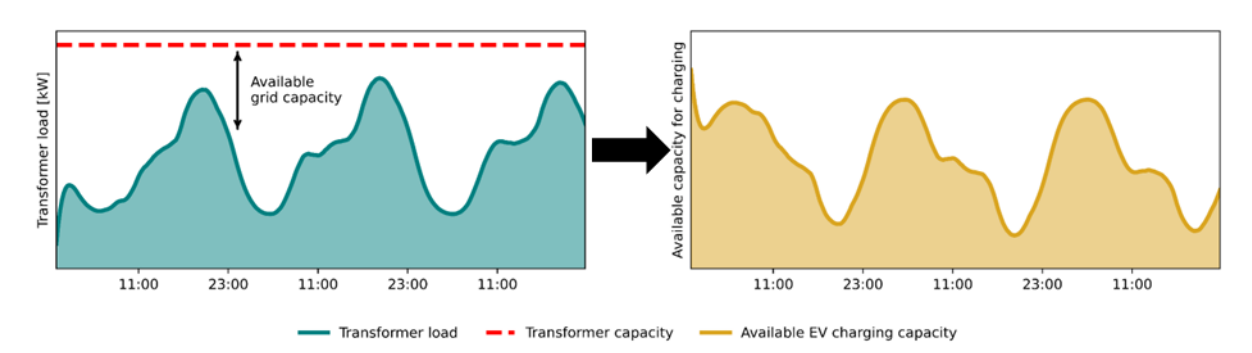


Figure 8: Explanation of the Grid Aware Charging ("netbewust laden") system considered in this tool. The available capacity for EV charging (right plot) is based on the available grid capacity (left plot).

The last charging strategy considers the use of V2G functions. These model simulations are still based on the Grid Aware Charging system but enable the ability to discharge EVs at moments with high grid load. In these simulations, it is assumed that minimum battery state-of-charge is 20% and that the maximum discharging power is equal to the maximum charging power.

 $\frac{\text{https://www.agendalaadinfrastructuur.nl/ondersteuning+gemeenten/documenten+en+links/documenten+in+bibliotheek/handlerdownloadfiles.ashx?idnv=2607151}{\text{for more information on this program.}}$ 

<sup>12</sup> See



## 9.6 Case study introduction

In this project, the approach outlined above has been applied to one specific case study, the wider Lombok district in the city of Utrecht, the Netherlands. This district will serve as the first district to implement the tool, with the intention of scaling the tool to other districts, the entire city, and potentially the wider city area.

The considered district is a residential area from the 1930s, which currently hosts a large number of EV charging stations. The considered district has approximately 11,000 inhabitants. The local grid operator serves around 9000 grid connections in this district, divided over 28 low-voltage grids, each with an individual transformer station.

The local grid operator has provided information about the capacity and location of each transformer station, as well as information on the number of grid connections served by each transformer station. Details of all grid connections in this district were retrieved from the national geo-information data platform of the Netherlands<sup>13</sup>. Grid connections were allocated to the nearest individual transformer stations, while considering the provided information on the number of grid connections per transformer station. Simulated transformer load profiles were compared with measured load profiles of each transformer station. Figure 9 presents a map of the considered city district and the considered low-voltage grids.

The analysis in this work considers EV charging session data from 384 public charging stations of We Drive Solar, covering 196,859 charging sessions. The model simulations were performed using 2022 weather and charging session data.

<sup>13</sup> https://www.pdok.nl/





Figure 9: The considered city district in this work. Different low-voltage grids are grouped using different colours.

### 9.7 Scenario assessment

The developed tool allows users to discover the grid impact in a specific city district for a very broad range of scenarios, as the scenario pane of the tool allows users to adjust parameter values for a wide range of technologies. This section will highlight the main results of the model simulations that have been performed using this tool for the considered city district.



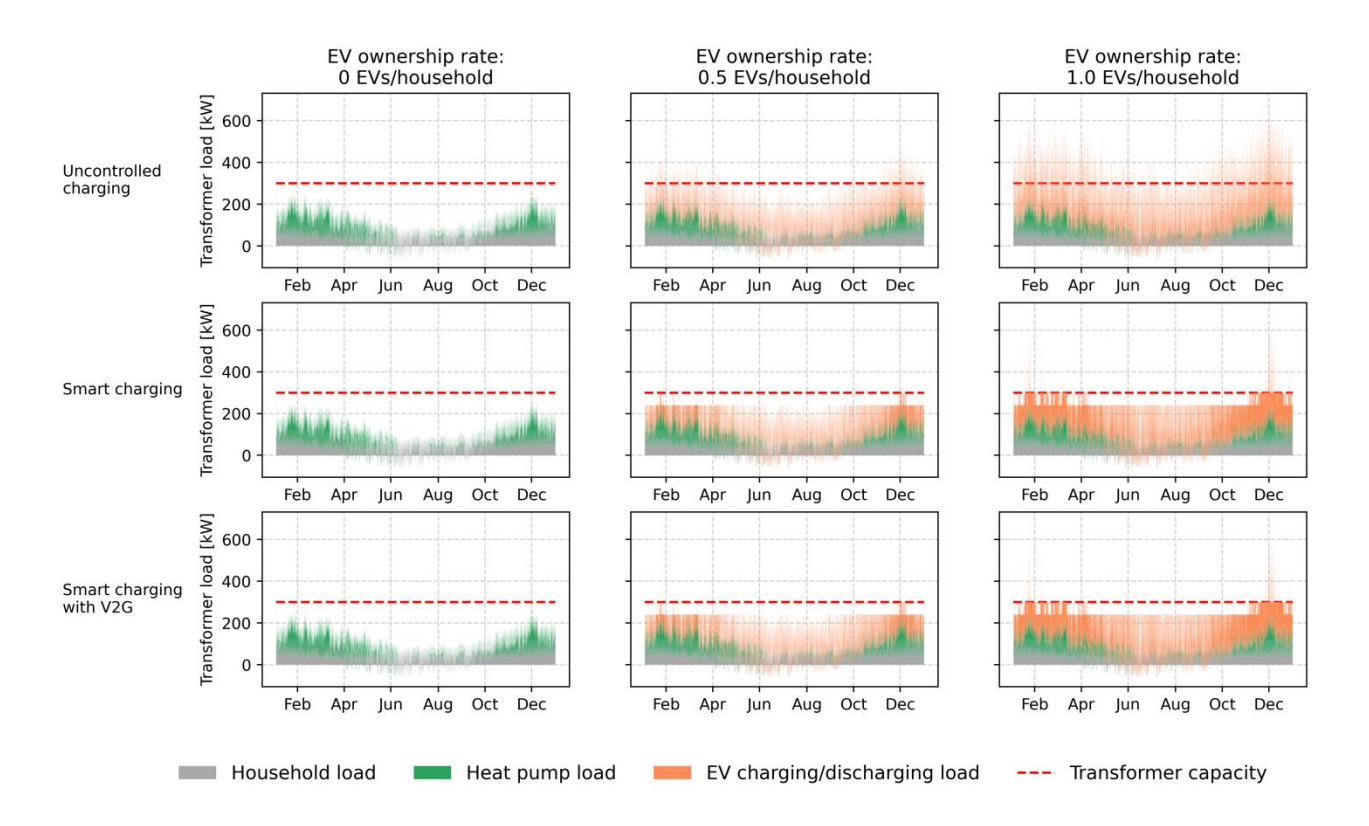


Figure 10: Examples of transformer load profiles for one example transformer for different EV ownership rates and EV charging strategies. The considered heat pump adoption rate is 100% for this figure. In this case, congestion problems occur both with smart charging and smart charging with V2G with an EV adoption rate of 1.0 EVs/household.

Figure 10 presents the yearly transformer load profiles for one transformer for different EV ownership rates and charging strategies. It is visible from these graphs that congestion problems mostly occur in winter periods, which is caused by a higher heating demand and lower PV generation rates. The profiles indicate that the deployment of smart charging can avoid congestion problems at this specific transformer station if the EV ownership rate equals 0.5 EVs/household. With an EV adoption rate of 1.0 EVs/household, congestion problems cannot be fully mitigated for this transformer station, even when considering V2G functions.

A more comprehensive insight into the impact of three main parameters on the transformer loading is presented in Figure 11: i) the EV adoption rate, ii) the considered EV charging strategy and iii) the heat pump adoption rate. The figure provides insight into the loading for all transformer stations considered. It should be noted that these results cannot be generalized, as these results only apply to the specific use case studied.



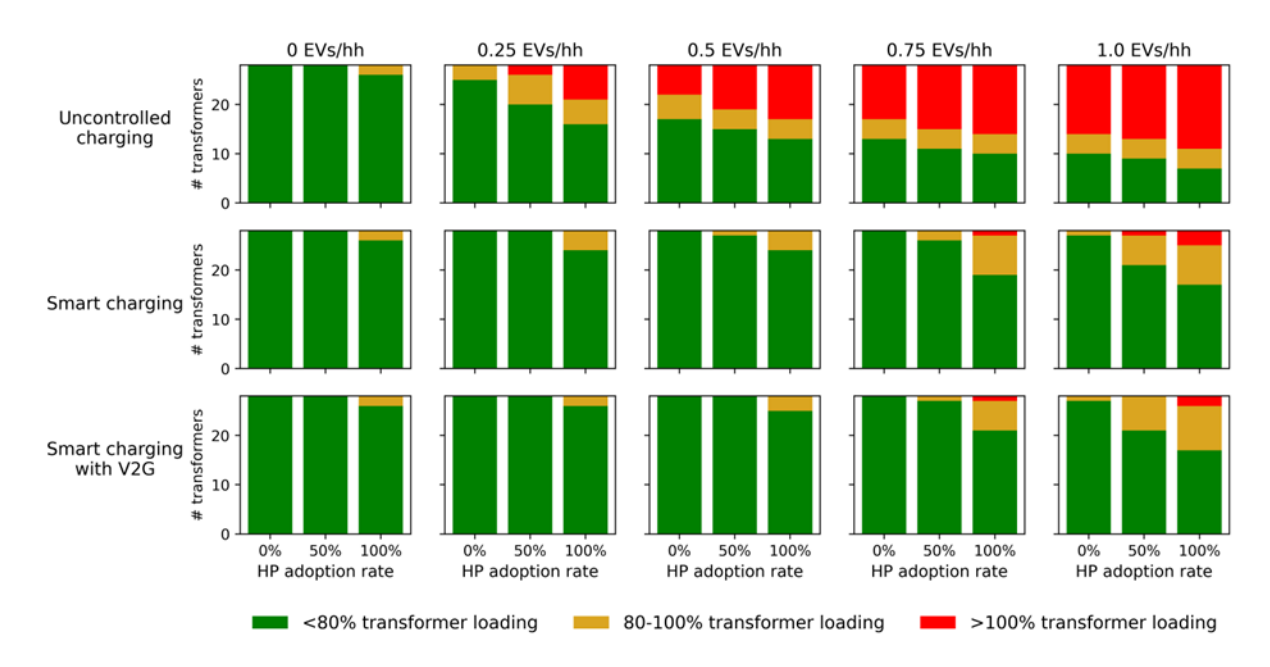


Figure 11: Transformer loading for all considered charging stations in the studied city district, considering different EV adoption rates, EV charging strategies and heat pump adoption rates.

The results show that when considering uncontrolled charging, grid congestion problems already occur in a significant number of the transformer stations at an EV adoption rate of 0.25 EVs/household if heat pumps are also deployed. If heat pumps are not considered, transformer stations will become congested from an EV adoption rate of 0.5 EVs/household. With a high EV adoption rate of 1.0 EVs/household, between 50-60% of the transformer stations in the specific district are congested, depending on the heat pump adoption rate.

It can also be concluded from Figure 11 that unidirectional smart charging can already solve a great share of the congestion problems for the specific case study. If the proposed system is rolled out, no grid congestion occurs in any of the considered scenarios with an EV adoption rate of 0.5 EVs/household or lower. With higher EV adoption rates, a small proportion of the grids can become congested with 50% and 100% heat pump adoption rates. When incorporating V2G functionality, the number of congested grids decreases slightly further. Even with a 50% adoption rate of heat pumps, no grids experience congestion. Additionally, the introduction of V2G further reduces the number of grids where transformer loading exceeds 80%. However, V2G cannot resolve all congestion issues in this specific case study. This limitation arises because the model ensures that EVs meet their charging demand before their departure time and cannot discharge below a 20% state-of-charge threshold.

The value of V2G compared to unidirectional smart charging becomes more pronounced if one steps away from the assumption that all EVs perform smart charging. If only a share of the EVs adjust their charging schedules to benefit the grid, for instance if specific EV owners are unwilling to participate in a smart charging scheme, the congestion levels between unidirectional smart charging and smart charging with V2G can show more considerable differences. This is visible in Figure 12 on page 31.

It shows that with lower EV adoption rates and low smart charging participation rates (e.g., 0.25 EVs/household and 25% smart charging), the number of congested grids is considerably lower when considering V2G functions. Such a situation, in which not all EVs are able to perform V2G functions, is



realistic for the upcoming years. Similarly, with high EV adoption rates and smart charging adoption rates of around 75%, the grid congestion levels are also considerably lower when considering V2G functions.

## 9.8 Conclusions and next steps

This chapter has introduced the first tool of Task 2.6, the *Transformer Load Capacity Tool for Integrated EV mobility and Energy Scenario planning* developed by the City of Utrecht and Utrecht University. This tool aims to assist cities in managing the ongoing energy transition, in particular by planning the integration of shared and private mobility, EV charging infrastructure, photovoltaic systems and heat pumps into the electricity system, without experiencing congestion problems. The developed tool is open-access and can potentially be implemented at any city in Europe. In this task, the tool has been tested and implemented in the City of Utrecht in the Netherlands. The City of Utrecht will now use the results of this tool to inform policy decisions regarding the ongoing energy transition. The next steps involve scaling up the tool to other districts within the city, a process we are already working on, with the goal of city-wide implementation. Additionally, the tool has been selected for evaluation by the Province of Utrecht to create energy scenarios for new housing projects and to report these to the grid operator.



In this chapter, it has been outlined how the tool can be set up, how it can be used and how it functions. In addition, Section 9.7 presented results from the tool for the specific case study considered.



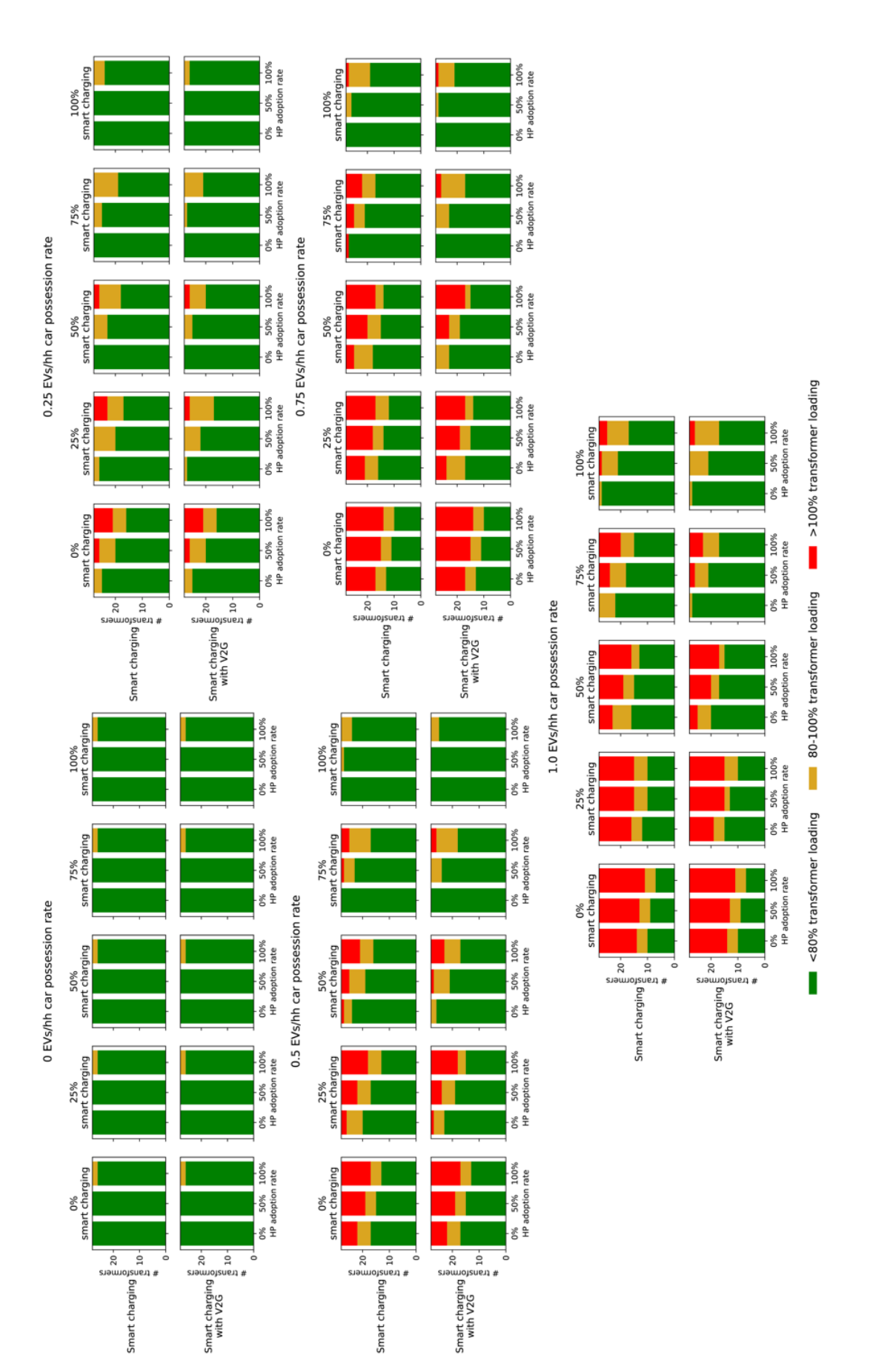


Figure 12: Transformer loading for all considered charging stations in the studied city district, considering different EV adoption rates, EV charging strategies, heat pump adoption rates and shares of EVs conducting smart charging.



# 10 Tool B – Tool developed by CERTH

As described above, two tools have been developed in this Task. Each tool has different functionality and is therefore treated in a different section. Also, a video is created for each tool, showing visually and verbally what the tools do and how they can be used by the target audience(s). Second, the tool developed by CERTH will be discussed.

# CERTH's in-house-developed optimal Energy Planning Tool and INTEMA.grid grid simulator

A demo video of this tool has been submitted together with this report, which provides a detailed explanation of the functioning of the tool. The video is titled "SCALE D2.6 – Demo tool B – CERTH – SCALE.mp4".

#### 10.1 Overview of the tool

#### 10.1.1 Literature review

Several challenges can be found in the route towards achieving an energy transition from a fossil fuel-based energy mixture to a state of significantly increased share of renewable energy sources (RES). Numerical simulation tools can be crucial in this long and demanding process mainly due to their advantage of accurately representing large and complex energy systems through digital twins. Through the concept of digital twin, the evaluation of design and operation options is enabled in a much more efficient manner in terms of required time and cost. By addressing the challenges that today's modelling tools are facing, it will be possible to enable the development and implementation of more sophisticated and reliable control over modern power grids, making them an essential component in the energy transition value chain. Modern power grids are characterised, inter alia, by high shares of RES in the energy mix, a significant contribution of plug-in electric vehicles (EVs) to the total power balance, smart energy management, energy storage and demand response facilities. The intermittency nature of RES and the uncertainty of EV charging demands and V2G availability result nowadays in significant challenges for the electrical grids in terms of stability, reliability, and resiliency. Available computational tools can aid the proper integration of these new elements into the grid ensuring system reliability in the event of unwanted incidents, such as disturbances, faults, etc. This can provide technical feasibility in the energy planning process. Also, modelling via simulation tools can provide grid designers and operators the availability to explore multiple design arrangements and operating and control strategies before the key results of these studies get actually tested and evaluated in the field; thus, saving costs and reducing risks. In the context of SCALE T2.6, the described advantages extend to the integration of V2G chargers into Utrecht's distribution network.

A series of studies have been recently conducted in the research field of power grids supporting V2G functionality. The Optimal Power Flow (OPF) problem is a typical study area of electrical grids leading to conclusions about a wide area of system power generation scheduling, from simple optimal power dispatch to more complex combined unit-commitment multiperiod OPF problems, taking into account further constraints, such as ramping costs or RES generation uncertainty. Zhang et al. [1] proposed a joint methodology for simultaneous OPF routing in a power grid and decentralised V2G scheduling with the regulation service, ensuring satisfaction of both voltage and frequency regulation. In [2], a multi-period OPF problem is solved with the utilisation of the IPOPT solver in GAMS, where a low-voltage (LV) distribution system with DSO partial controllability of residential flexibility resources, i.e. PVs, EVs and energy storage systems, is studied. Jadoun et al. [3] propose a fuzzy-based improved elephant herding optimization approach to solve a multiobjective optimisation problem for optimal scheduling of a microgrid considering a



mix of multiple dispatchable and non-dispatchable distributed energy resources (DERs) and compare the results with other methods over 3 different scenarios and 6 cases.

Several studies have been conducted related to the dynamic operation of grids supporting V2G functionality. Kuhada et al. [4] have proposed a V2G control strategy for an EV battery, testing its efficiency through real-time simulations using OPAL-RT real-time environment and MATLAB/Simulink. In [5], the authors proposed a V2G-based primary and secondary frequency control to mitigate frequency deviation in a microgrid. The testing facility includes a 10 kWe bidirectional off-board EV DC fast charger (DCFC), a V2G-capable Nissan Leaf EV, a 15 kVA grid simulator, two 4.5 kW AC/DC electronic loads and a 5 kW PV simulation combined with a 5 kW grid-tied micro-inverter and all of these elements are integrated into the Canadian Centre for Housing Technology (CCHT) and monitored by a local SCADA system. Simulations in this case were also conducted by using MATLAB/Simulink on a time-domain dynamic analysis through the phasor modelling technique. Furthermore, studies [6,7] have been conducted for the island of Porto Santo, Portugal, investigating the integration of renewable energy units into the existing power system, as well as developing V2G capabilities through the electrification of the transportation network. In [8] the effects of V2G in a non-interconnected island are compared between different scenarios of energy management without, however, following a dynamic grid modelling approach.

### 10.1.2 Application of CERTH's tools for the case of UTR demo site

In the context of SCALE T2.6 relevant activity, a Mobility and Energy Planning tool with a unified approach has been designed by CERTH to support the optimal integration of EVCI in the distribution grid of the Floresstraat neighbourhood in Utrecht, which is presented in Figure 13. The single-line diagram of the grid under study have been provided by the City of Utrecht.



Figure 13: View of Floresstraat distribution grid under study. The black circle is the Distribution Transformer

In this study, the approach followed aims to address research challenges in the field of V2G planning by introducing a three-step methodology that is applied in the Floresstraat distribution grid in Utrecht. An overview of the proposed methodology is presented in Figure 14. The methodology combines the EVCI position optimisation at the local grid while considering stochastic mobility and charging behaviour patterns,



cost-minimising optimal power flow problem and transient system response through dynamic models for the stress-test of the proposed topology.

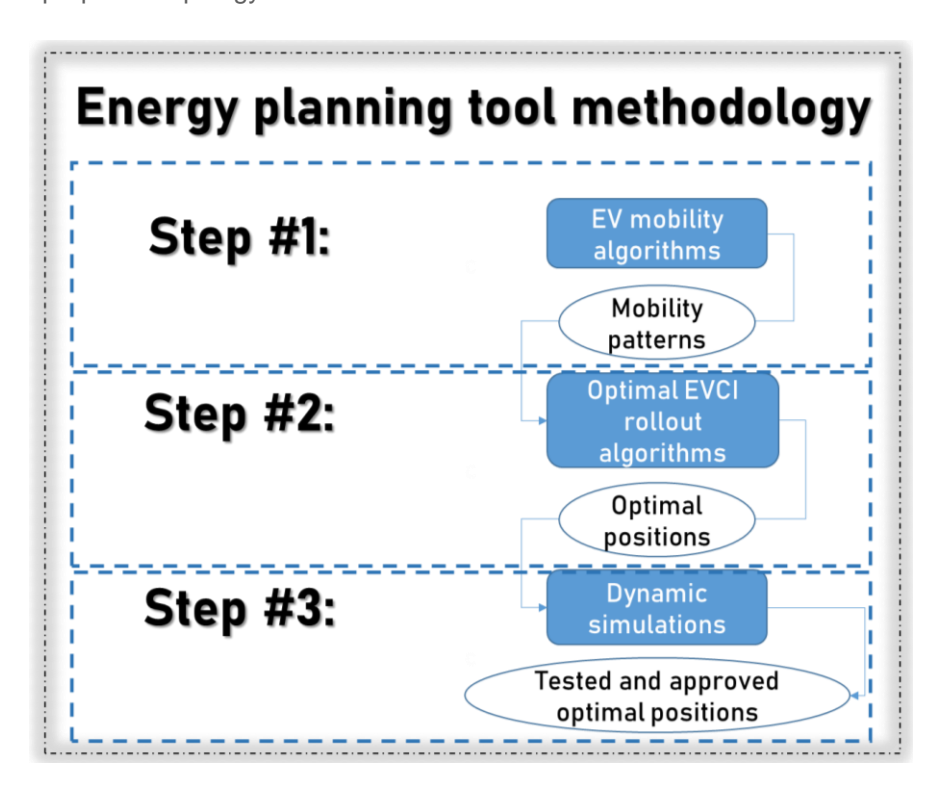


Figure 14: Overall methodology of the Energy Planning Tool designed and implemented by CERTH for T2.6

The first step of the methodology is described in Section 10.2 and involves the estimation of mobility data provided by the Mobility Tool. The results from this first step i.e. the estimated mobility patterns are used for the subsequent Step 2 and Step 3.

The second methodological step entails the Energy Planning Tool which executes an optimal power flow (OPF) problem that is solved repetitively for each discrete time point. Common optimal power flow (OPF) studies solve an optimisation problem at each time step leading to conclusions about the most financially beneficial allocation of the power demand to the available power plants, at each time step. Finally, the most profitable solutions in the long term are identified by comparing all possible EVCI spatial arrangements. The optimal EVCI positions and the optimal dispatch scheduling are given as the output of the optimization algorithms described in Section 10.3.

The final step of the proposed methodology (Section 10.4) includes the advancement and application of CERTH's in-house INTEMA.grid modelling tool [9] specially focusing on power grid dynamic operation and transient phenomena. A single feeder line of the Floresstraat neighbourhood distribution grid connected with the local transformer substation is isolated to act as a reference use case for the numerical testing of INTEMA.grid. Two cases, Case A and Case B, are examined to evaluate the technical feasibility of the proposed EVCI topology. In Case A, the optimal dispatch schedule is applied by the charger control system to ensure the provision of V2G power. In Case B, a grid disturbance is numerically introduced over a short period of a few seconds to evaluate the V2G capability to provide ancillary services to the grid, such as system frequency stability.



#### 10.1.3 SCALE's numerical innovation (in terms of model approaches followed)

An important advantage of the approach designed, and the model tested during SCALE, lies in the combination of a) the proposed technique for identifying the optimal EVCI rollout into the grid, b) the advanced transport models developed by CERTH and c) the dynamic simulations performed by INTEMA.grid. Different transport models are initially developed to extract mobility data estimations, such as users' driving behaviour patterns and, consequently, the vehicle availability for charging or the V2G power supply. The data exported from those transport models are imported to the optimisation algorithms of the EVCI positions in the existing grid, to ensure that unavailability resulting from user behaviour is considered. After extracting the optimal positions of the V2G chargers in the existing grid a post-process evaluation of the proposed solutions, through dynamic operation simulations, follows. In terms of grid dynamic operation, this last step guarantees the elimination of results that are technically infeasible.

Among the advantageous aspects of the dynamic modelling approach followed are i) the combination of detailed 3-phase AC power grid models using dq0 transformation [10], ii) the utilisation of exciter and turbine-governor models for all plants based on international standards (e.g. IEEE), iii) along with the inclusion of battery models at a cell level using the Equivalent Circuit Model (ECM) technique with 2 resistor-capacitor (RC) branches and iv) custom models developed for all subcomponents of the EV charger, including inverter and sophisticated control circuits.

The detailed subcomponent models ensure adequate accuracy ensuring that the built system model offers improved estimation of system response at all grid points (e.g. connection point of feeder line, V2G chargers, vehicle battery, etc.). All of these models are based on the equation-based Modelica language and the utilization of open-source libraries.

As regards the CERTH-CPERI own exploitation plan of the models developed, an important outcome is the development of INTEMA.EV, a standalone EV simulator that is expected to be included in the broader CERTH's suite of tools, INTEMA [11]. INTEMA.EV will offer novel services to different stakeholders through an open, easy-to-access, verified and technically sound web-based GUI. that includes dynamic battery models for different types of lithium-ion chemistry and sophisticated powertrain control algorithms. Additionally, this tool can be used to extract important information regarding the performance assessment of EV powertrain components based on the user's imported driving schedule.

In a nutshell, the advantageous features offered by the integrated EV Mobility and Energy Planning Tool, which can be considered as the added value of this tool, entail an advanced, beyond current state-of-the-art methodology for solving the problem of EVCI placement involving 3 aspects:

- Optimal EVCI location problem solving through specialised OPF python scripts
- Integration of mobility behaviour patterns
- Stress test of the proposed topology through dynamic component-based modelling



# 10.2 Different scenarios based on the transport model

#### 10.2.1 Introduction

In modelling electric vehicle (EV) charging behaviour, it is crucial to accurately capture the temporal patterns of when and where vehicles are being charged. Charging stations vary widely in their usage, from residential homes to public locations like shopping malls and highways, each presenting a unique set of behaviours for when EVs arrive and depart. To model these charging scenarios effectively, we rely on probabilistic methods, particularly **normal distribution**, as the primary tool for generating realistic arrival and departure times.

The normal distribution is widely used in statistical modelling due to its ability to represent real-world phenomena where events cluster around a central value with natural variation on either side. It forms a bell curve, where most data points (in this case, arrival or departure times) are centred around the average, but there are still occurrences of early or late events. This shape matches many of the charging behaviours observed in real life.

#### 10.2.2 Workplace Charging

Workplace charging is typically used by individuals who drive to work and stay for a full workday. In the scope of T2.6, this is imported as the user behaviour, whereas a detailed presentation of alternative scenarios is studied more thoroughly in the follow-up task T5.2. The arrival times reflect the common start times for office work, typically between 7:00 AM and 9:00 AM. Departure times are set between 4:00 PM and 6:00 PM, aligning with typical end-of-day work hours. The duration of charging, from 8 to 11 hours, reflects the length of an average workday, including some flexibility for late arrivals or early departures.

Arrival Time: Between 7:00 AM and 9:00 AM
Departure Time: Between 4:00 PM and 6:00 PM

Duration: 8 to 11 hours

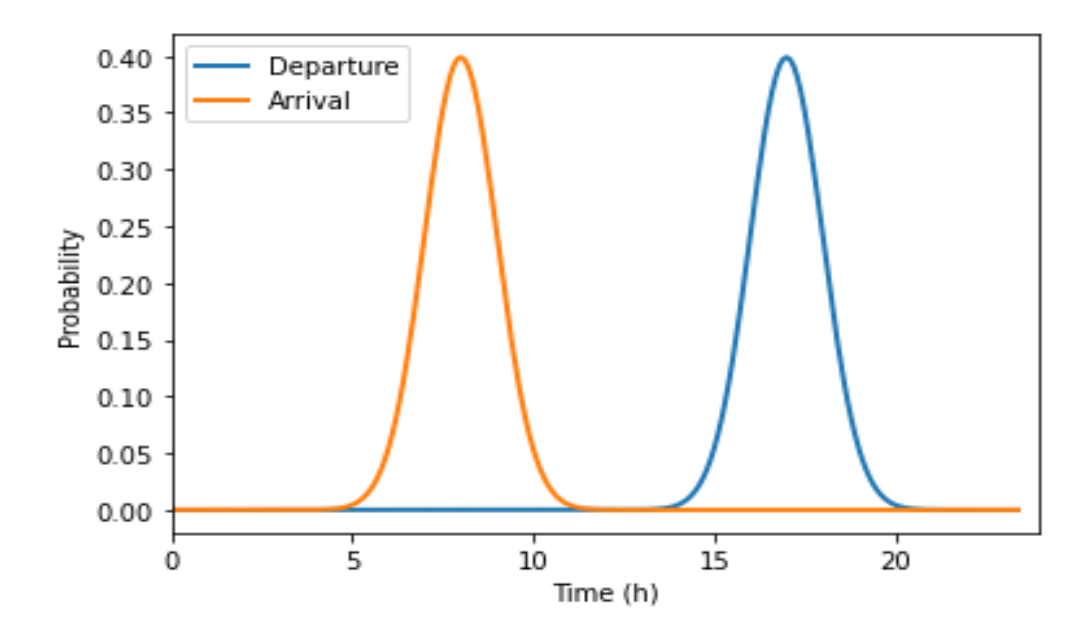


Figure 15: Probability distributions of workplace charging: Arrival peaks between 7-9 AM and departure between 4-6 PM, reflecting typical office hours.



# 10.3 EV charging infrastructure rollout optimisation methodology

## 10.3.1 Description of CERTH's Energy Planning Tool

CERTH's Energy Planning Tool is an optimization tool, which is developed to support the integration of EV V2G (Vehicle-to-Grid) and V2X (Vehicle-to-Everything) charging stations into a given Distribution Electric Grid. This tool identifies the optimal location and size (Nominal Apparent and Active Power) of the charging stations.

To determine the optimal location, the tool considers the following factors:

- Energy requirements (loads, battery efficiency)
- Grid saturation
- Impact on grid voltage, frequency, stability, and overall power losses caused by the chargers
- Forecasting the number of vehicles (transport model)

The tool calculates the optimal position and size of the chargers by minimizing total grid power losses and congestion after the introduction of EV chargers.

#### 10.3.2 Modelling

To achieve the goal of the description, the Energy Planning Tool contains an optimization algorithm whereby the grid's power flow is executed. By this process, the algorithm takes into account the following grid's specifications:

- Loads position and consumption
- DER position and energy production
- Number of grid's lines and buses
- Total line power losses
- Magnitude and angle of voltage on every bus
- Current magnitude on every line

Using the previous specifications, the algorithm chooses the optimal size and position of charger stations, minimizes the total line power losses and contributes to the normal operation of grid.

#### 10.3.2.1 Objective Function

The objective function includes the variables to be optimized, specifically total grid power losses and total grid congestion. As a result, the objective function is a vector function, represented by the following equation:

$$\vec{F} = \left(\sum_{l}^{N} g_{l} \big| V_{i}^{2} + V_{j}^{2} \big| - 2g_{l} |V_{i}| \left| V_{j} \right| cos(\theta_{i} - \theta_{j}), S_{oper} \right)$$

Where:

The first component is the total line power losses (kW)

The second component is the operational apparent power (kVA) of the grid's transformer, which represents the total grid congestion

N are the total lines of the grid



g<sub>1</sub> is the conductance of every line

i, j are the buses, which are connected via I line

V<sub>i</sub>, V<sub>i</sub> are the voltage magnitudes on i, j buses respectively

i, j are the voltage angles on i, j buses respectively

#### 10.3.2.2 Constraints

The constraints are the process whereby the algorithm ensures the grid's normal operation and the finding of at least position for a charge station in the grid. This process is shown as following:

- 1.  $\left(p_0S_{bmin}^0, p_1S_{bmin}^1, ..., p_KS_{bmin}^K\right) \leq \left(S_{b}^0, S_{b}^1, ..., S_{b}^K\right) \leq \left(p_0S_{bmax}^0, p_1S_{bmax}^1, ..., p_KS_{bmax}^K\right)$ . This inequality ensures that the values of nominal apparent power of charge stations do not fall under a minimum value and do not surpass a maximum value, predetermined by the pilot's administrator.
- 2.  $\sum_{i}^{K} (p_0 S_{bmin}^0, +p_1 S_{bmin}^1 + ... + p_K S_{bmin}^K) > 1 \text{ MVA}$ , This inequality ensures that the total installed nominal apparent power of Charge Stations is at least 1 MVA.
- 3.  $(V_{0min}, V_{1min}, ..., V_{Kmin}) \leq (V_0, V_1, ..., V_K) \leq (V_{0max}, V_{1max}, ..., V_{Kmax})$ , This inequality ensures that the magnitude values on every Grid's bus do not fall under a minimum value and do not surpass a maximum value, predetermined by pilot's administrator.
- 4.  $(I_0, I_1, ..., I_N) \le (I_{0max}, I_{1max}, ..., I_{Nmax})$ , This inequality ensures that the Grid's lines do not overload.

Where:

K is the number of total grid's buses.

N is the number of total grid's lines.

 $I_{0max}, I_{1max}, ..., I_{Nmax}$  are the nominal currents of every grid's line

In addition, the algorithm finds the bus where the grid's substation and transformers are connected and ensures that no charge station is introduced there. Therefore, another constraint is the following:

5. If  $i = \text{substation } i = \text{transfomer then } p_i = 0$ , Where  $p_i$  is the position binary on bus i.

## 10.3.3 Optimization Process Methodology

The operation of the Energy Planning Tool's optimization algorithm follows a methodology, which is separated into two parts.

- 1. The usage of **Pymoo** optimization tool, for minimising total line power losses and ensuring the non violation of the constraints.
- 2. The usage of **Pandapower** power flow tool, to execute the pilot's distribution grid power flow.



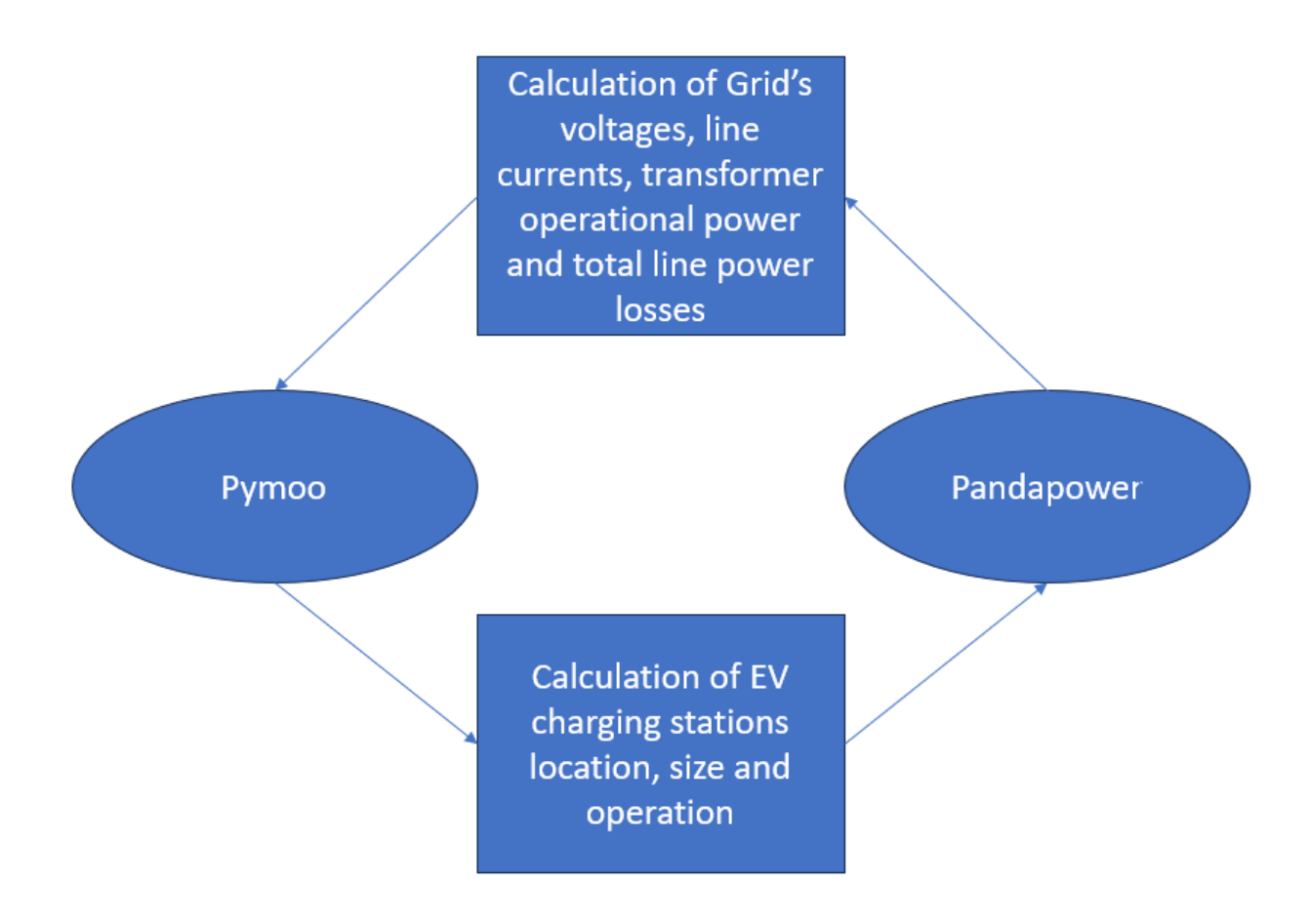


Figure 16: Communication between Pymoo and Pandapower.

#### 10.3.3.1 Pymoo Optimization Tool

Pymoo is a Python-based optimization tool designed for advanced single and multi-objective optimization tasks. It offers a range of features related to optimization, including visualization and decision-making support. Pymoo processes data from power flow simulations to determine the optimal placement and size of EV charging stations by optimizing the objective function, while ensuring that constraints are not violated.

Additionally, Pymoo provides iterative feedback, allowing for repeated power flow simulations with the inclusion of EV charging stations. This process continues until the optimal objective function is achieved or the maximum number of iterations is reached.

Thus, the Energy Planning Tool's optimization algorithm must ensure seamless communication between Pymoo and the power flow tool.

#### 10.3.3.2 Pandapower Power Flow Tool

Pandapower is a Python-based power flow tool that simulates the grid's power flow by using the EV charging station locations and sizes provided by Pymoo as input. Through power flow analysis, the following data are computed:

Load locations and consumption



- DER (Distributed Energy Resources) locations and energy production
- Number of grid lines and buses
- Total power line losses
- Voltage magnitude and angle at each bus
- Current magnitude on each line

This data is then fed back to Pymoo to calculate updated locations and sizes for the EV charging stations.

## 10.3.4 Implementation

The Energy Planning is implemented in the Floresstraat Distribution Grid, an area near Utrecht.



Figure 17: Floresstraat Distribution Grid, the pins indicate the grid's buses and the black circle is the bus with the Distribution Transformer

For the calculations, the Energy Planning Tool estimates the grid's worst-case scenario day by analysing consumption data from the entire year of 2022. Figure 18 indicates the monthly consumption values. From this figure it is clear that the month with the highest consumption was January 2022.



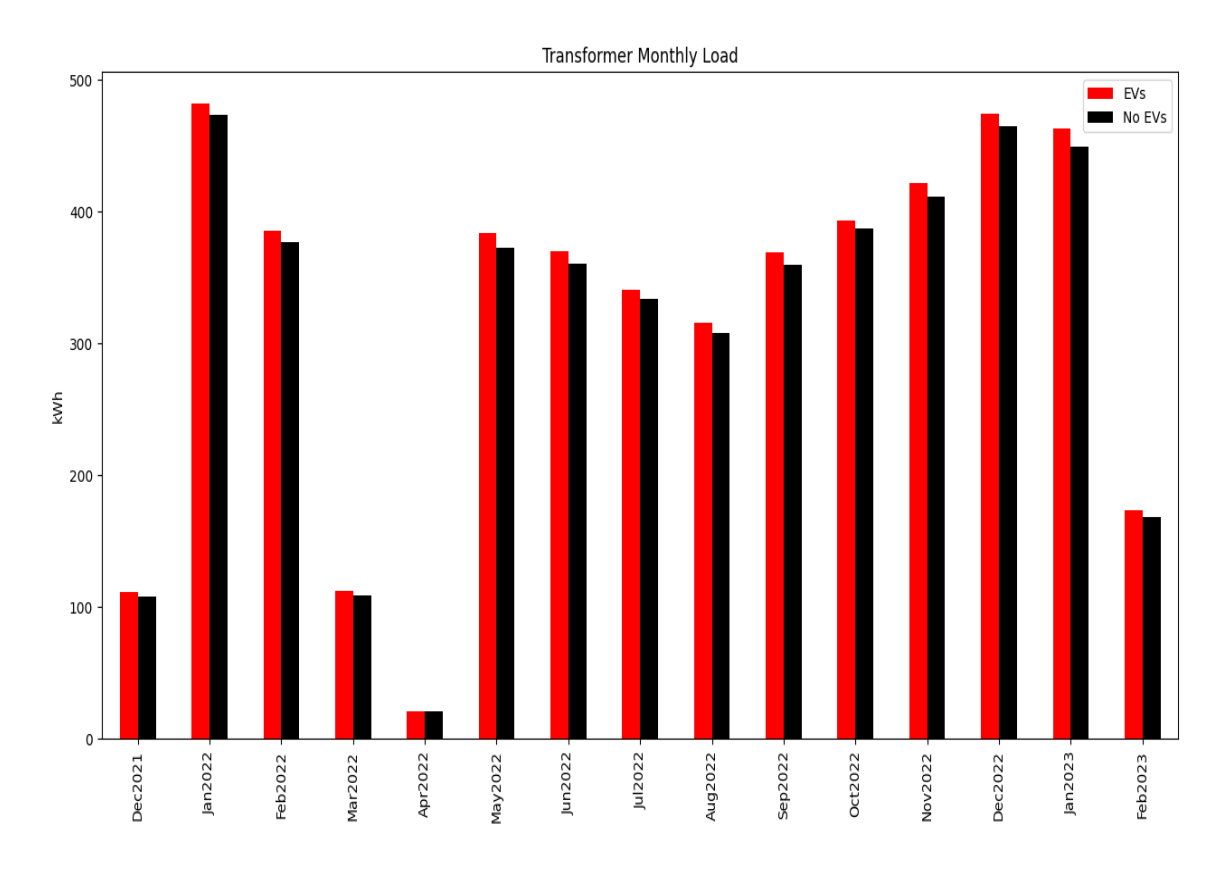


Figure 18: Monthly consumptions

Figure 19 shows the daily consumption for January 2022. As indicated, the day with the highest consumption is January 15<sup>th</sup>, making it the annual worst-case scenario that the Energy Planning Tool must manage.



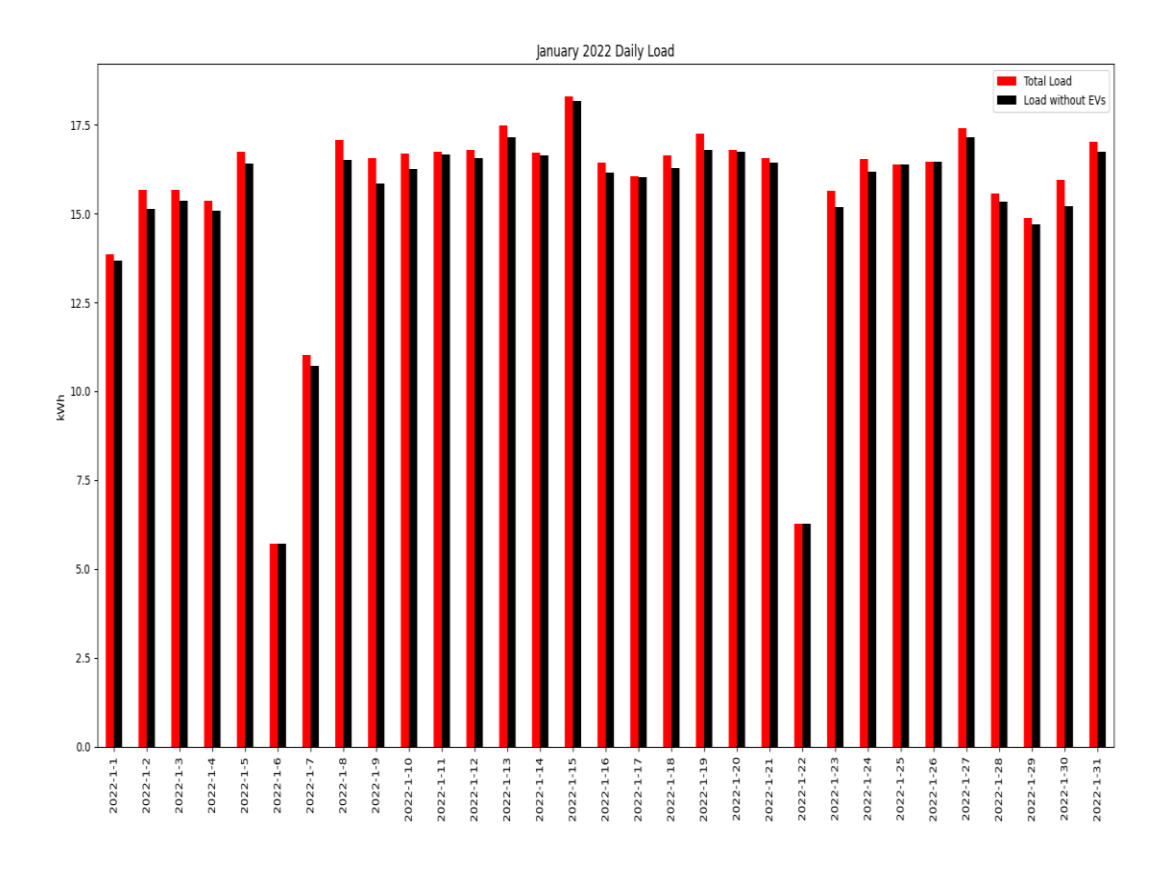


Figure 19: January 2022 Daily Consumptions

## 10.3.4.1 Load Configuration

The Floresstraat distribution grid contains 344 consumption loads and is an LV distribution grid so the exact demand data of each one of the loads is unavailable.

For this reason, the Total Power Demand of Figure 20 is evenly distributed on each one of the grid's loads. This assumption is crucial for the execution of the power flow.



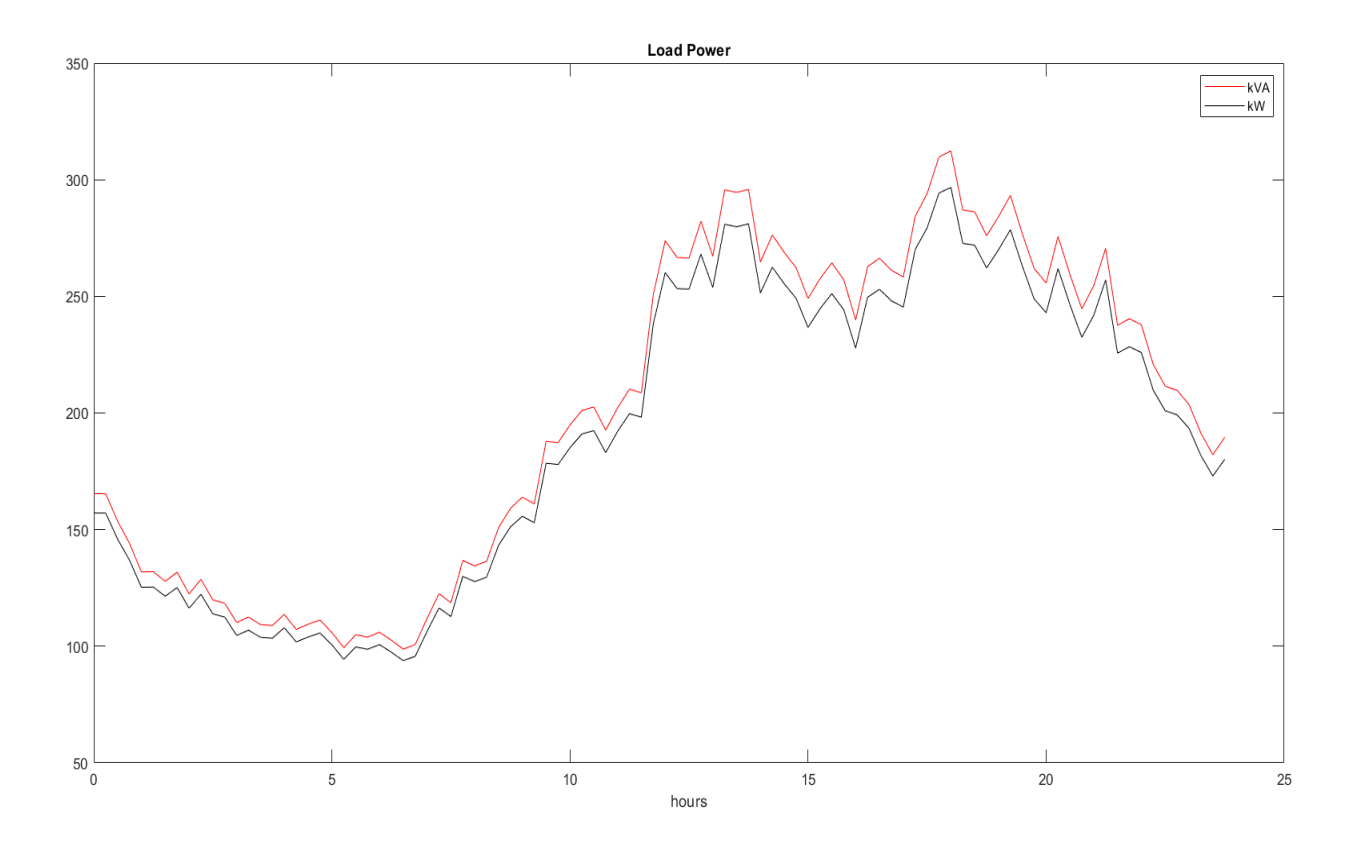


Figure 20: Total Power Demand of the Grid



#### 10.3.4.2 Results

As it is showed at the Figure 21, two charging station has been introduced by the Energy Planning Tool with **22 kVA** nominal power each.

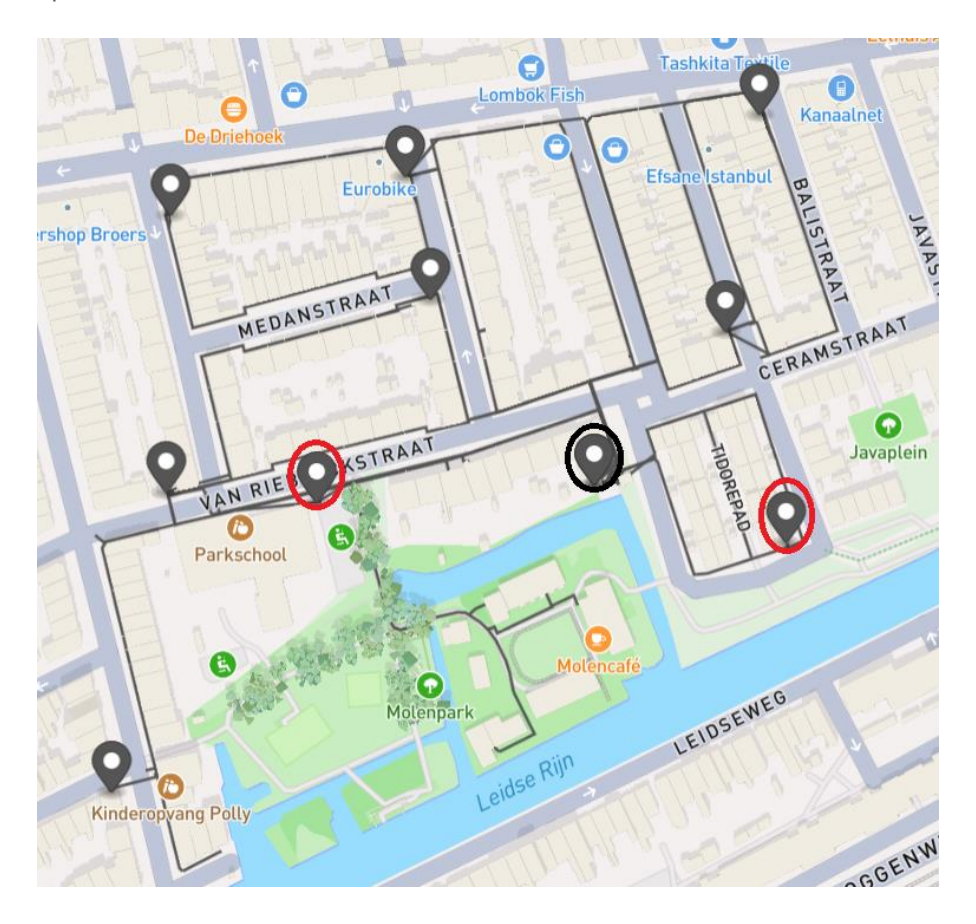


Figure 21: Floresstraat Distribution Grid after the introduction of the EV charging stations. The red circles indicate the buses where the EV charging stations are installed.

After the installation the Energy Planning Tool calculated the optimal operation of the charging stations for three cases, according to the transportation model of Section 10.2. These cases are:

- V2G Operation
- V1G or Smart Charging Operation
- V0G or Plug-in Operation

The transformer loading, given on the Y-axis in percentage, and as a result the Grid Congestion, is minimised after the introduction of the charging stations during the V2G operation, as it showed at the Figure 22. As we can see in the original state (black), the loading of the transformer follows, as usual the daily affairs of the area that services. If EVs are left to charge immediately as they plug in, i.e. V0G, (blue), it is evident that the situation worsens, with the loading increasing significantly, thus putting the substation under strain. This situation though, can be improved with the use of smart charging, or V1G, (yellow), and even more when not only smart charging is utilized but also smart discharging (red), where the congestion is mitigated thus releasing the strain from the substation.



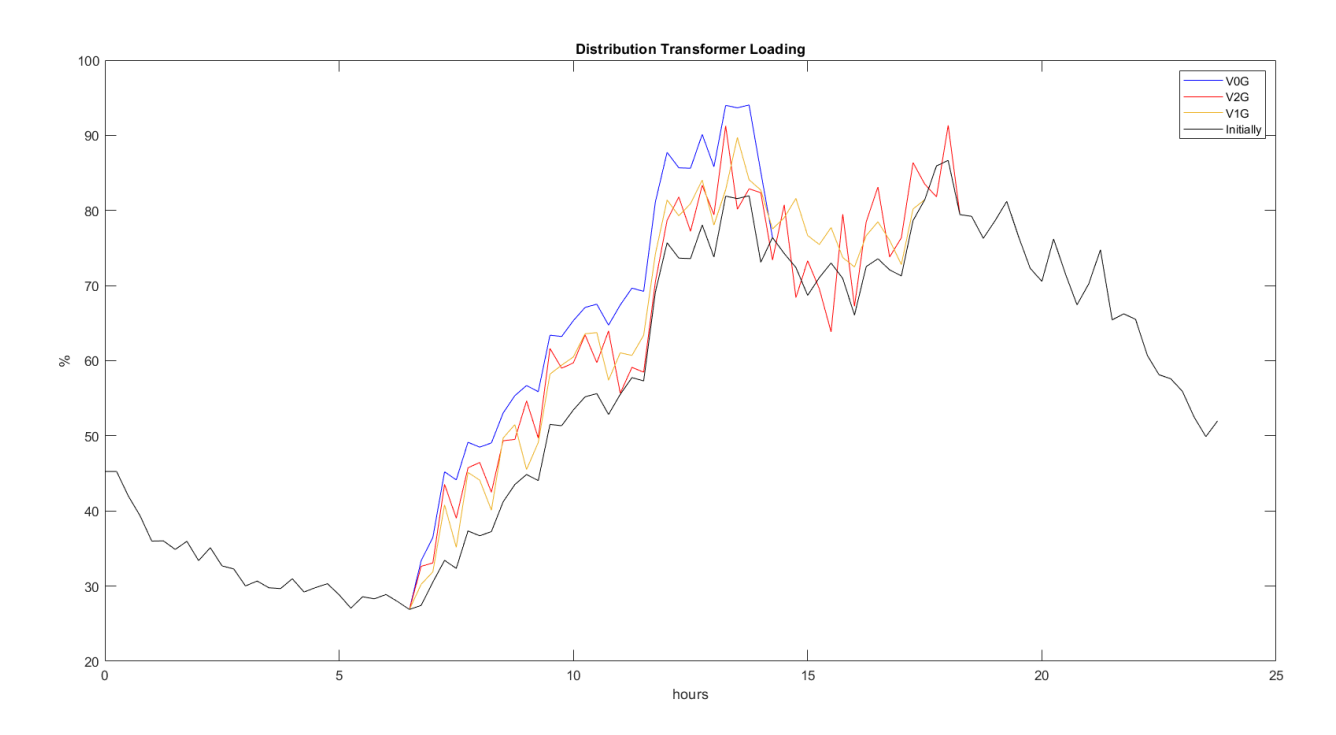


Figure 22: Transformer Loading Percentage

Figure 23 shows certain intervals where the State of Charge drops, indicating that the batteries are discharging during those periods, where **31150** and **31170** are the names of the Grid's buses where the charging stations are connected.

The time intervals where the State of Charge is zero, no EV is plugged at the charging station.

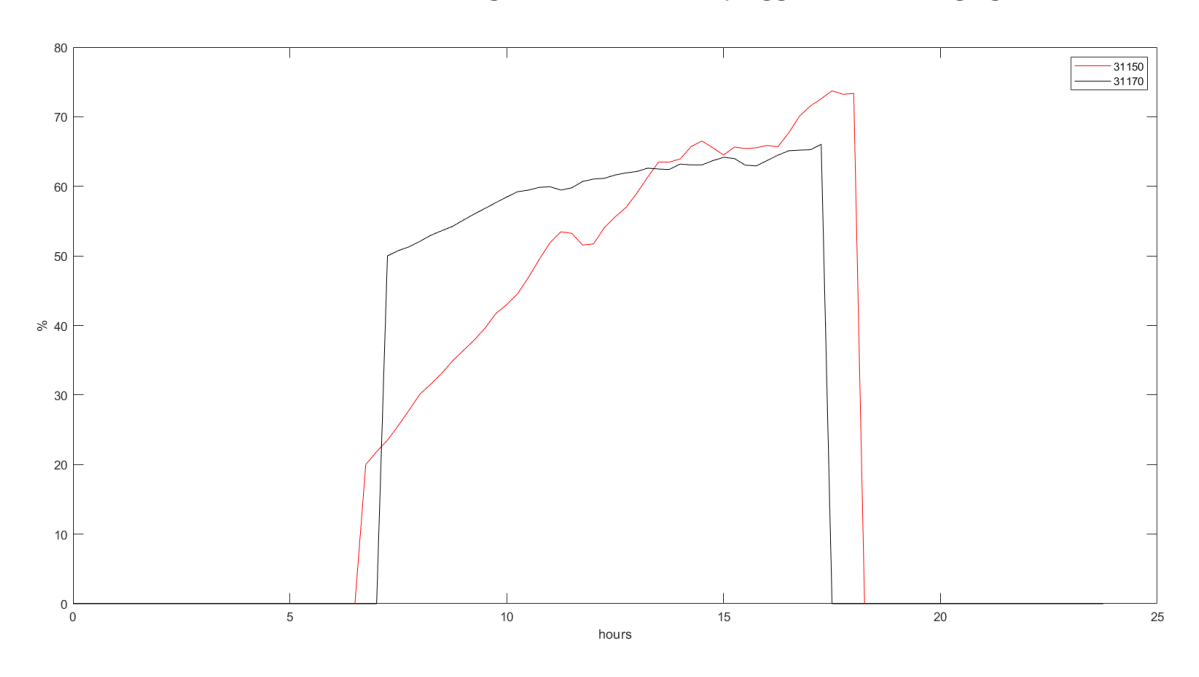


Figure 23: State of Charge of EV Battery during V2G operation



# 10.4 V2G dynamic models

# 10.4.1 Description of INTEMA simulation tool

To stress-test the network topology proposed and presented by the position optimisation algorithms in Section 10.3, studying the grid operation under a reference period is a necessary third step to verify that the system complies with a series of technical constraints. For the study of the operation of an electrical grid throughout time, a dynamic system model is a key prerequisite. A reliable environment to describe the operation and interaction of all system components with proper solvers for the multiple equations is necessary. For this purpose, the CERTH in-house INTEMA.grid tool, dedicated to the dynamic simulation of electrical grids, is utilised. This tool, formerly developed and tested in the IANOS [12] and SMILE [13] projects, eases the design and simulation of electrical grids of different kinds that can involve active and passive network elements, such as generators, transformers, lines, loads and grid-scale storage assets in an unrestricted variety of configurations. A powerful and effective modelling language underlies the physical representation and simulation of the grid. Namely, the component-oriented equation-based language Modelica, specialised in the modelling of multi-domain physics systems, is utilised within the Dymola software environment [14,15]. Models of the open-source libraries Modelica Standard Library [16] and PowerSystems [17] are used supportively or simply as a basis to create custom component models.

A classification of the key INTEMA.grid outputs by possible interested parties is presented in Figure 24.

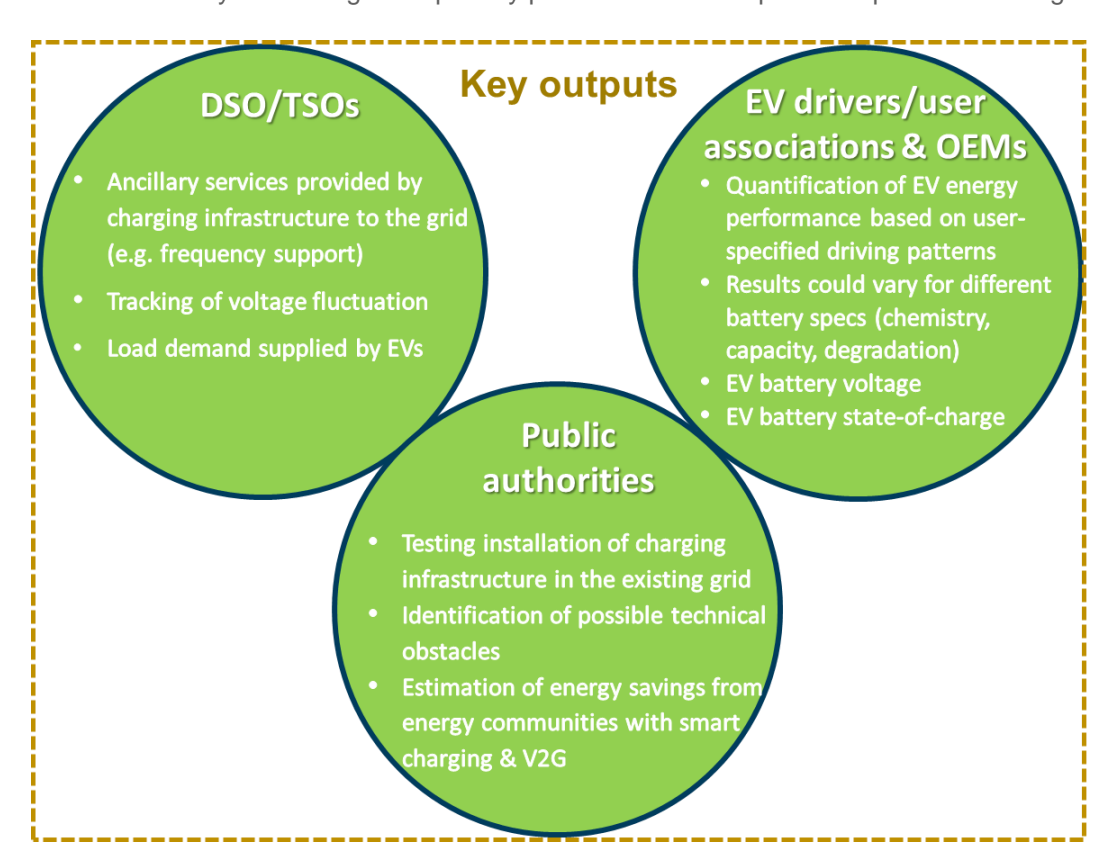


Figure 24: Key outputs of INTEMA.grid dynamic models classified by potential interested parties

To rise to the challenge of V2G simulations of Utrecht's grid, for the purposes of T2.6, the enrichment of INTEMA.grid capabilities is conducted in the context of SCALE. Proper models of the following key system



components have been developed and integrated into the existing model library, which basis is formulated for the case of AC-governed power systems:

- EV battery
- > Bidirectional/unidirectional charger
- > EV powertrain
- Utrecht distribution network

The steps followed for model development are described in detail in the following section.

#### 10.4.2 System modelling

#### 10.4.2.1 Background numerical framework: Three-phase AC system representation

For the study of power system dynamics, it is necessary to develop accurate models of large-scale power systems with the minimum possible complexity, also accounting for the minimum reduction of computation resources needed. A common practice is to use time-varying phasor models [18–21]. These models are based on the assumption that voltage and current quantities are nearly sinusoidal. As such, phasor models that incorporate a slow time variation of amplitude and phase can be used for their representation. They are mainly used for stability analysis and for modelling relatively slow transients. However, they can only be used if amplitude and phase variations evolve relatively slowly. An alternative modelling option is the dq0 transformation, which maps sinusoidal signals to constants, similar to the phasors representation, leading to more simple dynamic models. In contrast with the phasors technique, no approximations take place and the mapping is accurate. The dq0 models find extensive application in the modelling and analysis of fast transient power system phenomena. This technique is also a common way to proceed with the modelling of synchronous machine dynamic behaviour.

Through dq0 transformation, three-phase signals in the ABC reference frame are mapped to new quantities in a rotating dq0 reference frame. The definition of this transformation and its inverse is [10]:

$$T_{\theta}^{-1} = \frac{2}{3} \begin{bmatrix} \cos(\theta) & -\sin(\theta) & 1\\ \cos(\theta - \frac{2\pi}{3}) & -\sin(\theta - \frac{2\pi}{3}) & 1\\ \cos(\theta + \frac{2\pi}{3}) & -\sin(\theta + \frac{2\pi}{3}) & 1 \end{bmatrix}$$
 (2)

, where the angle  $\theta$  is the reference angle or the reference phase.

For 
$$x_{abc} = [x_a, x_b, x_c]^T$$
 and  $x_{dq0} = [x_d, x_q, x_0]^T$ :

$$x_{da0} = T_{\theta} x_{abc}$$
 , (3)

$$x_{abc} = Tx_{dq0}$$
 , (4)

, where the subscripts d, q, and 0 represent the direct, quadrature, and zero components respectively.

To implement this analysis with the Modelica language, the open-source library PowerSystems and its special features are utilised within INTEMA.grid. Custom sophisticated models have also been developed by



CERTH for various types of power plants (slack, PV or PQ) and their corresponding governor systems based on standardised international practices [22].

#### 10.4.2.2 EV battery

To proceed with the modelling of the EV battery at a satisfying representation level, certain aspects must be considered. Key operating variables such as cell and terminal voltage, state of charge, temperature, and injected or drawn current should be continuously calculated and controlled, so that their values always range in-between specific limits. This is important since technically inevitable configurations should be excluded from the final solution. To this end, the non-linearity of battery voltage as a function of battery state of charge (SoC), should be accounted for. This is because, when it comes to dynamic simulations over a significant period, neglecting this relationship with arbitrary simplifications, can result in large, accumulated errors in voltage and as a result in the power supplied or retrieved by the battery. This could lead to a significant error in the estimation of the actual available vehicle battery power at a certain time point, and therefore to misestimating the actual capability of injecting power to the grid through V2G technology.

Furthermore, since each EV battery pack consists of a unique arrangement of multiple battery cells connected in series and in parallel, it is essential that battery models are built at the cell level. The most widespread battery cell modelling technique that ensures a good trade-off between accuracy and computational complexity is the Equivalent Circuit Model (ECM) [23,24]. This is a key concept for reproducibility in an effective battery management system (BMS), in which high accuracy and minimum possible computational time must be ensured. The topology of an equivalent circuit with 2 RC branches is presented in Figure 25.

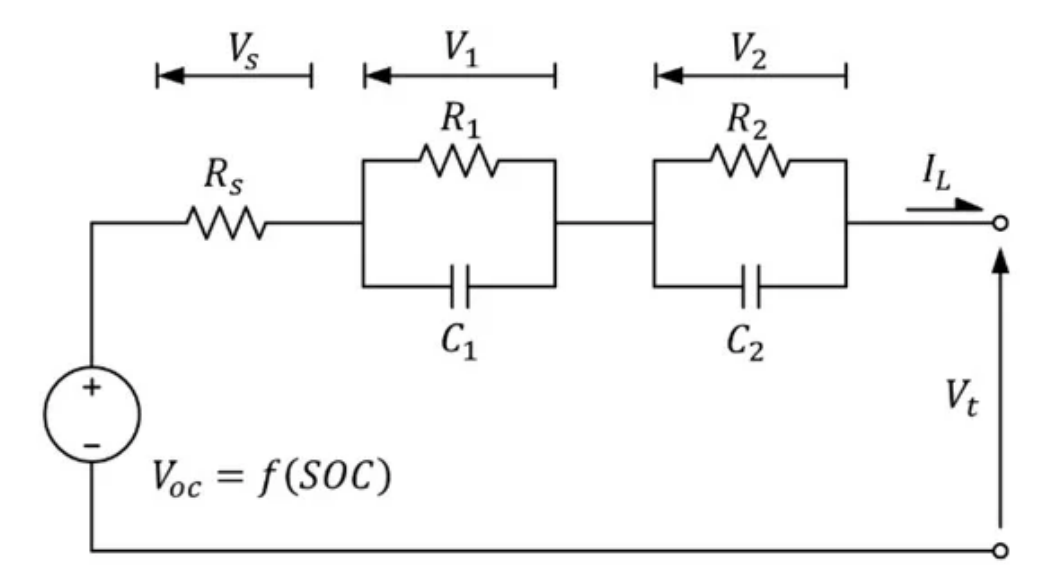


Figure 25: Schematic representation of the topology of an Equivalent Circuit Model with 2 RC branches [25]

ECM represents the complex internal electrochemical phenomena of the battery cell with an equivalent electric circuit. The voltage source of the circuit, usually named open-circuit voltage (denoted as  $V_{\text{oc}}$  in the figure circuit) corresponds to the available battery energy, whereas voltage drop across the series resistance (denoted as  $R_s$  in the circuit) is equivalent to the instantaneous voltage drop due to an applied load and RC branches (denoted as R1-C1 and R2-C2 in the circuit) introduce time constants to capture the voltage transient response connected with diffusion effects.



The graphical representation of the model of a single cell developed in Modelica within the Dymola user interface is presented in Figure 26. A variable voltage source model component is used to incorporate the open-circuit voltage whereas the components of a series resistance and 2 RC branches correspond to the  $R_s$  and  $R_1C_1$ ,  $R_2$ - $C_2$  circuit elements, respectively. SoC is continuously estimated based on the applied terminal current and available capacity varies depending on the cell temperature and whether a charging or discharging operation is underway. Heat is stored through a heat capacitor with a mass equal to the battery cell mass, whereas heat transfer with the surroundings takes place through the convection mechanism. The cooling load for keeping the temperature value between the desired levels is calculated through a PI controller. According to the array configuration of the single battery cells in the entire pack, the connections between cells are achieved. The model developed by CERTH has been thoroughly described in a recent journal publication [26].

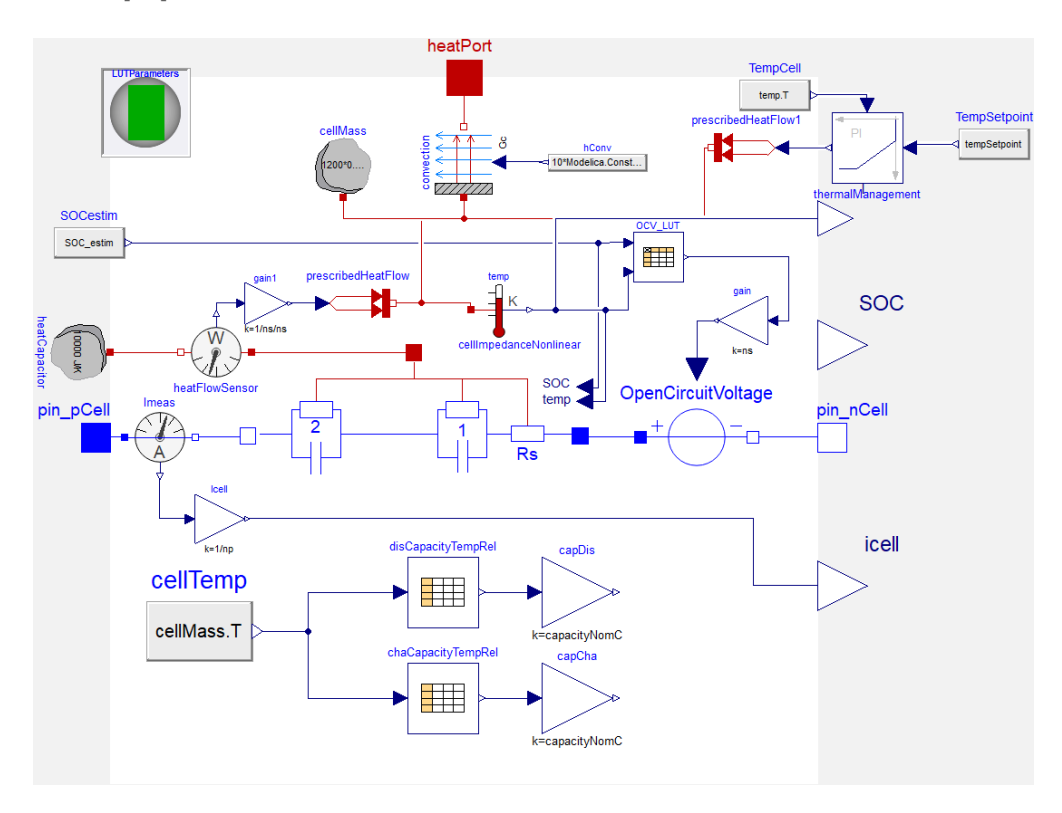


Figure 26: Graphical representation of the battery cell model developed in Modelica

A detailed presentation of the model components and equations together with the step-by-step process to extract the parameter datasets necessary for the simulations are available in the Annex. Regarding the retrieved parameter datasets, they can be used to accurately represent the operation of four (4) different battery cell chemistry types, namely the most widely used in EV applications. These chemistry types classified by the positive electrode material, are lithium-iron phosphate (LFP), lithium-manganese oxide (LMO), lithium-nickel cobalt aluminium oxide (NCA) and lithium-nickel manganese cobalt oxide (NMC). This important feature extends the model capability to be used to accurately describe a wide range of applications with different operating requirements (e.g. high-power or high-energy battery cells could be selected depending on the application). Model users can select the look-up table parameters between the 4 available chemistry types. An additional remark for future tool replication is that although the 4 considered chemistry types are sufficient for the scope of SCALE, the INTEMA modelling technique allows the extension of the model application to any particular battery parameter dataset and, hence, any cell chemistry type and specifications.



#### 10.4.2.3 Bidirectional V2G charger

Another key component in the grid system model development is the bidirectional V2G charger, coupling the DC side of the EV battery with the AC side of the grid. From a modelling perspective, the operation control of a battery energy storage system (BESS) is mainly governed by the operation control of the energy storage power converter of the BESS. BESS operation control can be classified as grid-connected, off-grid and dual mode (on-/off- grid) switching control. Grid-connected operation is the case of Utrecht's grid under study. An important requirement is that the model should be able to couple with the overall power system model, and hence be aligned with the dq0 representation introduced in 10.4.2.1.

Bidirectional AC/DC converters can be classified in various ways.

- According to the DC energy storage form to voltage-source or current-source,
- According to the number of phases to single-phase, three-phase or multi-phase circuit
- According to switching modulation to hard-switching or soft-switching modulation
- · According to the bridge circuit structure to half-bridge or full-bridge circuit
- According to the modulation level to two-level, three-level or multi-level circuit

A closed-loop PI modulation is adopted to realise the converter control. The purpose of the outer loop is to protect stability, while the inner loop is used to enhance system dynamic performance and ensure the limitation of current values for protection purposes. The output of the outer ring is the reference value of the inner ring input current. The current error signal is retrieved and a PI regulation to reduce mutation of current in the dynamic process is performed. After getting the voltage in dq0, an inverse transformation takes place to yield the voltage in the ABC coordinate system.

An ESS connected to the grid directly adopts the grid frequency and voltage, controlling the input and output power, the voltage on the DC side, or charging and discharging current. As mentioned above the ESS control is implemented with a dual closed loop. The inner loop controls the input and output current of the energy storage and the outer loop applies constant power (P/Q) control. This control mode aims to maintain the active (P) and reactive (Q) power of the ESS close to their reference values. The P/Q control block diagram can be seen in Figure 27.

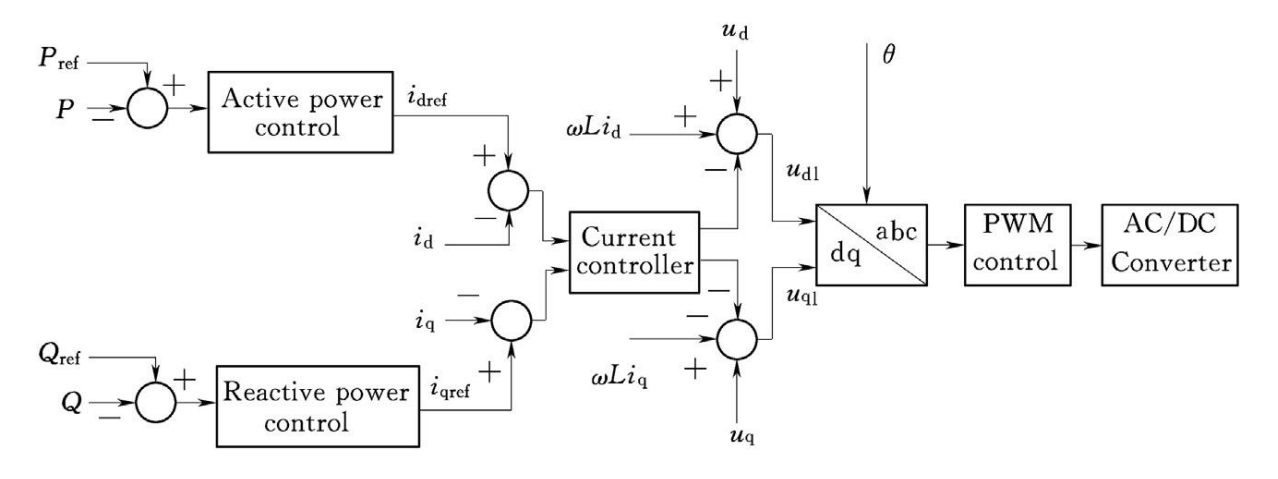


Figure 27: P/Q control block diagram of AC/DC converter [27]

P<sub>ref</sub> and Q<sub>ref</sub> are the power reference values, as provided by the calculations of the previous step where the chargers' optimal position is solved simultaneously with the OPF problem and P and Q are the power values as measured during the simulations. i<sub>dref</sub> and i<sub>gref</sub> are the reference values of the dq0 axis components of the



AC-side current.  $i_d$  and  $i_q$  are the measured values of the AC-side current dq0 axis components.  $u_d$  and  $u_q$  are the actual values of the inverter output voltage dq0 axis components.  $u_{d1}$  and  $u_{q1}$  are reference values of the inverter output voltage dq0 axis components. L is the AC-side coupling inductance and  $\theta$  is the initial phase angle of voltage.

The decoupled equations of inverter output power are:

$$\begin{cases} P = u_d i_d + u_q i_q \\ Q = u_d i_q - u_q i_d \end{cases}$$

Detailed documentation for this operation control technique can be found in [27].

The model, as developed in the Dymola user interface is presented in Figure 28.

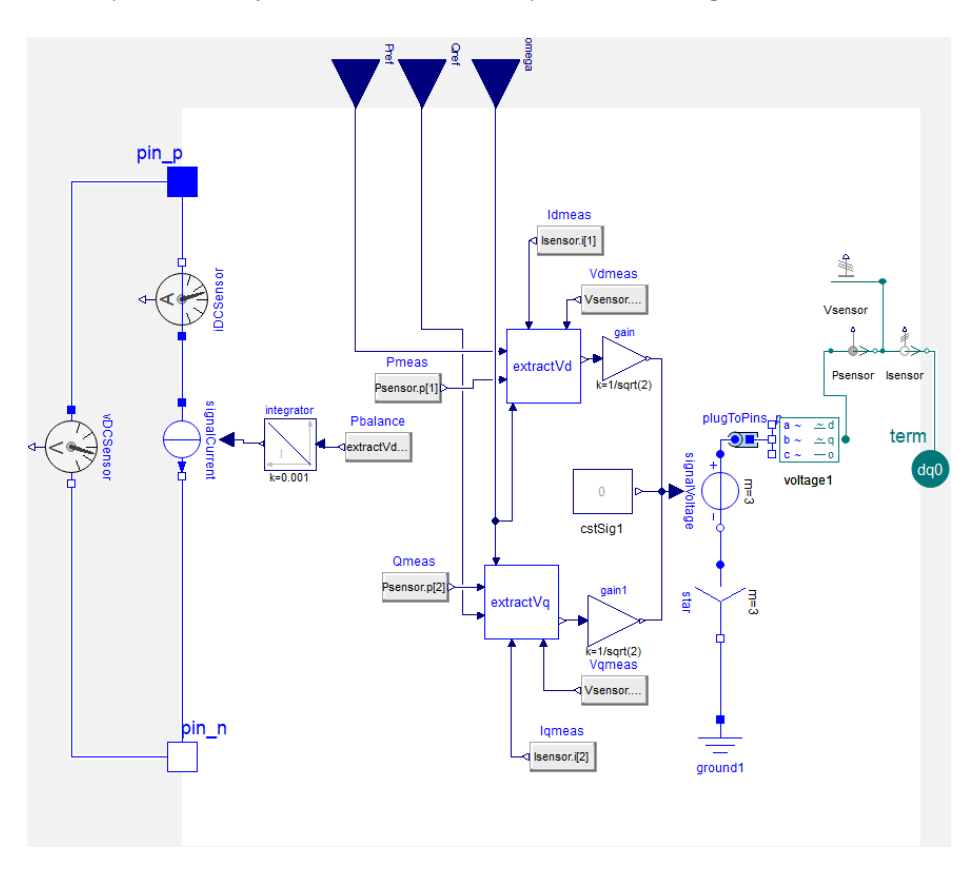


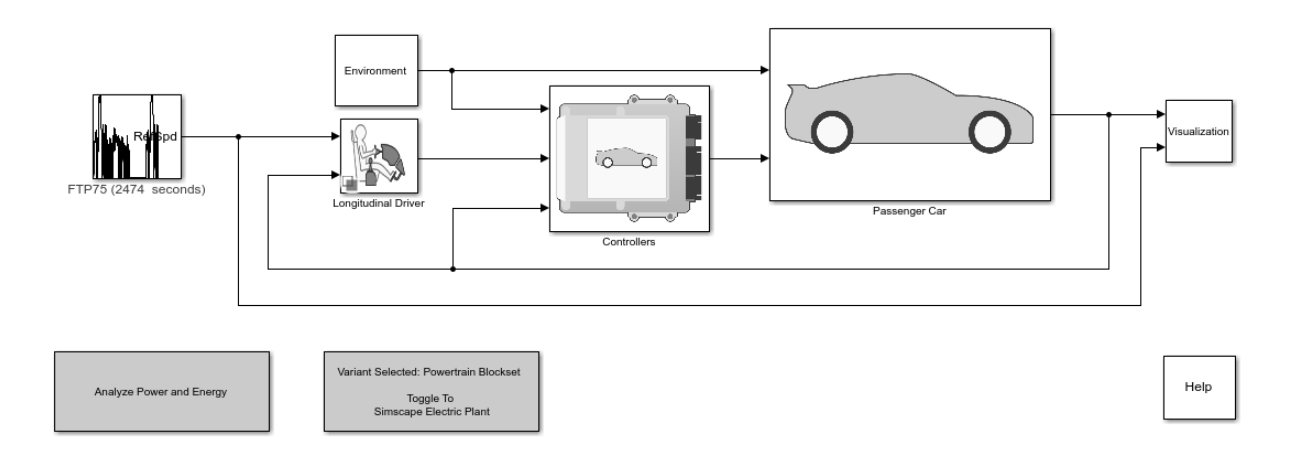
Figure 28: Model of EV AC/DC inverter in Dymola user interface

#### 10.4.2.4 EV application model for verification

To verify the SCALE's developed battery model, an EV simulation application has been selected as a test case, due to its operating conditions, characterised by intense load fluctuation in time and therefore highly transient response of battery quantities. In this report, the recently published and well-documented MATLAB/Simscape EV reference application [28] is selected as the software for benchmarking the CERTH's house-built one, developed for the scope of SCALE, among several available software solutions for EV simulation. Such include Simcenter AMESim [29] and AVL Cruise [30] among others. The selected application focuses on the simulation of a full EV energy system, taking into account all of its powertrain, drivetrain and control subsystems.



These include i) the driver's control actions to close the gap between the actual and the reference vehicle velocity, ii) the controllers of the battery management system (BMS) that ensure operation within allowed technical limits, iii) the power recovery through regenerative braking, iv) the EV powertrain including physical models of the battery pack (array of cells connected in series and in parallel) and v) the motor and the mechanical drivetrain of the vehicle. The US Environmental Protection Agency (EPA) Federal Test Procedure FTP75 driving cycle [31] has been used to import the velocity user profile. A representation of the system in the graphical environment of MATLAB Simulink is shown in Figure 29. The assumed velocity profile of FTP75 is depicted in Figure 30.



Copyright 2015-2023 The MathWorks, Inc.

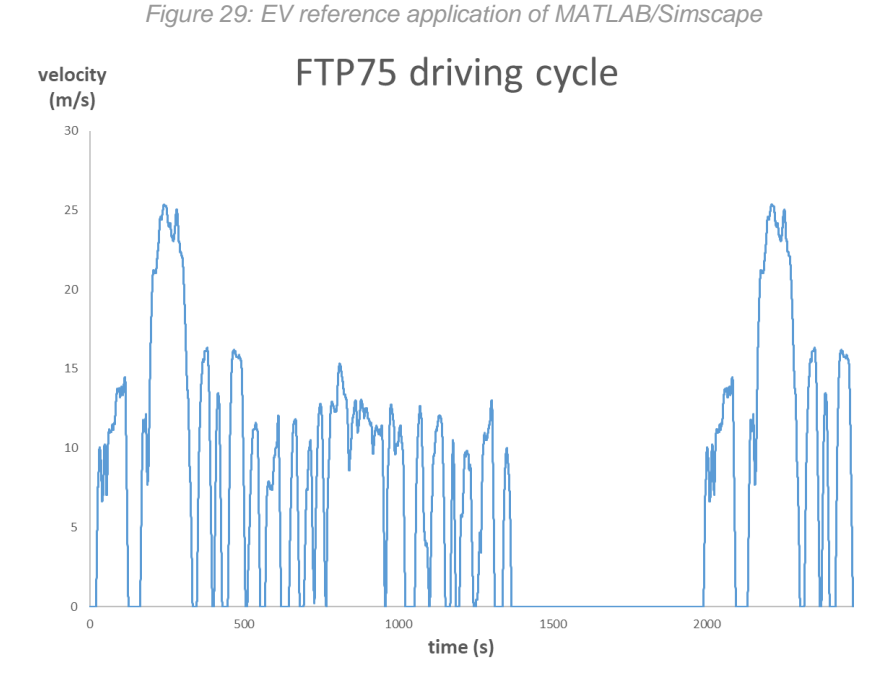


Figure 30: FTP75 driving cycle velocity profile

On top of the verification process, an additional outcome that could be considered as an added value to SCALE T2.6 activities is that the developed EV application could also be beneficial for the evaluation of EV charging strategies in terms of quantified vehicle energy performance since it also involves the more detailed



representation of EV batteries behaviour. This could provide better insight to SCALE stakeholders such as manufacturers of V2G chargers or EV users.

In the previous decade, a few Modelica open-source libraries have been developed, aiming to simulate vehicle performance. EHPT [32] and EVLibrary [33] are libraries specialising in EV modelling. In the scope of SCALE verification, a Modelica package library has been built by CERTH, including the model of the EV powertrain and drivetrain systems and all involved subcomponents (e.g. battery, motor, electric drive, vehicle dynamics, etc.). Certain models already developed in the EHPT library have been utilised to build the new library. This verification stage is capitalised in the development of INTEMA.EV, a new standalone EV simulation tool within CERTH's INTEMA suite of tools. All models developed by CERTH are described in the Annex. In Section 10.3, a comparison of the results extracted from the two software is presented in terms of verification. The results of this study have been presented in two journal publications [34,35].

#### 10.4.2.5 Utrecht's local distribution grid model

The afore-presented INTEMA models are utilised to perform the dynamic simulation of the power grid of the Floresstraat distribution network in Utrecht, with the inclusion of the charging infrastructure topology proposed in Section 10.3 as required for T2.6. Dynamic simulation of the proposed grid topology can provide positive feedback on system transient operation under variable conditions. Therefore, on top of the features of network congestion minimisation and mobility needs' satisfaction, the examination of the technical feasibility of the proposed topology of chargers' integration into the local power system is added to the Energy Planning Tool. The single-line diagram of the local grid status before SCALE, as provided by the City of Utrecht in the graphical environment of Powerfactory, is presented in Figure 31.

To proceed with the demonstration of the model results for Utrecht's local grid some necessary assumptions have been made. The complexity and nonlinearity of system subcomponents in an electrical grid can significantly increase simulation time intervals. Studying the entire local grid would result in longer simulation time without adding much value value to the demonstration described in this section. Therefore, it is considered outside the scope of SCALE T2.6. Instead, a smaller area of the local grid is studied, specifically the feeder line outlined in Figure 31.



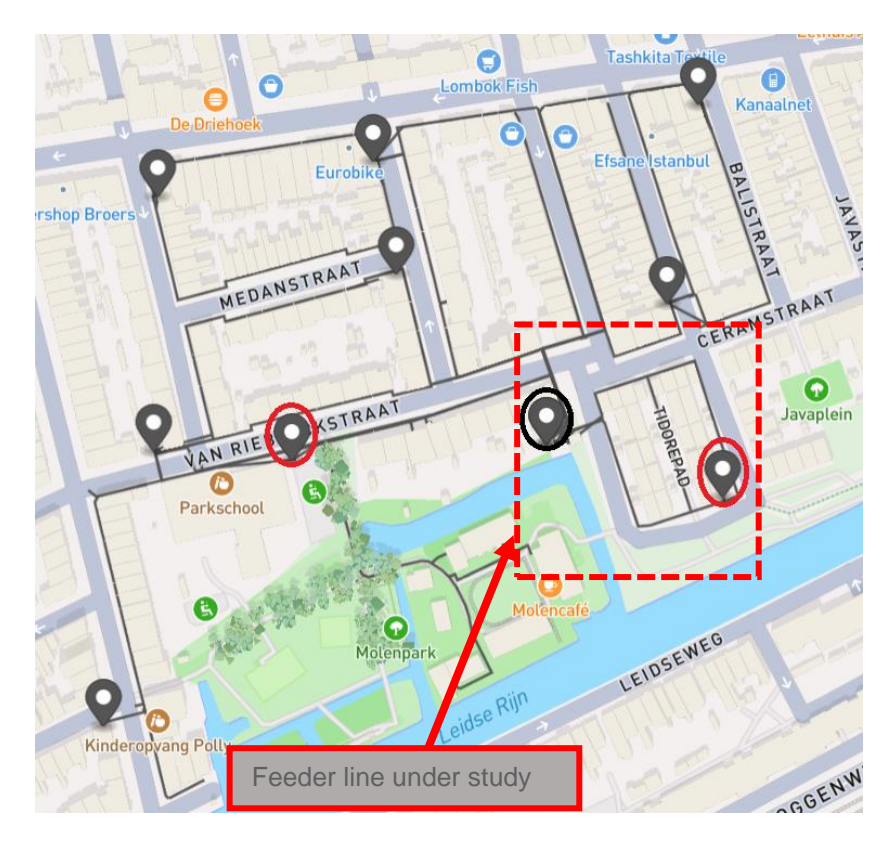


Figure 31: Line diagram of the Floresstraat distribution network under study. The feeder line selected for the simulations is outlined.

For the representation of the grid with the INTEMA.grid library models, the provided line diagrams are used. The methodology followed for the load consumption timeseries is:the nominal capacity of the 19 loads is multiplied with a normalised reference load distribution. A more detailed description of this assumption is also available in Section 10.3. Additional necessary input information about mobility and charging behaviour patterns and EV fleet characteristics (e.g. number of active vehicles, vehicle specifications, etc.) is given by the results of Section 10.3's optimization tool. At the moment, the simplification of a single motionless vehicle that is continuously connected at each proposed V2G point takes place since adding vehicle switching would add no valuable information for unwanted effects in the dynamic response of the grid or the battery.

Regarding the EVCI, all charger units have been assumed to be installed in the locations provided by the results of Section 10.3. Moreover, through the undergone OPF study the optimal dispatch schedule of the chargers over a 24-hour period is taken as input from Section 10.3 results. The INTEMA models of EV battery and bidirectional charger utilised for the grid simulations have already been described thoroughly in Section 10.4.2.

Combining all of the assumptions described above, the overall system representation can be seen in Figure 32.



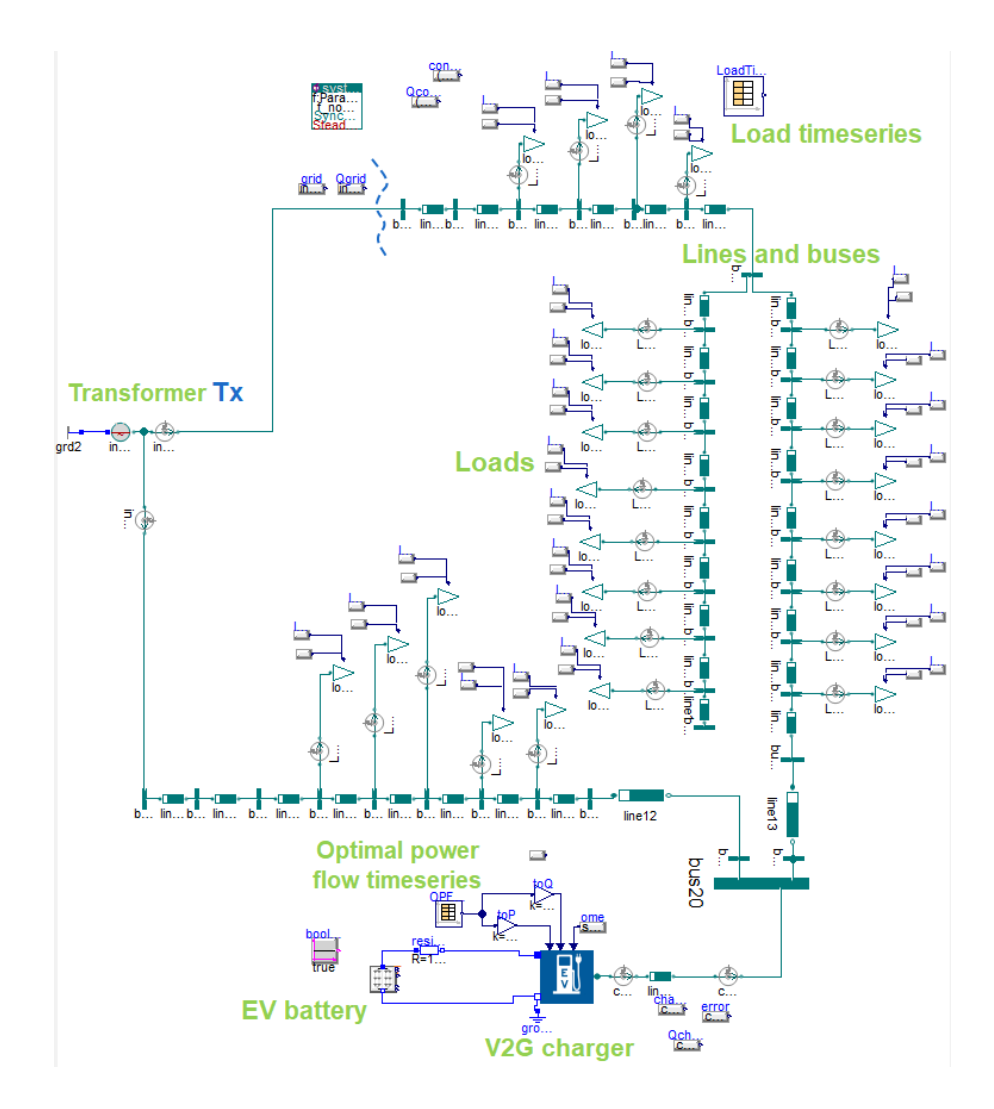


Figure 32: Graphical representation of the Floresstraat distribution network feeder line under study in the Dymola interface

The feeder line is connected to the local substation transformer at the highlighted transformer connection point. All loads and the V2G EV charger are connected to the feeder line and their contribution to the power balance is imported in the form of timeseries tables. The distribution system can be considered as ring.

# 10.4.3 Dynamic simulations of Utrecht local distribution grid

To stress-test the EVCI rollout topology proposed in Section 10.3, two (2) case studies have been simulated. The two case studies focus on testing the grid dynamic response, for the case of two different applied conditions, namely i) a long-term charging schedule and ii) a short-term disturbance. The system model of Utrecht's Floresstraat distribution network developed by CERTH as presented in Section 10.4.2.5 is used for the simulations.

#### 10.4.3.1 Case study A: 24-hour simulation

The first application involves the 24-hour simulation of the feeder line under study. The purpose is to examine the operation of EV chargers, i.e. the adjustment of inverter outputs to ensure that the active and reactive power injection or absorption takes place according to the setpoint values, as provided by the optimal dispatch schedule calculated and presented in Section 10.3. This practice could be thought of as equivalent



to checking the grid dynamic operation and responsive behaviour, after applying a day-ahead energy planning and, therefore, could give useful insights to DSOs about grid services provided by EVCI.

Utilising INTEMA.grid and Modelica advantageous features, quantities at all system points can be tracked and controlled. The results of the active power, given in Y-axis, supplied by the EV battery to the grid and the requested setpoint based on the optimal scheduling performed in Section 10.3 are presented in Figure 33. An accurate match between the setpoint curve and the simulation result is consistently succeeded.

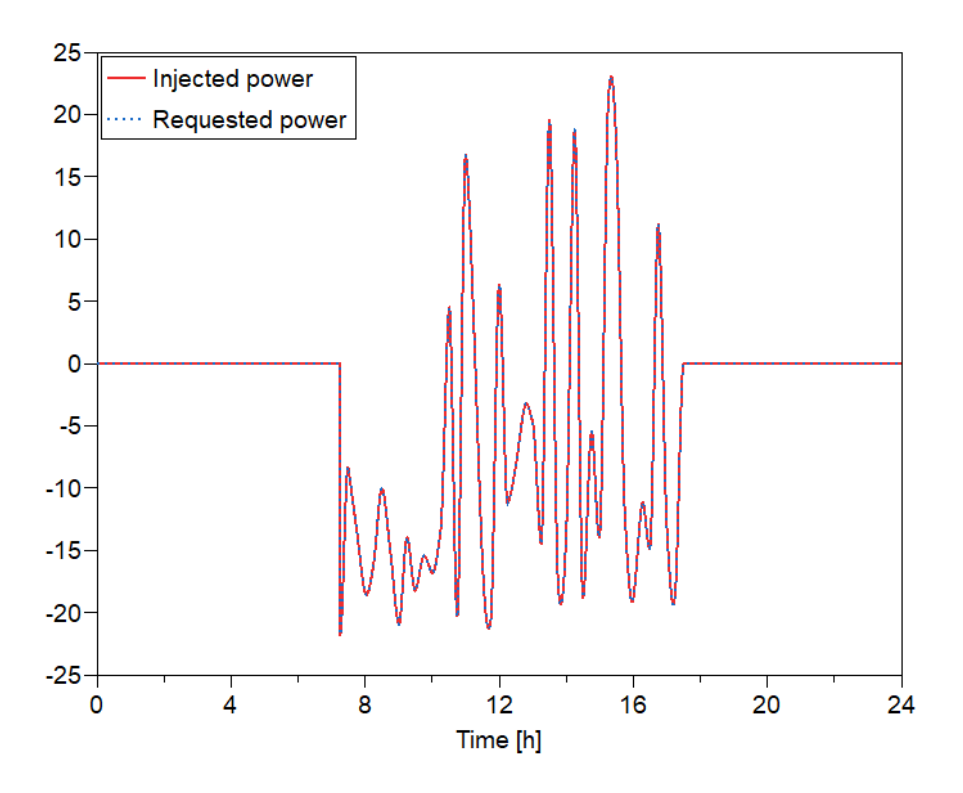


Figure 33: Requested and injected active power by V2G charger #2

As already mentioned, the power consumption of each line load is considered as a known input. The main modelling challenge is to ensure that the charging infrastructure control system is able to adjust and regulate the actual power to follow the desired optimal power contribution schedule proposed in Section 10.3. As can be seen, the EV chargers manage to inject or absorb the requested active power to or from the grid. The relevant error is plotted in Figure 34 with a maximum absolute value below 20 W, which equals to a neglegible percentage of the power requested.



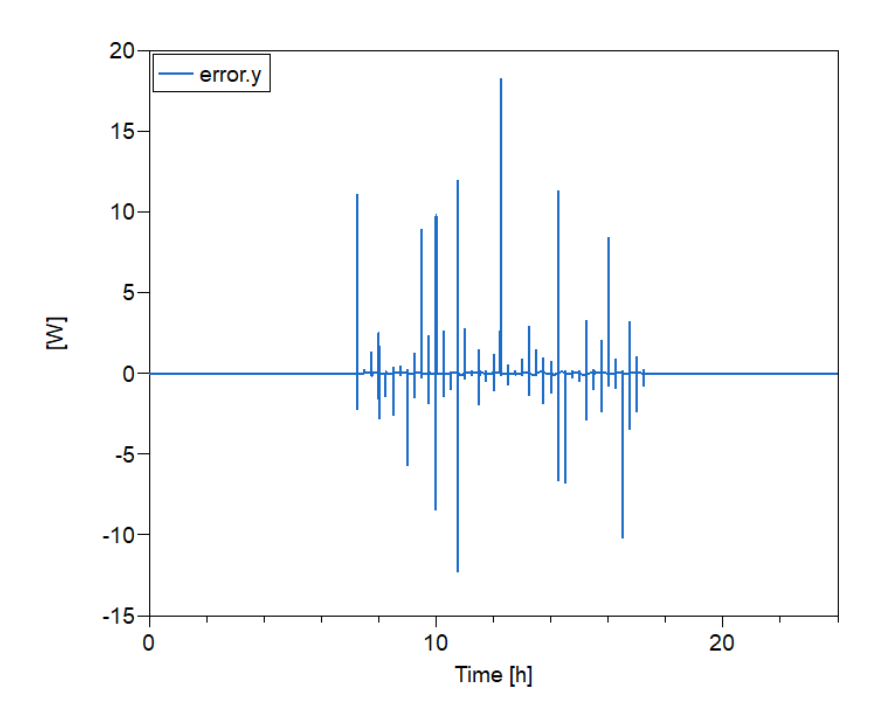


Figure 34: Error between requested and injected power by V2G charger

The evaluation of the technical feasibility of the proposed charging infrastructure topology and power dispatch schedule is based on the examination, of whether critical system quantities remain within accepted quality levels. These quantities include grid voltage and frequency and battery voltage or SoC. The evolution of voltage response at four different system points is monitored in Figure 35. The four system points correspond to buses 20, 345, 357 and 365 as previously numbered in the model presentation in Figure 32. The voltage response is kept at satisfying levels, between 0.9995 and 1.0005 pu, throughout the 24 hours of operation and, thus, system stability is achieved. Indeed, voltage fluctuation reaches its maximum level of 0.0004 per unit at bus 345 slightly after 4 am.



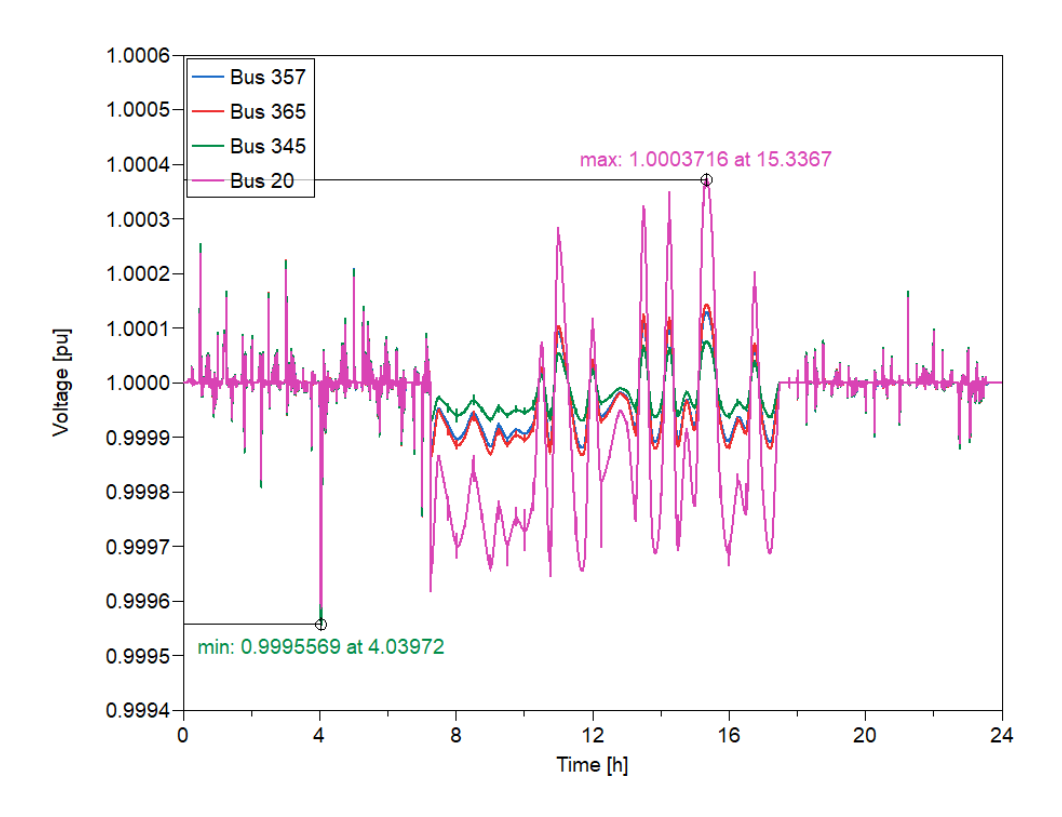


Figure 35: Voltage evolution at 4 system points, namely buses 20, 345, 357 and 365

The evolution of state of charge corresponds to the relevant result of the method described in Section 10.3, as plotted in Figure 36.

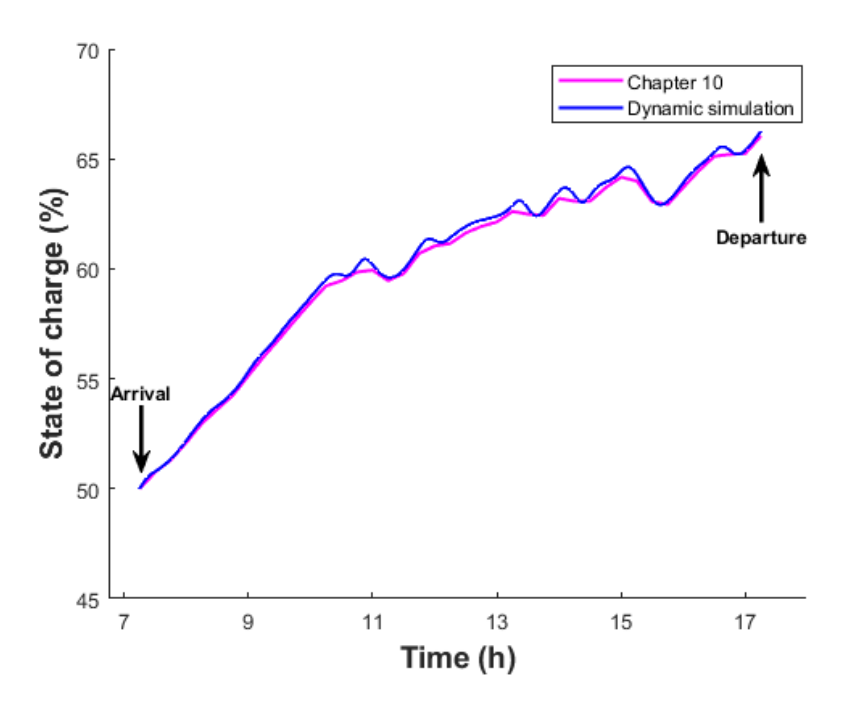


Figure 36: Evolution of EV battery state of charge (SoC) for both methods



The evolution of the injected current (negative for charging) of each of the installed charger is plotted in Figure 37. The current curve of the charger corresponds to the desired power exchange profile, which is the outcome of Section 9.3.

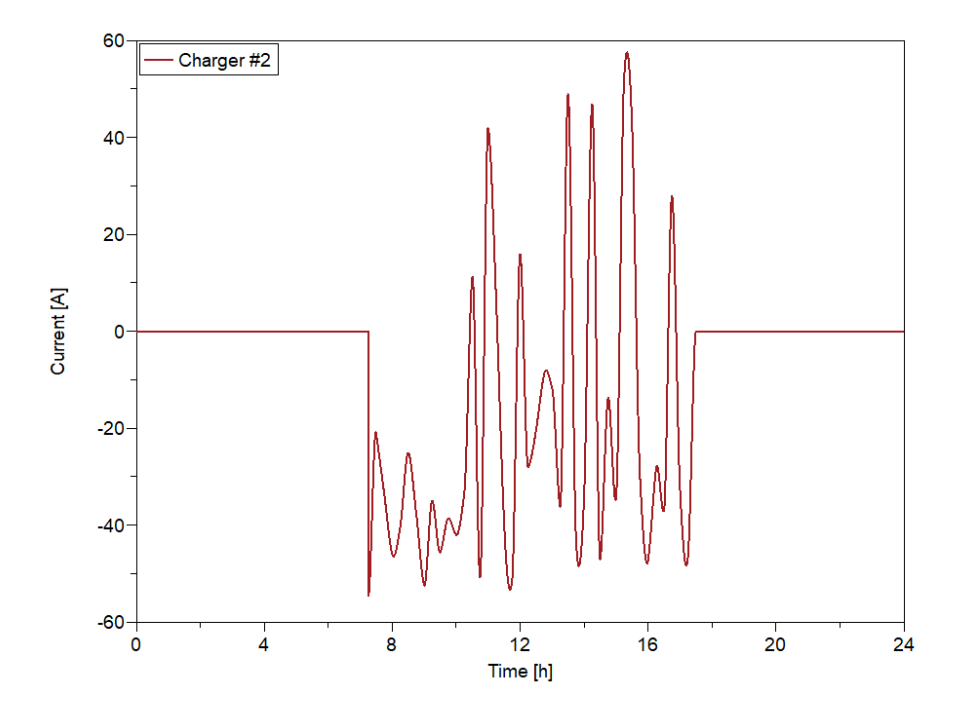


Figure 37: Current exchange between the V2G charger #2 and the local grid. Positive values correspond to current injection and negative values to vehicle charging

Next, the EV battery terminal voltage response during the proposed V2G operation, is examined in Figure 38.



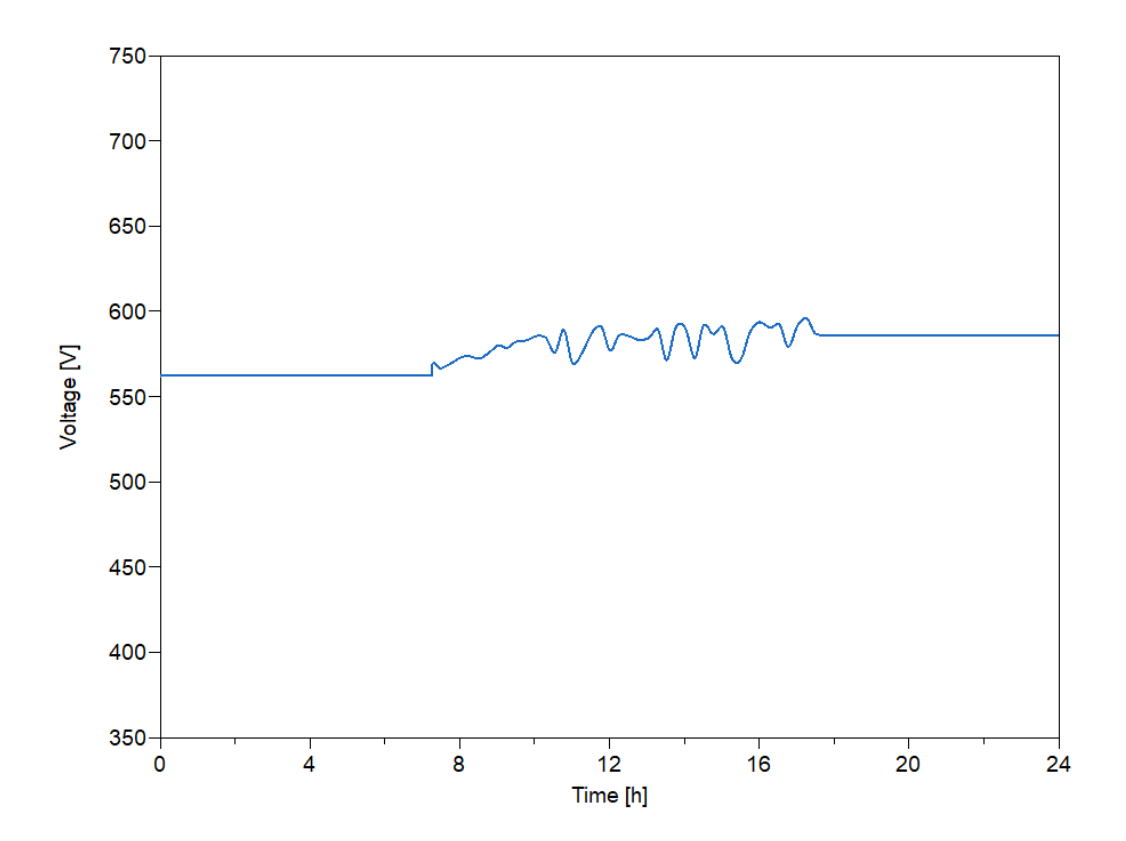


Figure 38: Battery terminal voltage evolution of the EV connected to Charger #2

The modelling technique followed makes sure that the evolution of battery SoC is monitored and, therefore, that the EV battery performance is within allowed operating limits. Moreover, the nonlinear voltage response to the requested current is clear in Figure 38. Voltage dependence on the varying SoC of the battery is taken into account with the modelling technique of ECM providing accurate information on the EV battery DC voltage. This is a significant factor that should be considered for charging infrastructure manufacturers and DSOs since grid planning should not neglect in any case the technical constraints implied by vehicle manufacturers to the EV users.

#### 10.4.3.2 Case study B: Short disturbance simulation

The second application of the local grid model focuses on the transient aspects of system operation. It primarily examines whether grid performance remains within acceptable limits under rapidly changing conditions. This is expected to be achieved through the EV charger inverter's response time, which is measured in milliseconds.

Power systems that rely heavily on renewable energy sources (RES) face unique challenges related to grid stability and inertia. Unlike conventional power plants, most RES sources lack inherent inertia and stability due to their intermittent nature. This absence of inertia makes the grid susceptible to i) sudden frequency fluctuations, ii) relay tripping leading to under-frequency load shedding (UFLS), iii) unintended outages, and even blackouts. In high RES penetration scenarios, continuous monitoring and control of grid frequency becomes critical to prevent these issues. To address these challenges, power system operators are implementing several strategies, including i) deploying energy storage systems, ii) adopting smart grid technologies, and iii) initiating demand response programs.



This case study aims to evaluate the responsiveness and effectiveness of EV batteries in managing demand fluctuations and facilitating the integration of intermittent RES into the electricity grid. Specifically, it assesses a scenario where RES accounts for 30% of the local grid. The system is analysed both with and without battery storage capacity, as depicted in Figure 39 and Figure 40.

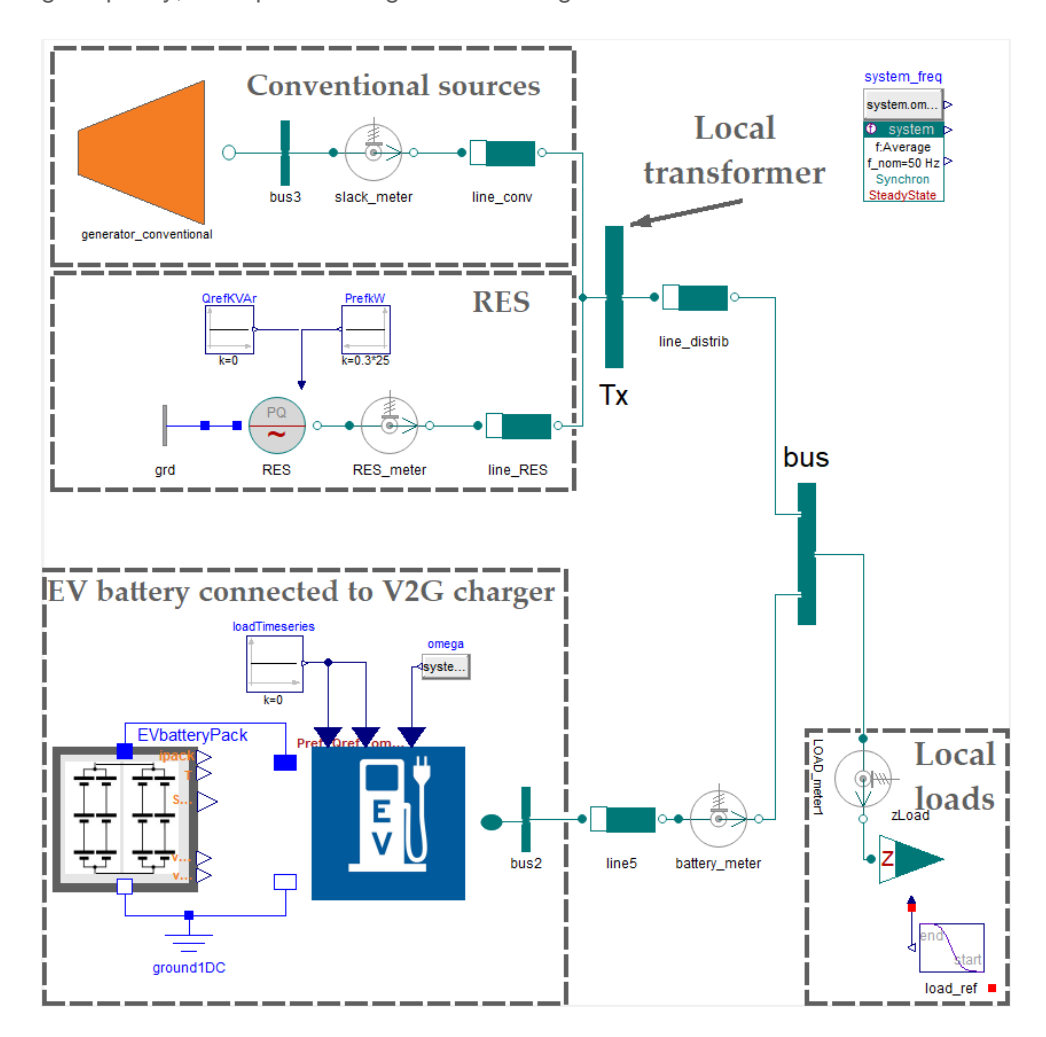


Figure 39: The local grid with an EV battery connected to the V2G charger



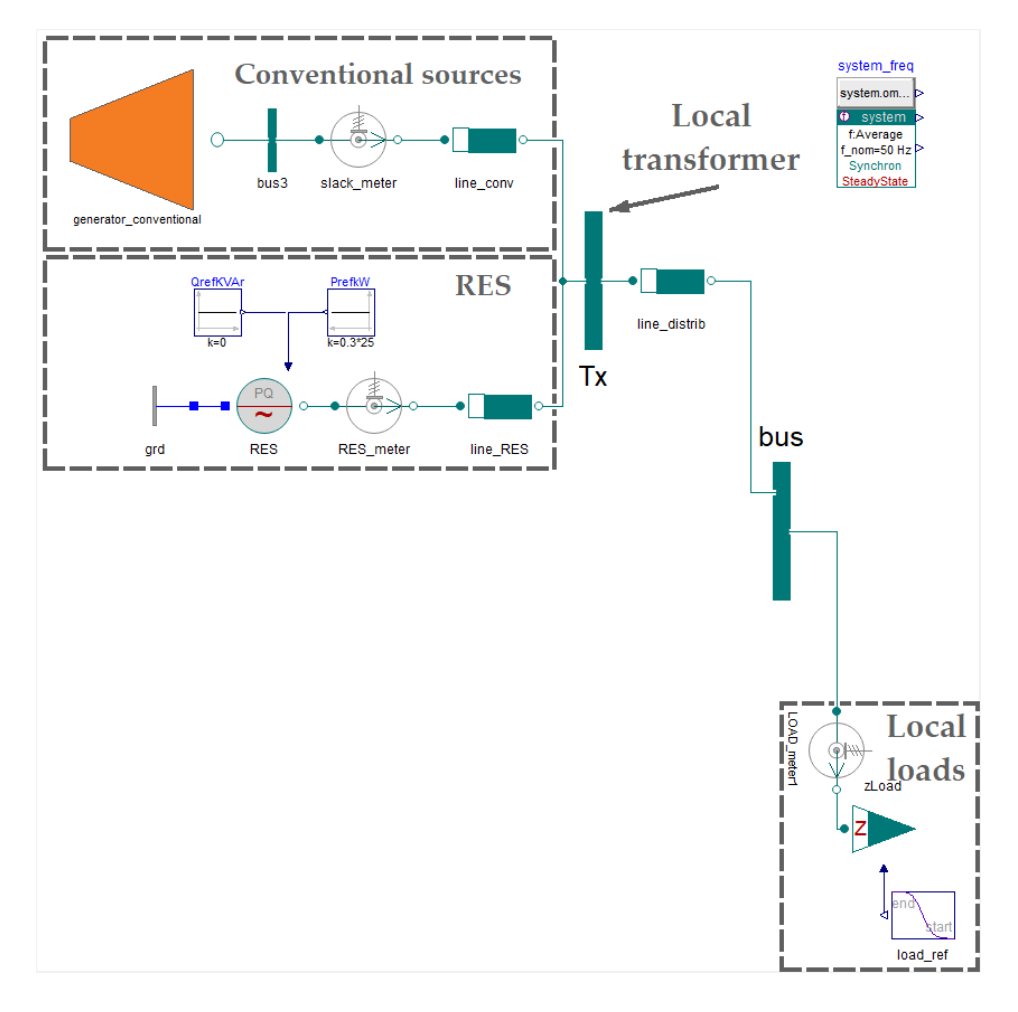


Figure 40: The local grid without an EV battery connected to the V2G charger

Given the study's specific focus on the Battery Energy Storage System's (BESS) contribution to grid stability, certain simplifying assumptions have been introduced, as outlined below. The power demand is modeled as a single aggregated load. In power systems, the balance between power demand and generation is closely tied to system frequency, which must be maintained at all times to ensure stability.

To analyze the system's ability to maintain frequency stability, a sudden load increase of 10% (0.1 per unit) is applied to the local load demand in both BESS and no-BESS scenarios, while the system frequency is monitored over a 30-second period. The load change is illustrated in Figure 41.



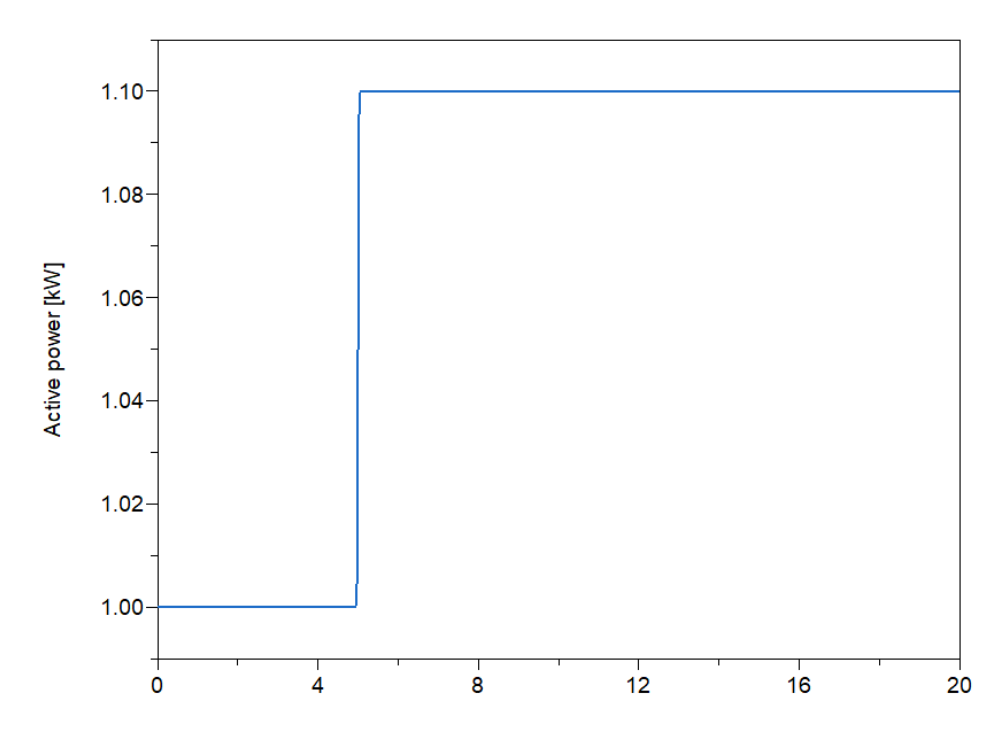


Figure 41: The load change assumed for this case study

The load change occurs instantaneously at t=5 s. A dip in frequency is expected due to the prompted instability between power demand and generation. The contribution of V2G to keeping the frequency at 50 Hz is studied and its importance to the system's stability is highlighted. V2G assists in frequency support until secondary response measures take action (10-30 minutes).

As presented in Figure 42, when examining both cases, with and without BESS, the new steady state frequency reaches a value of around 49.9996. The frequency with no storage available reaches a nadir of 49.9989 Hz. This nadir value changes to 49.9993 Hz with the contribution of BESS, which is 57% closer to the new steady state value. Nevertheless, it is clear that the frequency response of the BESS-supported grid approaches the steady state value faster, approximately 0.45 seconds after the disturbance at t=5.45 s, while without the BESS integration the new steady state is reached around 0.99 seconds later at t=5.99 s



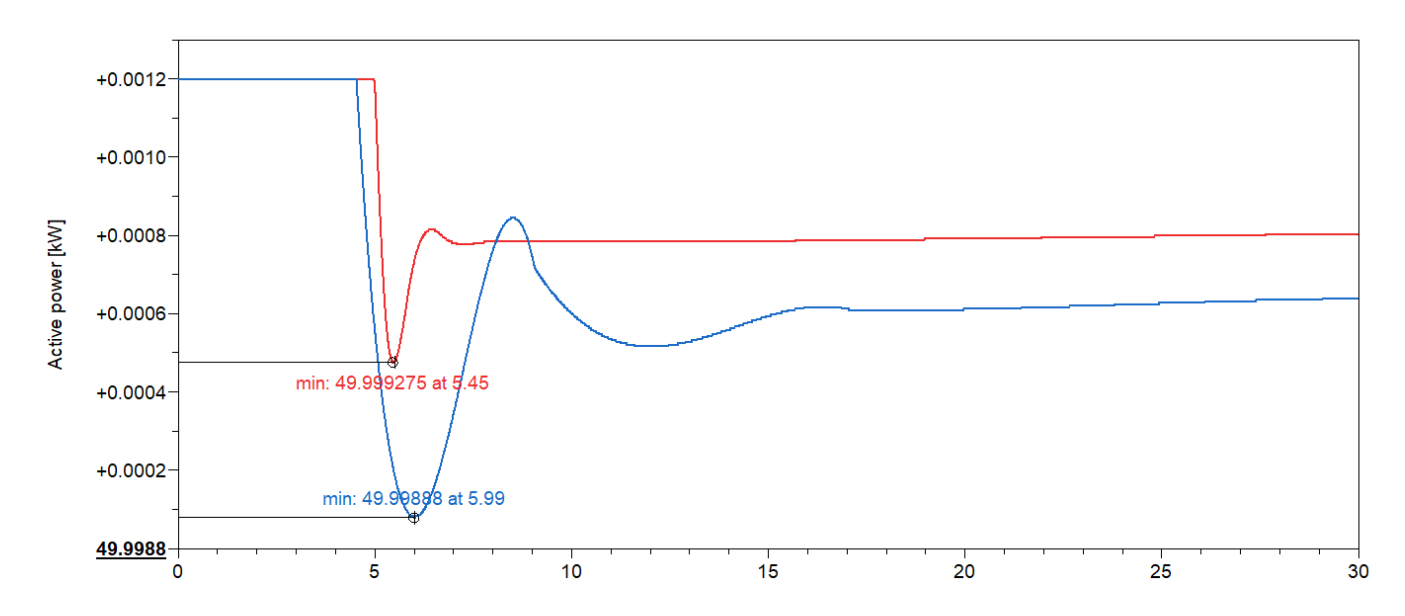


Figure 42: Frequency correction with the battery contribution



#### 10.5 Conclusions of Tool B

In the context of SCALE T2.6 relevant activity, CERTH has designed and applied a unified methodology to support the optimal integration of EVCI in the distribution grid of the Floresstraat neighbourhood in Utrecht. The approach followed aims to address the research challenges in the field of V2G planning by introducing a three-step methodology that is applied in the Floresstraat distribution grid. The methodology combines the EVCI position optimisation at the local grid while considering stochastic mobility and charging behaviour patterns, cost-minimising optimal power flow problem and transient system response through dynamic models for the stress-test of the proposed topology.

The advantageous features offered by the integrated approach, which can be considered as the added value of this tool, entail an advanced, beyond current state-of-the-art methodology for solving the problem of EVCI placement involving 3 aspects:

- Optimal EVCI location problem solving through specialised OPF python scripts
- Integration of mobility behaviour patterns
- Stress test of the proposed topology through dynamic component-based modelling

Taking into account the specifications of the Distribution Network, the Energy Planning Tool introduced two charging stations for the buses with the code names 31150 and 31170. Both of these charging stations have a nominal power of 22 kVA. As mentioned in the Section 10.3, the optimization process of the Energy Planning Tool calculates the operation of chargers for the V0G, V1G, and V2G scenarios. By comparing these three scenarios, it is found that the V2G scenario is the one that stresses the distribution transformer the least, and thus has the least impact on the overall stress of the distribution network. This is also confirmed by the results.

The dynamic simulation of the proposed topology verified the feasibility of the proposed topology of the V2G chargers. The optimal scheduling was followed accurately with a maximum active power deviation of less than 20 W, while the deviation of the voltage response from the nominal value remained below 0.0005 pu at the evaluated system nodes. The system's transient behaviour was also assessed following an applied disturbance (a sudden 10% load increase) and the integrated V2G technology demonstrated superior performance. Specifically, it achieved a lower nadir value, 57% closer to the new steady state value compared to the existing grid configuration, and a faster response, improving by 0.44 s.

As regards the exploitation plan of the models developed, an important outcome is the development of INTEMA.EV, a standalone EV simulator that is expected to be included in the broader CERTH's suite of tools, INTEMA [11].



# 11 References

- 1. Zhang, S.; Leung, K.-C. Joint Optimal Power Flow Routing and Vehicle-to-Grid Scheduling: Theory and Algorithms. IEEE Trans. Intell. Transp. Syst. 2022, 23, 499–512, doi:10.1109/TITS.2020.3012489.
- 2. Avramidis, I.I.; Capitanescu, F.; Deconinck, G. A Comprehensive Multi-Period Optimal Power Flow Framework for Smart LV Networks. IEEE Trans. Power Syst. 2021, 36, 3029–3041, doi:10.1109/TPWRS.2020.3040502.
- 3. Jadoun, V.K.; Sharma, N.; Jha, P.; S., J.N.; Malik, H.; Garcia Márquez, F.P. Optimal Scheduling of Dynamic Pricing Based V2G and G2V Operation in Microgrid Using Improved Elephant Herding Optimization. Sustainability 2021, 13, 7551, doi:10.3390/su13147551.
- 4. Kuhada, R.B.; Chauhan, A.P.; Pindoriya, N.M. Real-Time Simulation of V2G Operation for EV Battery. In Proceedings of the 2020 21st National Power Systems Conference (NPSC); IEEE: Gandhinagar, India, December 17 2020; pp. 1–6.
- 5. Yoo, Y.; Al-Shawesh, Y.; Tchagang, A. Coordinated Control Strategy and Validation of Vehicle-to-Grid for Frequency Control. Energies 2021, 14, 2530, doi:10.3390/en14092530.
- 6. Torabi, R.; Gomes, Á.; Morgado-Dias, F. Energy Transition on Islands with the Presence of Electric Vehicles: A Case Study for Porto Santo. Energies 2021, 14, 3439, doi:10.3390/en14123439.
- 7. Duić, N.; Da Graça Carvalho, M. Increasing Renewable Energy Sources in Island Energy Supply: Case Study Porto Santo. Renew. Sustain. Energy Rev. 2004, 8, 383–399, doi:10.1016/j.rser.2003.11.004.
- 8. Mele, E.; Natsis, A.; Ktena, A.; Manasis, C.; Assimakis, N. Electromobility and Flexibility Management on a Non-Interconnected Island. Energies 2021, 14, 1337, doi:10.3390/en14051337.
- 9. Ntomalis, S.; Iliadis, P.; Atsonios, K.; Nesiadis, A.; Nikolopoulos, N.; Grammelis, P. Dynamic Modeling and Simulation of Non-Interconnected Systems under High-RES Penetration: The Madeira Island Case. Energies 2020, 13, 5786, doi:10.3390/en13215786.
- 10. Levron, Y.; Belikov, J. Modeling Power Networks Using Dynamic Phasors in the Dq0 Reference Frame. Electr. Power Syst. Res. 2017, 144, 233–242, doi:10.1016/j.epsr.2016.11.024.
- 11. INTEMA Available online: https://intema.cperi.certh.gr/dashboard (accessed on 31 January 2024).
- 12. The Project. IANOS.
- 13. SMILE H2020 Available online: https://www.h2020smile.eu/ (accessed on 15 February 2022).
- 14. Fritzson, P. Principles of Object-Oriented Modeling and Simulation with Modelica 3.3: A Cyber-Physical Approach; IEEE, 2015;
- 15. WISTROeM, U. Dymola Dynamic Modeling Laboratory. 40.
- 16. Modelica/ModelicaStandardLibrary Available online: https://github.com/modelica/ModelicaStandardLibrary (accessed on 10 January 2024).
- 17. Franke, R.; Wiesmann, H. Flexible Modeling of Electrical Power Systems -- the Modelica PowerSystems Library.; March 10 2014; pp. 515–522.
- 18. Definition and Classification of Power System Stability IEEE/CIGRE Joint Task Force on Stability Terms and Definitions. IEEE Trans. Power Syst. 2004, 19, 1387–1401, doi:10.1109/TPWRS.2004.825981.
- 19. Machowski, J.; Lubosny, Z.; Bialek, J.W.; Bumby, J.R. Power System Dynamics: Stability and Control; Third edition.; John Wiley: Hoboken, NJ, USA, 2020; ISBN 978-1-119-52636-0.
- 20. Van Cutsem, T.; Vournas, C. Voltage Stability of Electric Power Systems; Power electronics and power systems; Springer: New York, 2008; ISBN 978-0-387-75535-9.
- 21. Wood, A.J.; Wollenberg, B.F.; Sheblé, G.B. Power Generation, Operation, and Control; Third edition.; Wiley-IEEE: Hoboken, New Jersey, 2013; ISBN 978-1-118-73391-2.
- 22. Power System Dynamic Performance Committee; Power System Stability Subcommittee; Task Force on Turbine-Governor Modeling Dynamic Models for Turbine-Governors in Power System Studies 2013.
- 23. Chen, M.; Rincon-Mora, G.A. Accurate Electrical Battery Model Capable of Predicting Runtime and I-V Performance. IEEE Trans. Energy Convers. 2006, 21, 504–511, doi:10.1109/TEC.2006.874229.



- 24. Huria, T.; Ceraolo, M.; Gazzarri, J.; Jackey, R. High Fidelity Electrical Model with Thermal Dependence for Characterization and Simulation of High Power Lithium Battery Cells. In Proceedings of the 2012 IEEE International Electric Vehicle Conference; IEEE: Greenville, SC, March 2012; pp. 1–8.
- 25. Poopanya, P.; Sivalertporn, K.; Phophongviwat, T. A Comparative Study on the Parameter Identification of an Equivalent Circuit Model for an Li-lon Battery Based on Different Discharge Tests. World Electr. Veh. J. 2022, 13, 50, doi:10.3390/wevj13030050.
- 26. Rotas, R.; Iliadis, P.; Nikolopoulos, N.; Tomboulides, A.; Kosmatopoulos, E. Dynamic Simulation and Performance Enhancement Analysis of a Renewable Driven Trigeneration System. Energies 2022, 15, 3688, doi:10.3390/en15103688.
- 27. Grid-Scale Energy Storage Systems and Applications; Wu, F.-B., Yang, B., Ye, J.-L., Eds.; Academic Press, an imprint of Elsevier: London; San Diego, CA, 2019; ISBN 978-0-12-815292-8.
- 28. EV Reference Application MATLAB & Simulink Available online: https://www.mathworks.com/help/autoblks/ug/electric-vehicle-reference-application.html (accessed on 24 January 2024).
- 29. Simcenter Amesim Available online: https://plm.sw.siemens.com/en-US/simcenter/systems-simulation/amesim/ (accessed on 24 January 2024).
- 30. AVL CRUISETM M | AVL Available online: https://www.avl.com/en/simulation-solutions/software-offering/simulation-tools-z/avl-cruise-m (accessed on 24 January 2024).
- 31. US EPA, O. EPA Federal Test Procedure (FTP) Available online: https://www.epa.gov/emission-standards-reference-guide/epa-federal-test-procedure-ftp (accessed on 24 January 2024).
- 32. Ceraolo, M. Max-Privato/EHPT Available online: https://github.com/max-privato/EHPT (accessed on 24 January 2024).
- 33. Dominguez-Jimenez, J.A.; Campillo, J. Object-Oriented Mathematical Modeling for Estimating Electric Vehicle's Range Using Modelica. In Advances in Computing; Serrano C., J.E., Martínez-Santos, J.C., Eds.; Communications in Computer and Information Science; Springer International Publishing: Cham, 2018; Vol. 885, pp. 444–458 ISBN 978-3-319-98997-6.
- 34. Rotas, R.; Iliadis, P.; Nikolopoulos, N.; Rakopoulos, D.; Tomboulides, A. Dynamic Battery Modeling for Electric Vehicle Applications. Batteries 2024, 10, 188, doi:10.3390/batteries10060188.
- 35. Rotas, R.; Iliadis, P.; Nikolopoulos, N.; Tomboulides, A. Evaluating Synergies between Electric Vehicles and Photovoltaics: A Comparative Study of Urban Environments. World Electr. Veh. J. 2024, 15, 397, doi:10.3390/wevj15090397.
- 36. Tran, M.-K.; DaCosta, A.; Mevawalla, A.; Panchal, S.; Fowler, M. Comparative Study of Equivalent Circuit Models Performance in Four Common Lithium-Ion Batteries: LFP, NMC, LMO, NCA. Batteries 2021, 7, 51, doi:10.3390/batteries7030051.
- 37. US EPA, O. Text Version of the Electric Vehicle Label Available online: https://www.epa.gov/fueleconomy/text-version-electric-vehicle-label (accessed on 26 January 2024).



# 12 Annex

# 12.1 List of figures

Figure 1: Forecast for the growth of EVs in the City of Utrecht. 'Midden scenario' is Dutch for Mid-Scenario. Others are the high scenario and low scenario. Source: ElaadNL
Figure 2: Expected rollout for charging infrastructure for the city of Utrecht by 2030. Source: City of Utrecht.
Figure 3: The considered city planning tool, with the scenario pane highlighted using a red frame18
Figure 4: The considered city planning tool, with the mapping pane highlighted using a red frame19
Figure 5: The considered city planning tool, with the simulation pane highlighted using a red frame20
Figure 6: Examples of figures for the yearly simulation function of the tool. The left graph shows a load duration curve for a specific object. The right graph shows the annual consumption/generation volumes of a specific object
Figure 7: Detailed simulation pane for one individual household.
Figure 8: Explanation of the Grid Aware Charging ("netbewust laden") system considered in this tool. The available capacity for EV charging (right plot) is based on the available grid capacity (left plot)24
Figure 9: The considered city district in this work. Different low-voltage grids are grouped using different colours
Figure 10: Examples of transformer load profiles for one example transformer for different EV ownership rates and EV charging strategies. The considered heat pump adoption rate is 100% for this figure. In this case, congestion problems occur both with smart charging and smart charging with V2G with an EV adoption rate of 1.0 EVs/household.
Figure 11: Transformer loading for all considered charging stations in the studied city district, considering different EV adoption rates, EV charging strategies and heat pump adoption rates
Figure 12: Transformer loading for all considered charging stations in the studied city district, considering different EV adoption rates, EV charging strategies, heat pump adoption rates and shares of EVs conducting smart charging.
Figure 13: View of Floresstraat distribution grid under study. The black circle is the Distribution Transformer
Figure 14: Overall methodology of the Energy Planning Tool designed and implemented by CERTH for T2.6
Figure 15: Probability distributions of workplace charging: Arrival peaks between 7-9 AM and departure between 4-6 PM, reflecting typical office hours
Figure 16: Communication between Pymoo and Pandapower



Figure 17: Floresstraat Distribution Grid, the pins indicate the grid's buses and the black circle is the bus wi the Distribution Transformer	
Figure 18: Monthly consumptions4	41
Figure 19: January 2022 Daily Consumptions	42
Figure 20: Total Power Demand of the Grid	43
Figure 21: Floresstraat Distribution Grid after the introduction of the EV charging stations. The red circle indicate the buses where the EV charging stations are installed	
Figure 22: Transformer Loading Percentage	45
Figure 23: State of Charge of EV Battery during V2G operation	45
Figure 24: Key outputs of INTEMA.grid dynamic models classified by potential interested parties	46
Figure 25: Schematic representation of the topology of an Equivalent Circuit Model with 2 RC branches [2	
Figure 26: Graphical representation of the battery cell model developed in Modelica	49
Figure 27: P/Q control block diagram of AC/DC converter [27]	50
Figure 28: Model of EV AC/DC inverter in Dymola user interface	51
Figure 29: EV reference application of MATLAB/Simscape	52
Figure 30: FTP75 driving cycle velocity profile	52
Figure 31: Line diagram of the Floresstraat distribution network under study. The feeder line selected for the simulations is outlined	
Figure 32: Graphical representation of the Floresstraat distribution network feeder line under study in the Dymola interface	
Figure 33: Requested and injected active power by V2G charger #2	56
Figure 34: Error between requested and injected power by V2G charger	57
Figure 35: Voltage evolution at 4 system points, namely buses 20, 345, 357 and 365	58
Figure 36: Evolution of EV battery state of charge (SoC) for both methods	58
Figure 37: Current exchange between the V2G charger #2 and the local grid. Positive values correspond current injection and negative values to vehicle charging	
Figure 38: Battery terminal voltage evolution of the EV connected to Charger #2	60
Figure 39: The local grid with an EV battery connected to the V2G charger	61



Figure 40: The local grid without an EV battery connected to the V2G charger
Figure 41: The load change assumed for this case study63
Figure 42: Frequency correction with the battery contribution64
Figure 44: SOC-OCV curves for each lithium-ion battery chemistry tested. (a) LFP, (b) NMC, (c) LMO, and (d) NCA [36]
Figure 45: System-level model of a fully electric vehicle INTEMA.EV application
Figure 46: Driver block in Dymola user interface
Figure 47: Powertrain Control Module block in Dymola user interface
Figure 48: EV motor efficiency map used for the simulations
Figure 49: Model of available regenerative torque and brake command in the Dymola user interface78
Figure 50: Overall powertrain block79
Figure 51: Motor torque - speed curve used for the simulations80
Figure 52: Simplified drivetrain model in MATLAB Simulink environment80
Figure 53: Drivetrain model developed in Dymola user interface8
Figure 54: Comparison of output results between MATLAB and Modelica. Simulation velocity of both software against FTP75 velocity profile
Figure 55: Comparison of output results between MATLAB and Modelica. The error between the velocity results of both software and the FTP75 velocity profile
Figure 56: Comparison of battery pack current results between MATLAB and Modelica. Positive for charge and negative for discharge
Figure 57: Comparison of power in battery pack terminals between MATLAB and Modelica. Positive for charge and negative for discharge
Figure 58: Comparison of state-of-charge (SoC) of battery pack results between MATLAB and Modelica .84
Figure 59: Comparison of battery pack voltage results between MATLAB and Modelica86
Figure 60: Comparison of output results between MATLAB and Modelica. Torque supplied by the EV moto in both software
Figure 61: Comparison of EV motor rotational speed results between MATLAB and Modelica8
Figure 62: Comparison of EV fuel economy results between MATLAB and Modelica88
Figure 63: Comparison of EV brake force results between MATLAB and Modelica



Figure 64: Comparison of the sum of drag and friction forces applied to the EV results between MATI Modelica.	
Figure 65: Overview of the visualization tool	89
Figure 66: Visibility control button, toggle buses, PVs and lasso tool.	90
Figure 67: Playback and Optimisation tool buttons.	91
Figure 68: Line highlight using the map selection.	92
Figure 69: Line highlight using the table button.	92
Figure 70: Lasso tool utilization.	93
Figure 71: Map legend showing for the line loading and bus voltage.	93
Figure 72: Download CSV button utilization.	94
12.2 List of tables	
Table 1: Cell specifications for each chemistry [36]	72
Table 2: List of parameter values for 4 different Li-ion cell chemistry types [36]	74
Table 3: Parameters used for the verification of INTEMA.EV	82

# 12.3 Li-ion battery cell dynamic model

A set of 6 circuit parameters, namely open-circuit voltage ( $V_{oc}$ ), series resistance ( $R_s$ ) and two pairs of RC branches ( $R_1$ ,  $C_1$ ,  $R_2$ ,  $C_2$ ), is extracted from recursive data fitting to experimental measurements and allows the representation of a battery cell as an equivalent electric circuit, considering its unique manufacturing identity, i.e. chemistry, capacity and geometry. After the stage of the parameter extraction, the values of these parameters are stored in two-dimensional (2D) look-up tables that incorporate their nonlinear variation depending on the levels of SoC and operating temperature. This model allows accurate prediction of battery cell terminal voltage without diving into complex electrochemical phenomena or time-consuming and sophisticated measurements.

The equation set of the 2-RC ECM is as follows:

$$SoC=SoC(0)-\frac{\int_{0}^{t}I_{L}dt}{C_{available}}$$
 
$$V_{s}=I_{L}\cdot R_{s}$$
 
$$I_{C_{1}}=C_{1}\cdot \frac{dV_{1}}{dt}$$



$$I_{C_2} = C_2 \cdot \frac{dV_2}{dt}$$

 $V_{OC} = f(SoC,T)$ 

 $R_s = f(SoC,T)$ 

 $R_1=f(SoC,T)$ 

 $C_1 = f(SoC,T)$ 

 $R_2=f(SoC,T)$ 

 $C_2=f(SoC,T)$ 

 $V_{t} = V_{OC} - V_{s} - V_{1} - V_{2}$ 

Characterization tests may include (i) the capacity test; (ii) the pulse discharge test; and (iii) the hybrid pulse power characterization (HPPC) test. The battery cell is discharged through constant current pulses at certain SoC level points (e.g. every 10%) after successive intermittent periods of rest. Voltage response is monitored and the measurements are utilised for parameter fitting. A detailed description of the parameterisation process through experimental measurements is available in [26]. Tran et al. [36] have recently published the parameter datasets extracted from measurements of four different lithium-ion battery chemistry types. An important aspect covered by this research work is that these cells refer to all 4 most common chemistry types of battery cells that are being found in EV applications. This is important for the reproduction of the model of most types of EV batteries. These chemistry types classified by the positive electrode material, are lithium-iron phosphate (LFP), lithium-manganese oxide (LMO), lithium-nickel cobalt aluminium oxide (NCA) and lithium-nickel manganese cobalt oxide (NMC). The research work also includes the validation of the 4 battery models after the application of certain current profiles.

The specifications of the four cells are listed in Table 1.

Chemistry	Manufacturer	Cell name	Nominal capacity (mAh)	Nominal voltage (V)	Voltage range (V)
LMO	EFEST	IMR18650V1	2600	3.70	2.50-4.20
LFP	K2 Energy Solutions, Inc.	LFP26650P	2600	3.20	2.00–3.65
NMC	Samsung SDI	INR18650-20S	2000	3.60	2.50-4.20
NCA	Panasonic	NCR18650B	3200	3.60	2.50-4.20

Table 1: Cell specifications for each chemistry [36]

The OCV-SOC curves for each lithium-ion battery chemistry exported from the parameterisation process are plotted in Figure 43.



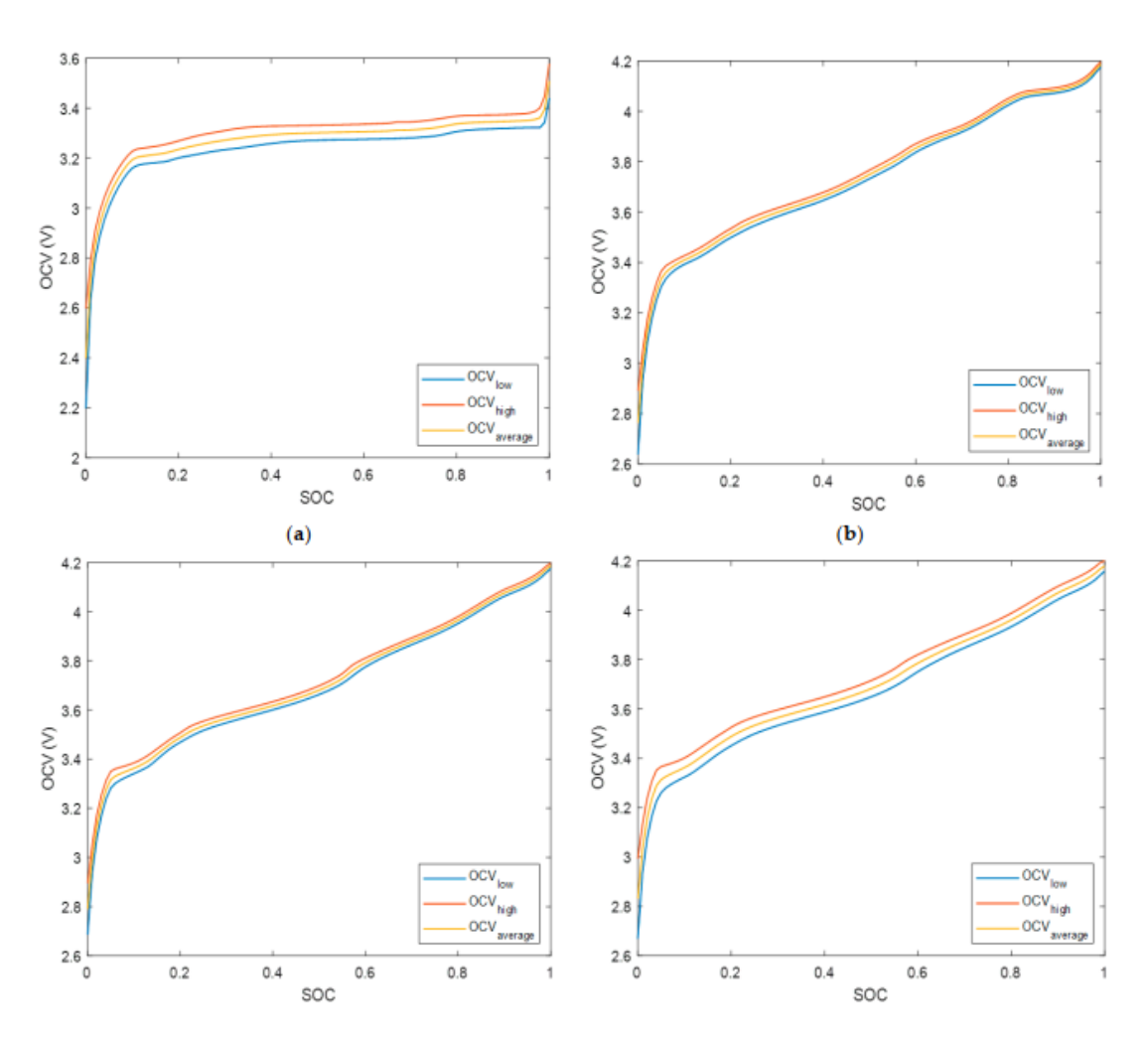


Figure 43: SOC-OCV curves for each lithium-ion battery chemistry tested. (a) LFP, (b) NMC, (c) LMO, and (d) NCA [36] The values of the lookup tables of the parameter datasets that are used in this study are listed in Table 2.

Chemistry type: Li-ion NMC					Chemistry type: Li-ion NCA						
SOC	R0 (Ω)	R1 (Ω)	C1 (F)	R2 (Ω)	C2 (F)	SOC	R0 (Ω)	R1 (Ω)	C1 (F)	R2 (Ω)	C2 (F)
0.9	0.0619	0.115	2206.02	0.0078	965.1	0.9	0.1325	0.0498	747.54	0.0096	639.61
0.8	0.0605	0.0854	2237.54	0.0056	1224.73	0.8	0.107	0.0272	982.5	0.0076	746.24
0.7	0.063	0.0511	2076.67	0.0048	1098.68	0.7	0.1042	0.0272	1128.74	0.0077	788.39
0.6	0.0619	0.046	2098.65	0.0049	1102.26	0.6	0.104	0.0275	1161.67	0.0077	791.77
0.5	0.0599	0.0389	1902.48	0.0045	884.1	0.5	0.1024	0.0271	1131.4	0.0078	789.73
0.4	0.06	0.1139	1395.74	0.0067	855.04	0.4	0.1023	0.039	929.76	0.0078	613.48



0.3	0.0598	0.1017	1852.54	0.0094	794.67	0.3	0.102	0.0315	766.53	0.0105	575.44	
0.2	0.0601	0.0942	2310.05	0.0099	758.97	0.2	0.1016	0.0302	734.1	0.0102	594.41	
0.1	0.0586	0.022	2254.18	0.0058	671.31	0.1	0.1063	0.0303	726.32	0.0099	636.78	
Chem	Chemistry type: Li-ion LMO					Chemistry type: Li-ion LFP						
SOC	R0 (Ω)	R1 (Ω)	C1 (F)	R2 (Ω)	C2 (F)	SOC	R0 (Ω)	R1 (Ω)	C1 (F)	R2 (Ω)	C2 (F)	
0.9	0.051	0.0884	1144.14	0.0136	315.48	0.9	0.0287	0.1047	754.39	0.0164	214.49	
0.8	0.0426	0.0494	1690.6	0.004	1036.82	0.8	0.0268	0.0539	834.83	0.0118	202.02	
0.7	0.0413	0.0472	1848.58	0.0036	1258.78	0.7	0.0257	0.0402	836.13	0.0094	210.55	
0.6	0.0405	0.0332	1805.97	0.0031	1074.47	0.6	0.0253	0.0373	863.25	0.0078	238.12	
0.5	0.0402	0.0362	1744.5	0.0033	981.4	0.5	0.0248	0.0315	887.06	0.0067	271.69	
0.4	0.0411	0.0808	1017.97	0.0044	668.99	0.4	0.0247	0.0311	935.5	0.0061	321.02	
0.3	0.0417	0.0912	1488.5	0.0079	911.13	0.3	0.0242	0.0284	962.9	0.0055	355.45	
0.2	0.041	0.0919	1384.18	0.0062	776.83	0.2	0.237	0.0361	967.72	0.0052	420.79	
0.1	0.0417	0.1061	1251.12	0.0078	846.01	0.1	0.0228	0.0278	1011.76	0.0047	456.43	

Table 2: List of parameter values for 4 different Li-ion cell chemistry types [36]

# 12.4 EV powertrain dynamic model for verification

# 12.4.1 System-level model

The system-level model of the INTEMA.EV application is presented in Figure 44. Based on the input velocity profile (FTP75 standard for the current application) controllers actuate on the EV powertrain, which in turn transfers the required power to the vehicle drivetrain. Considering that the interaction of mechanical parts is of low value for the scope of the current study, the sophisticated MATLAB drivetrain model is replaced with a simplified one developed by CERTH in Simscape. The simplified model is presented in more detail in the relevant subsection below.



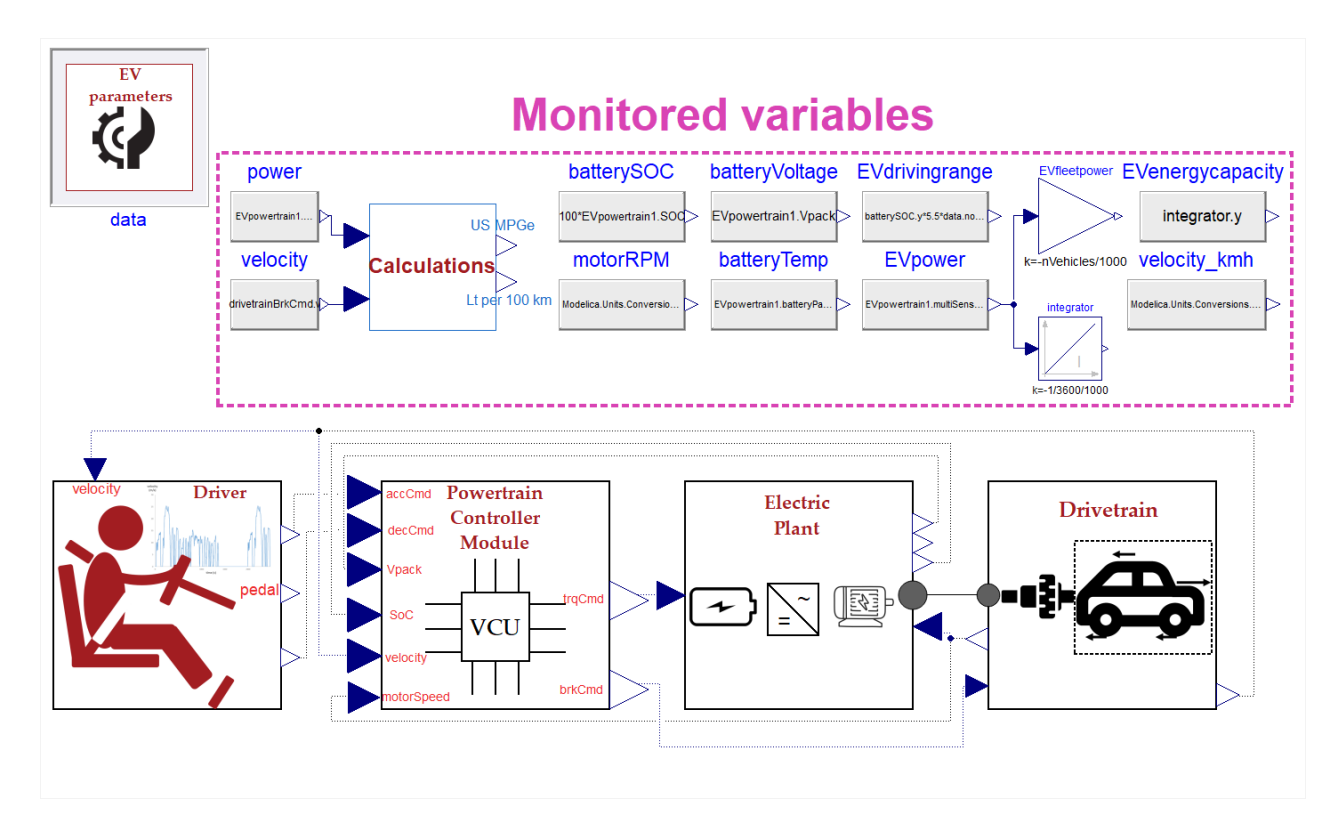


Figure 44: System-level model of a fully electric vehicle INTEMA.EV application

#### 12.4.2 Driver block

In this paragraph, the model of the driver's control actions is presented in Figure 45 described. Through a PI controller, a normalised signal of the pedal position command is adjusted to minimise the error between the reference signal (driving cycle velocity profile) and the measured velocity of the vehicle body. These signal values range from -1 to 0 when decelerating and from 0 to 1 when accelerating.

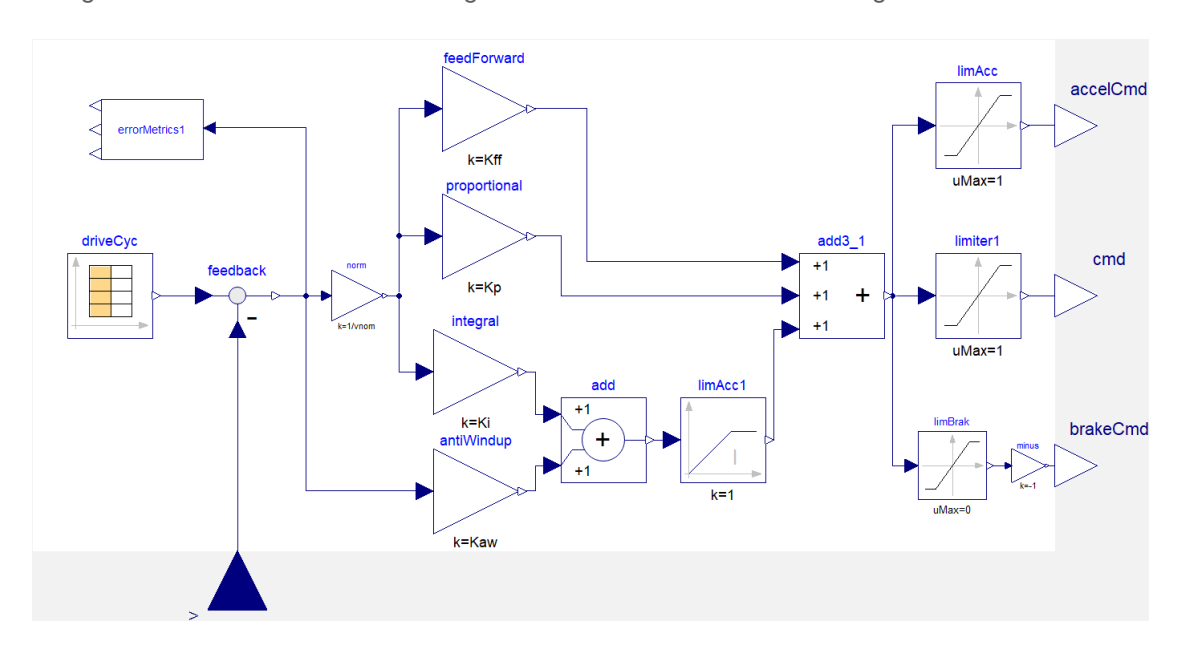


Figure 45: Driver block in Dymola user interface



#### 12.4.3 Powertrain Control Module block

The Powertrain Control Module (PCM) is the operation control centre of the EV. Based on the desired pedal position, which is received as input from the Driver block, the torque that should be applied by the motor with respect to the operating limits is produced as the output. Intermediate blocks are designed to limit discharge or charge power according to SoC and current limits and to arbitrate torque according to the wheel's rotational speed. The model block is presented in Figure 46.

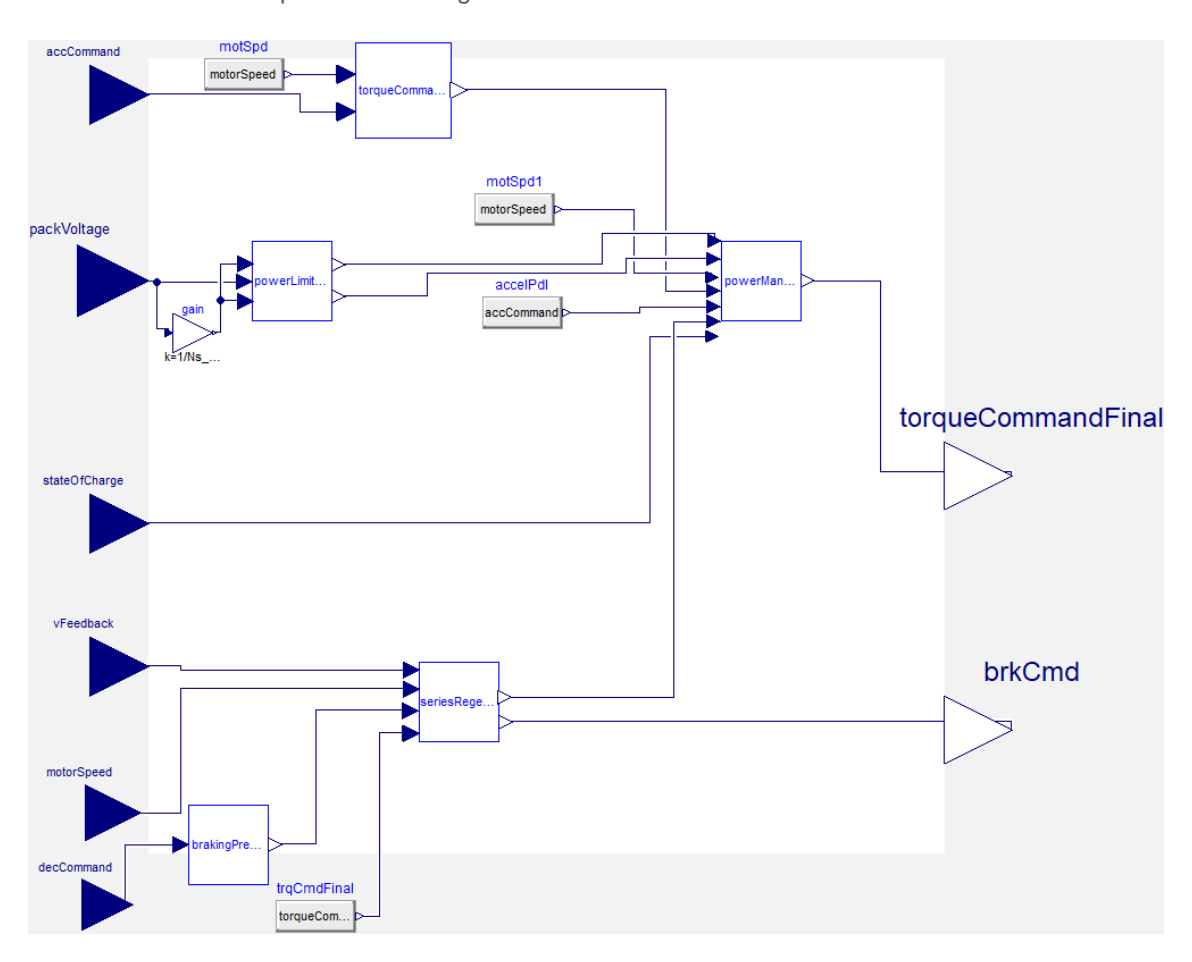


Figure 46: Powertrain Control Module block in Dymola user interface

Moreover, a power management algorithm is incorporated into the PCM block. Except for the power limits, it is responsible for the estimation of the required electric power to supply the necessary mechanical power based on the motor efficiency map. The efficiency map of the EV motor used for the simulations is plotted in Figure 47.



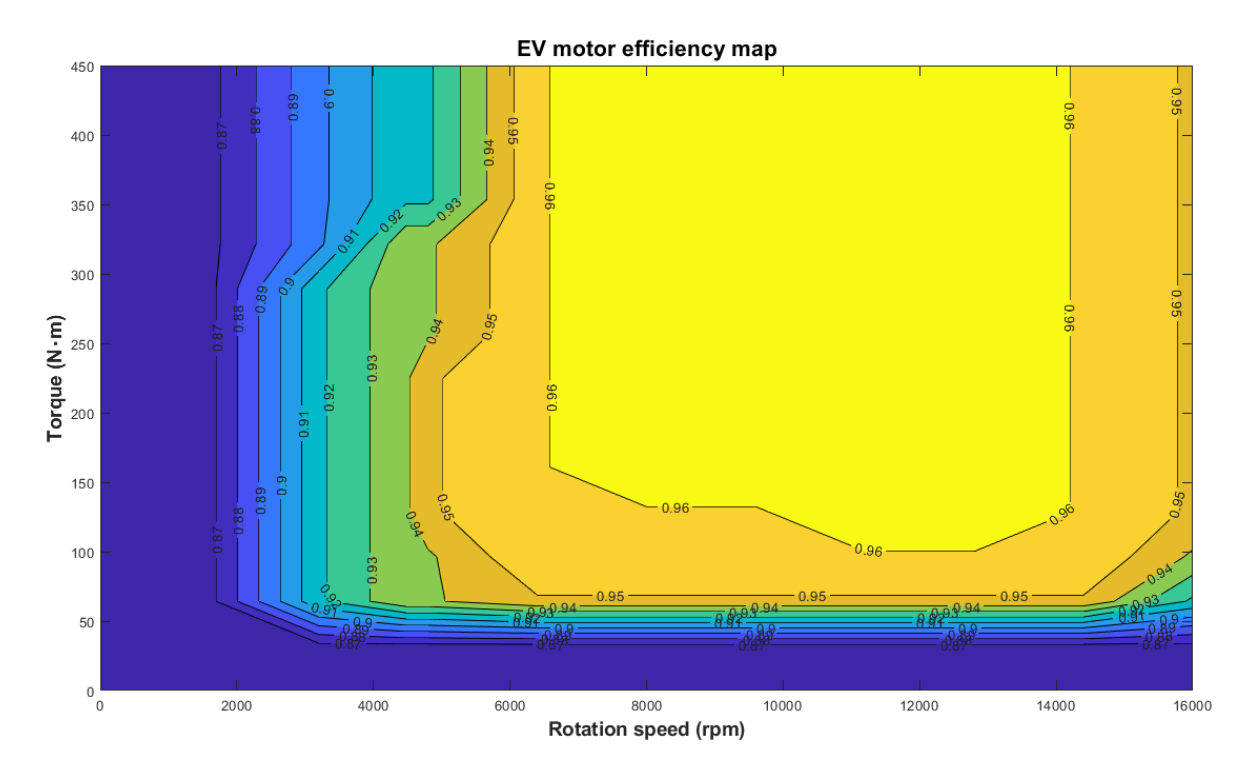


Figure 47: EV motor efficiency map used for the simulations

Regarding deceleration, based on the deceleration normalised command (-1 to 0) the brake pressure that should be applied to the wheels is calculated. Next, the maximum available regenerative torque is exploited for motor braking. The mechanical parts of the transmission system and the dependence of the regenerative torque on the vehicle's instant speed are considered. The regenerative torque limits the torque applied by the brake on the wheel during deceleration. The regenerative torque is subtracted from the total required brake torque and the residual is a block output that is sent to the drivetrain to be applied to the vehicle wheels. The algorithm described above is presented in a block diagram in Figure 48.



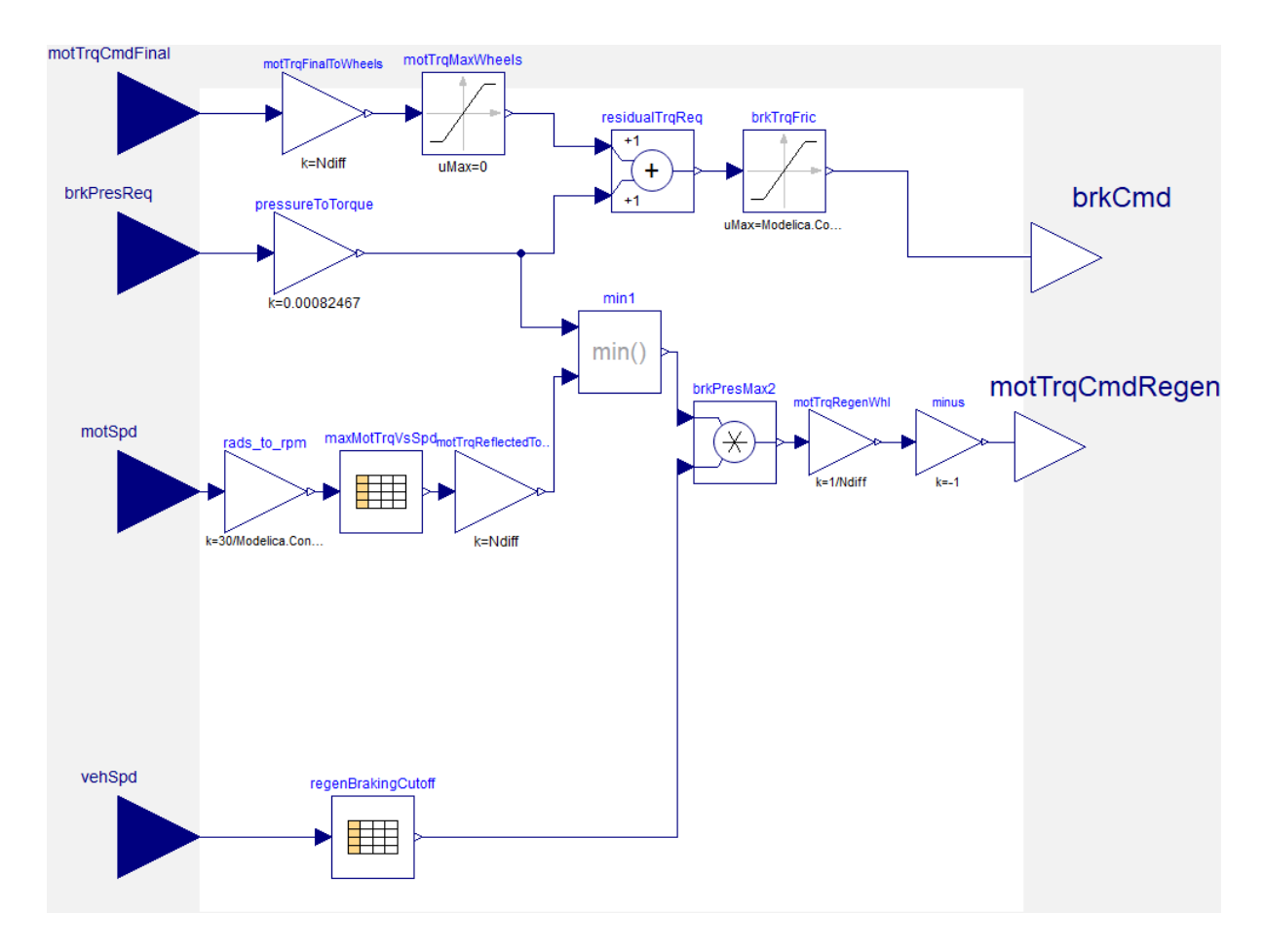


Figure 48: Model of available regenerative torque and brake command in the Dymola user interface

### 12.4.4 Powertrain block

The powertrain block models all the vehicle components engaged in power transfer, i.e. the battery, the power converter and the motor. A graphical representation of the model can be seen in Figure 49.



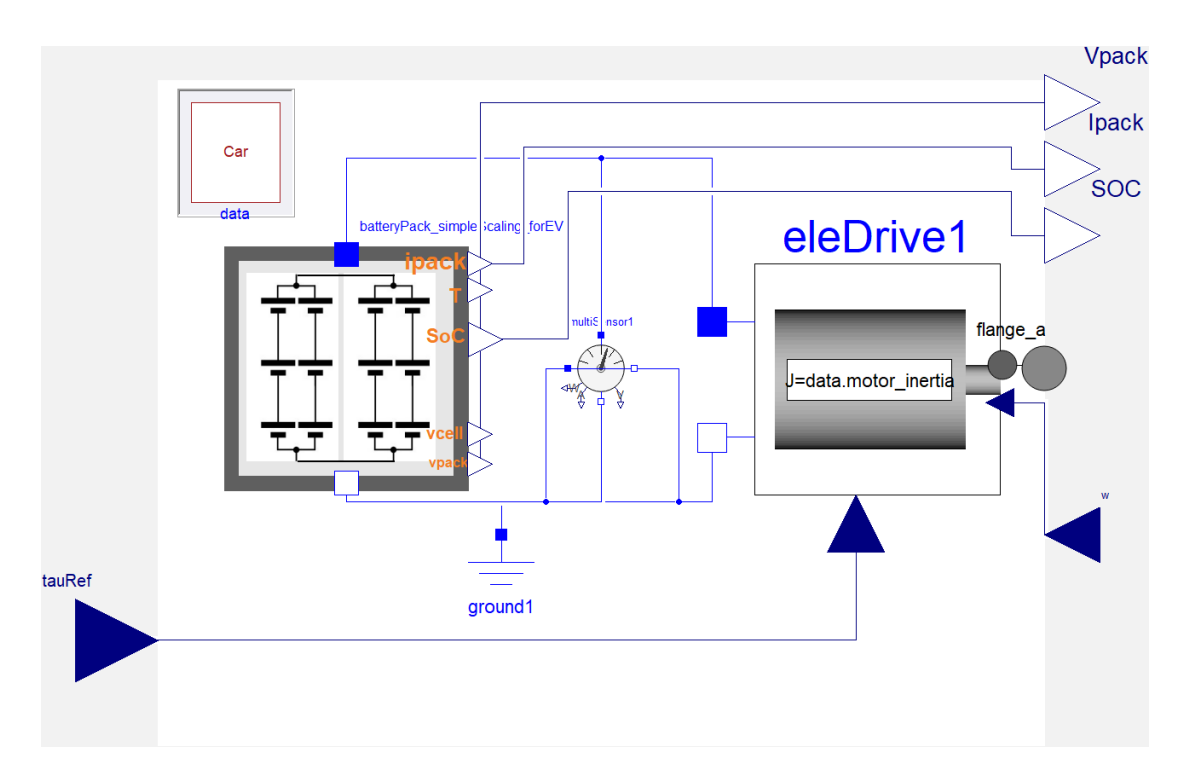


Figure 49: Overall powertrain block

The battery pack model is based on the battery cell model described thoroughly in Section 10.4.2.2 and can provide instantaneous response estimations of battery voltage and SoC. The battery pack arrangement (number of cells in series and in parallel), as well as nominal capacity, current and voltage thresholds, are considered inside the battery pack block. In the scope of SCALE, an option to select between 4 lithium-ion common chemistry types, based on the positive electrode material, is given. The available options include NMC, LFP, NCA, and LMO.

Inside the electric drive block, the operation of both motor and power converter are incorporated. Namely, depending on the instantaneous value of the wheels' rotation speed, the requested torque is limited. The torque-speed curve depicted in Figure 50 is used.



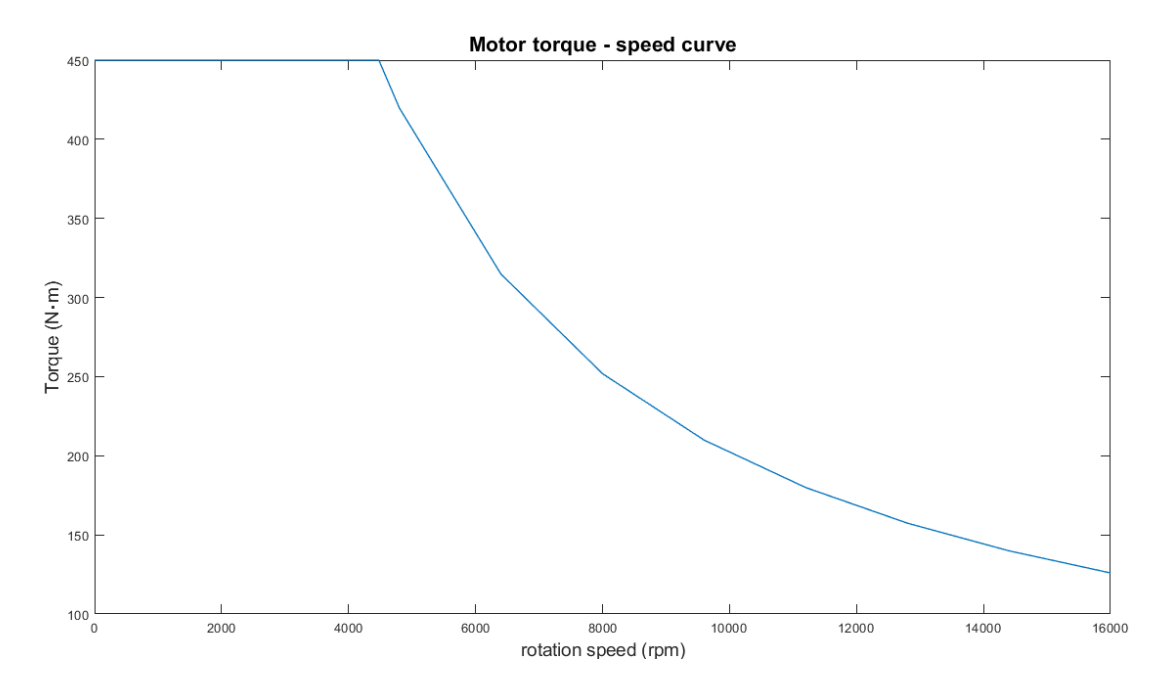


Figure 50: Motor torque - speed curve used for the simulations

Furthermore, the efficiency map, presented in Figure 47, is used to consider the electric drive losses. The final power requirement is covered by a variable resistance continuously adjusted by an integrator and connected with battery pack terminals.

### 12.4.5 Drivetrain block

To proceed with the EV simulations a model for the drivetrain is necessary. However, since special focus is given in the powertrain system the drivetrain can be kept simple and effective in terms of computational time. For this reason, the detailed existing model in the MATLAB EV application which can give quantity estimations of high accuracy for the mechanical components is simplified. The model developed in the Simulink environment with the utilisation of the Simscape libraries is presented in Figure 51.

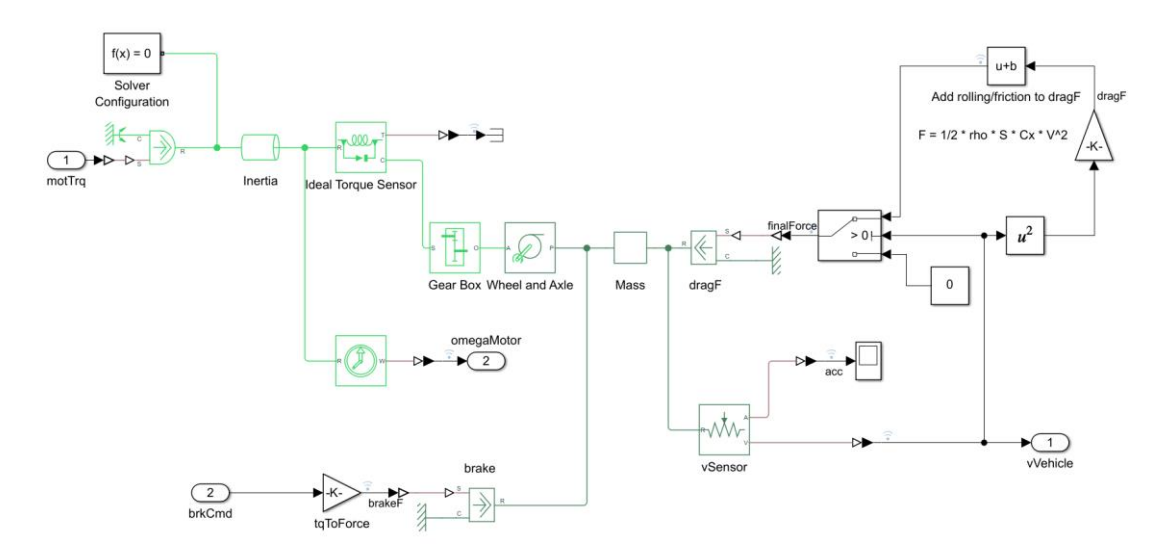


Figure 51: Simplified drivetrain model in MATLAB Simulink environment



The corresponding model built with the use of components of the Modelica Standard Library 4.0.0 and with an extension of the main idea of the drivetrain model of the EHPT Modelica library is presented in Figure 52.

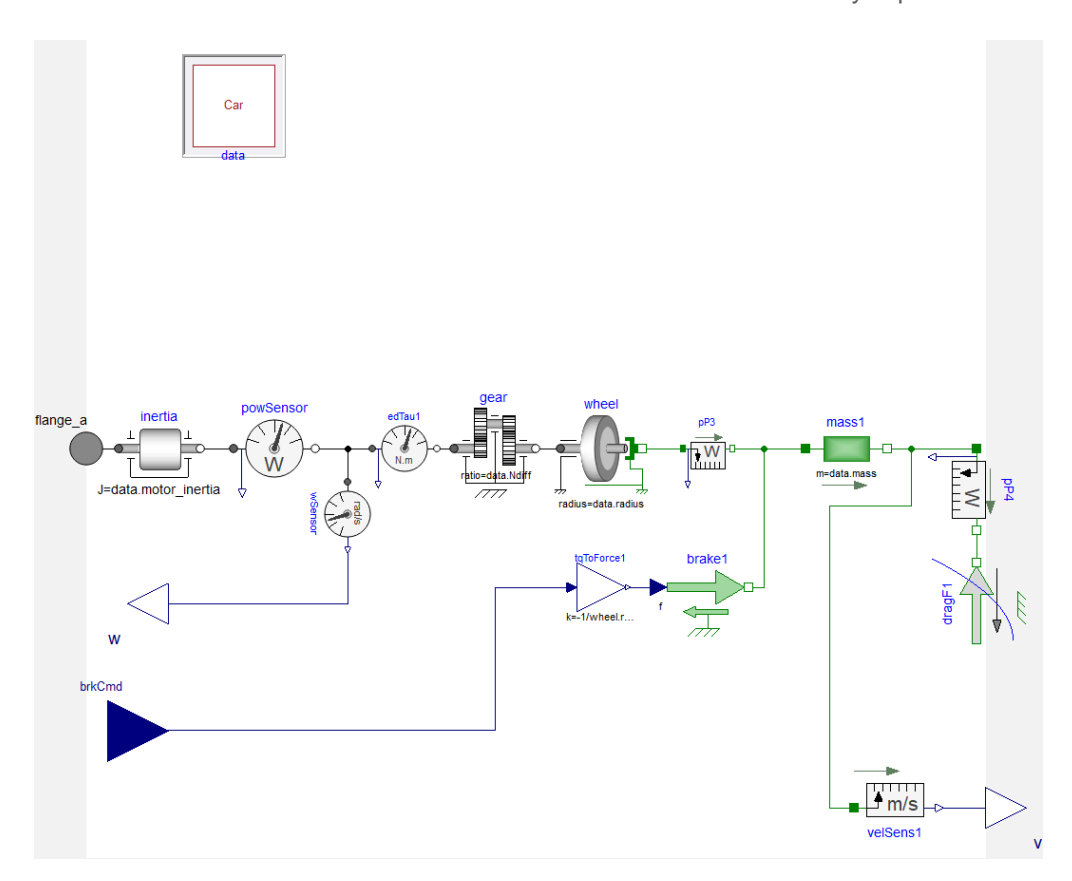


Figure 52: Drivetrain model developed in Dymola user interface

In both cases, the applied forces in the vehicle body include the motor tractive force, the braking force, the aerodynamic drag force and the rolling resistance force. A flat ground is considered, neglecting the effect of gravitational force on vehicle motion. For this study, all of the required drivetrain data, such as differential gear ratio and wheel radius, are retrieved by the MATLAB application to achieve a meaningful comparison of the results of the two software.



## 12.5 Detailed results of the verification of battery models

The results of the model verification process introduced in Section 10.4.2.4, are presented in this section. First, some necessary points of the verification process followed, are highlighted. The models of the system components presented in block diagram form in the Annex are used to set up the verification of the results of the dynamic battery models developed by CERTH with the well-established MATLAB EV application. However, to proceed to meaningful data comparison multiple parameters used and assumptions made must be common in both cases. The input data of both applications are listed as follows:

- Overall EV technical parameters
- User velocity profile
- Battery specifications
- Electric motor specifications

The parameters used for the simulations in both software are listed in Table 3.

General EV parameters		Battery specifications				
Vehicle mass (with 4 passengers)	1500 kg	Battery chemistry type	Lithium-ion NMC			
Longitudinal aerodynamic drag coefficient	0.26	Number of cells in series	96			
Gear ratio	7.94	Number of cells in parallel	31			
Wheel radius	0.31 m	Nominal cell capacity	4.8 Ah			
Rolling resistance coefficient	0.014	Nominal cell voltage	3.6 V			
Cross-sectional vehicle area	2.2 m <sup>2</sup>	Nominal battery pack energy capacity	51.4 kWh			
Maximum brake pressure	5 MPa	Maximum allowed discharge rate	5C			
Electric motor specifications		Initial state-of-charge	0.75			
Maximum power	211 kW	Thermal mass	1364 J/K			
Maximum torque	450 N·m	Minimum cell operating voltage	2.5 V			
Total rotational inertia	1.5 kg·m <sup>2</sup>	Maximum cell operating voltage	4.2 V			
User velocity profile						
Driving cycle		FTP75				

Table 3: Parameters used for the verification of INTEMA.EV



Moreover, to proceed with a proper evaluation of the simulation results, some critical quantities have been selected to verify the accuracy of the developed models at certain system points. These include:

- the vehicle velocity against the imported driving cycle velocity profile (requested setpoint),
- the error between simulated vehicle velocity and driving cycle velocity profile,
- the current injected to/supplied by the battery from/to the motor,
- the power injected to/supplied by the battery from/to the motor,
- the battery pack state-of-charge,
- the voltage at battery pack terminals,

The key verification results of the battery models are presented in the following figures. All results show a good match between the results of the two software. More specifically, in Figure 53 the simulated vehicle velocity of both software is plotted against the requested velocity profile, imported by the FTP75 driving cycle. With the designed control algorithm, the operation of all subsystems ensures that the desired driving behaviour is achieved in INTEMA models.

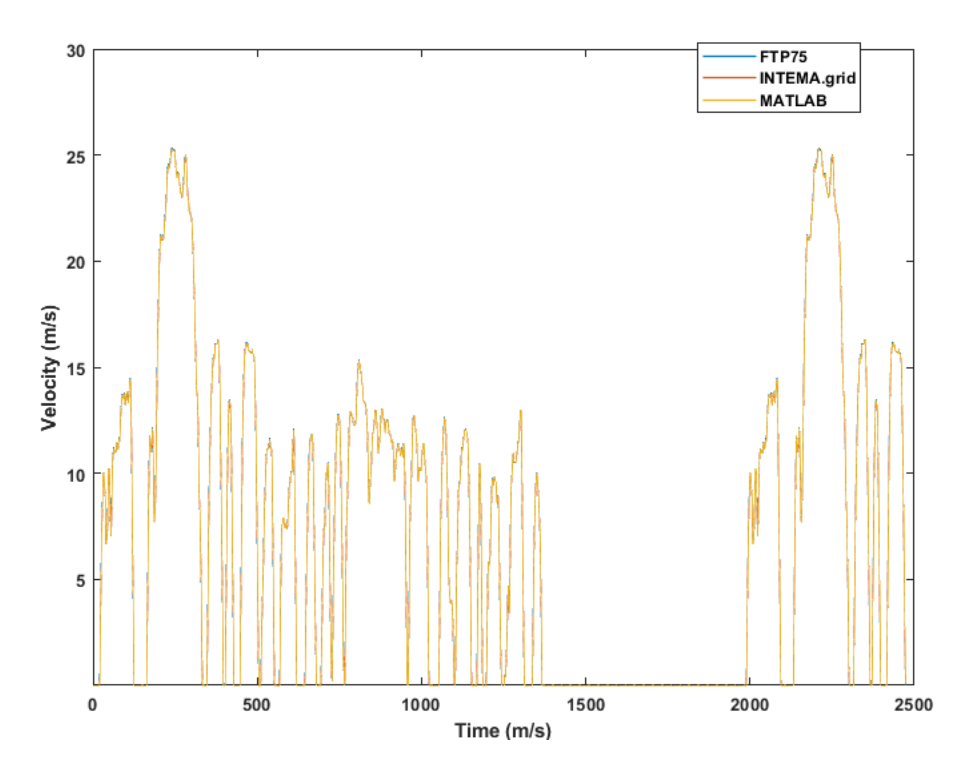


Figure 53: Comparison of output results between MATLAB and Modelica. Simulation velocity of both software against FTP75 velocity profile

In Figure 54, the relatively low instantaneous error between the desired and output velocity values strengthens model validity. The maximum absolute value of 0.38 m/s is equivalent to 1.38 km/h, which can be considered acceptable for a driving application.



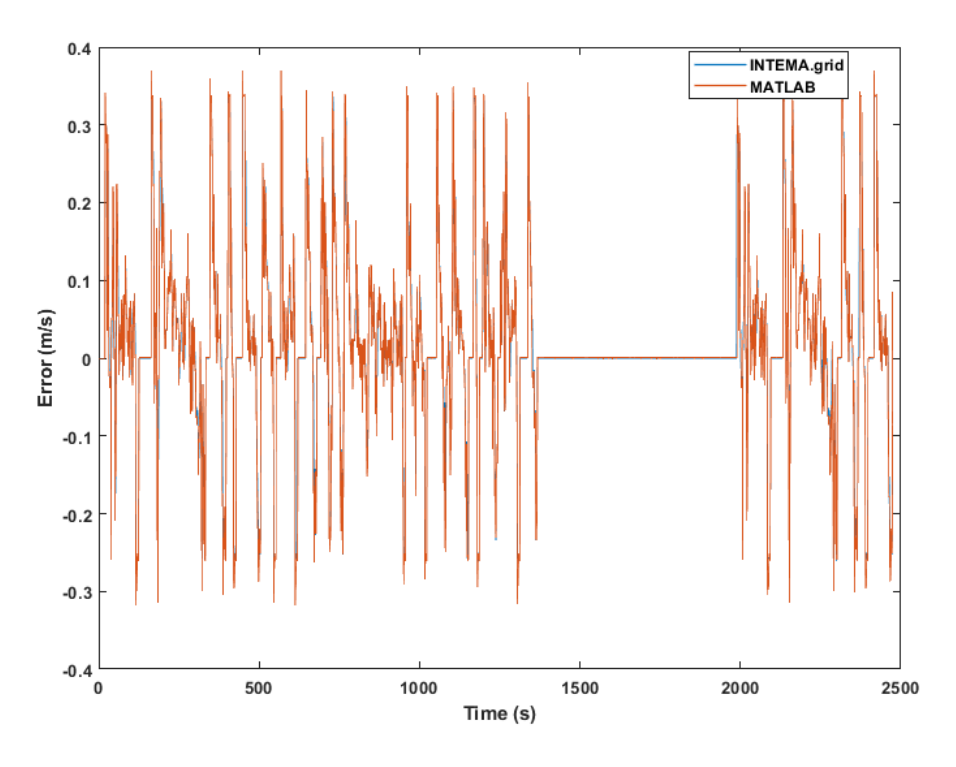


Figure 54: Comparison of output results between MATLAB and Modelica. The error between the velocity results of both software and the FTP75 velocity profile

In Figure 55 and Figure 56, the results of the torque provided by the EV motor, the battery current (positive for charging and negative for discharging) and the battery power (same convention as battery current), respectively show an accurate match of the solutions of the two software. This is a key result to come to the conclusion of accurate estimations of power transactions throughout the EV powertrain.

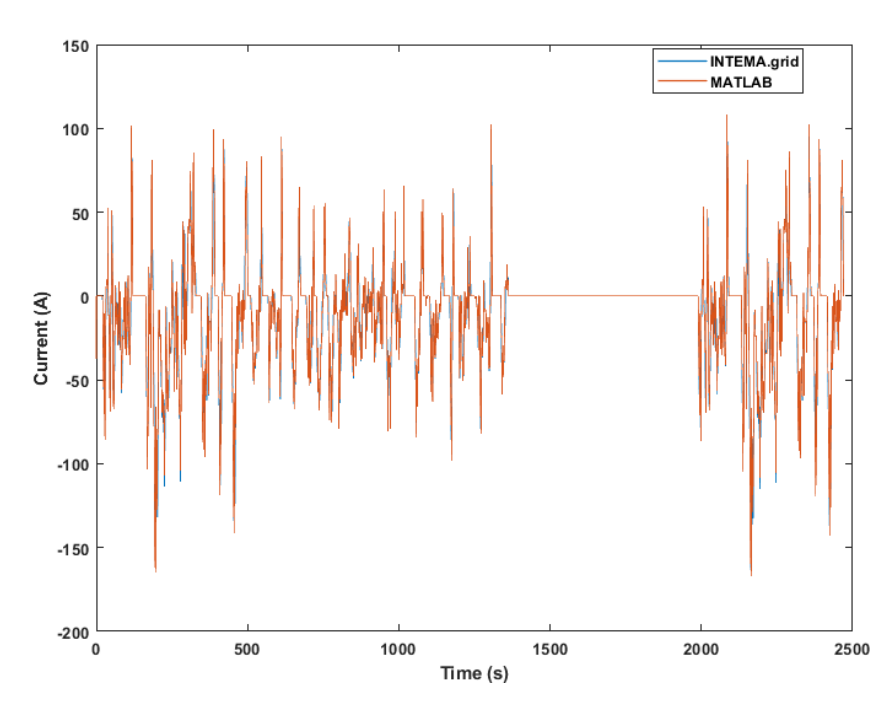


Figure 55: Comparison of battery pack current results between MATLAB and Modelica. Positive for charge and negative for discharge



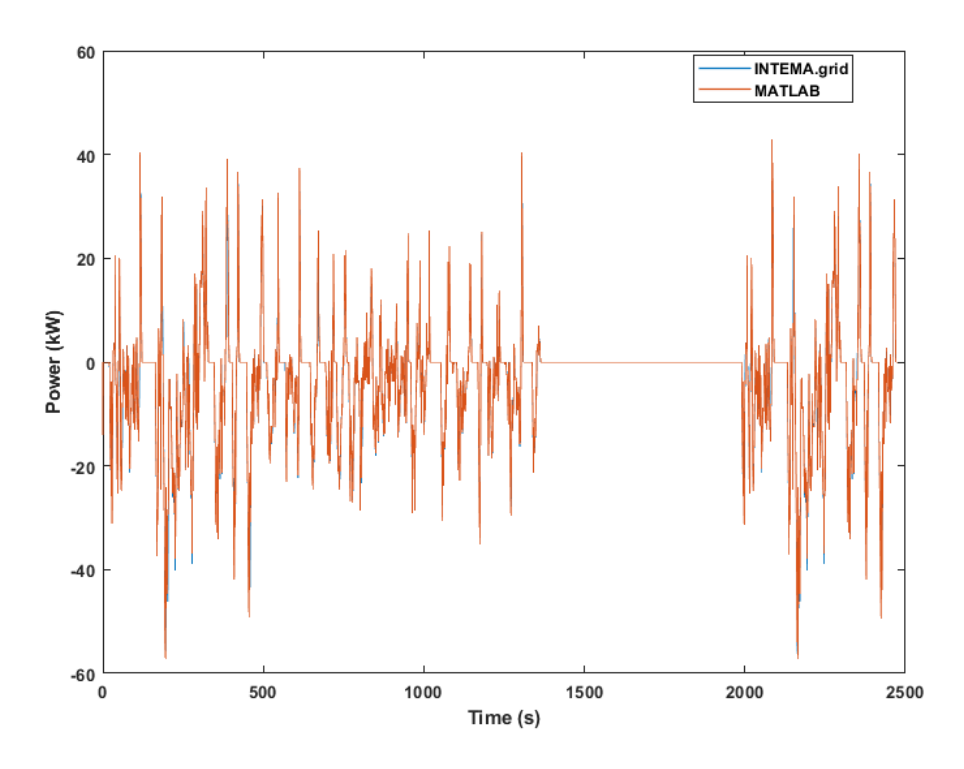


Figure 56: Comparison of power in battery pack terminals between MATLAB and Modelica. Positive for charge and negative for discharge

The results of the estimated SoC are plotted in Figure 57, from which it can be seen that the maximum deviation between the two software results is limited to 0.08%. The comparison of voltage response in Figure 58 shows an insignificant difference between the two curves in the larger part which is expected since the same set of ECM parameters is used for the simulations and, thus, the same instantaneous and transient response should be extracted. Instantaneous deviation can be seen only at time points of mismatch between current instantaneous values.

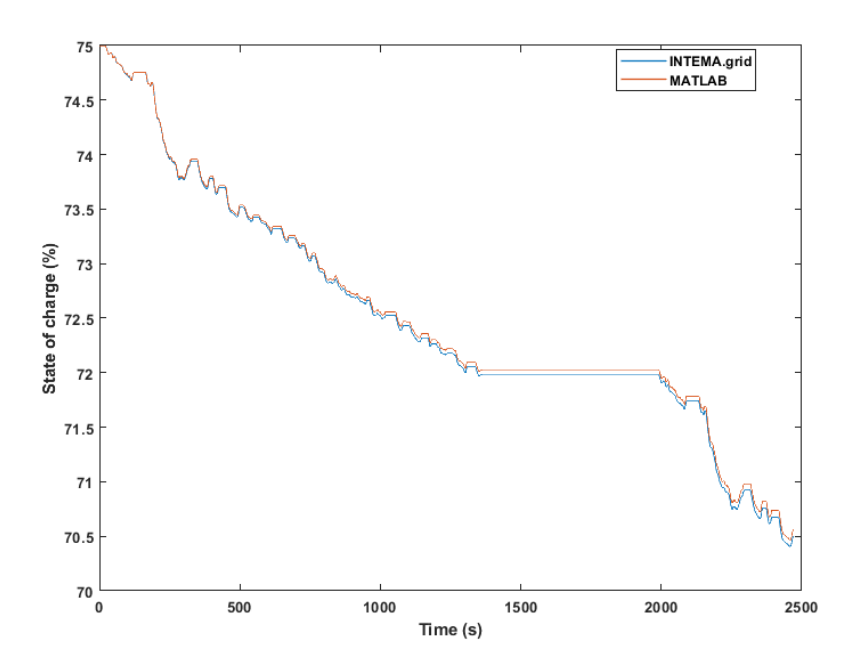


Figure 57: Comparison of state-of-charge (SoC) of battery pack results between MATLAB and Modelica



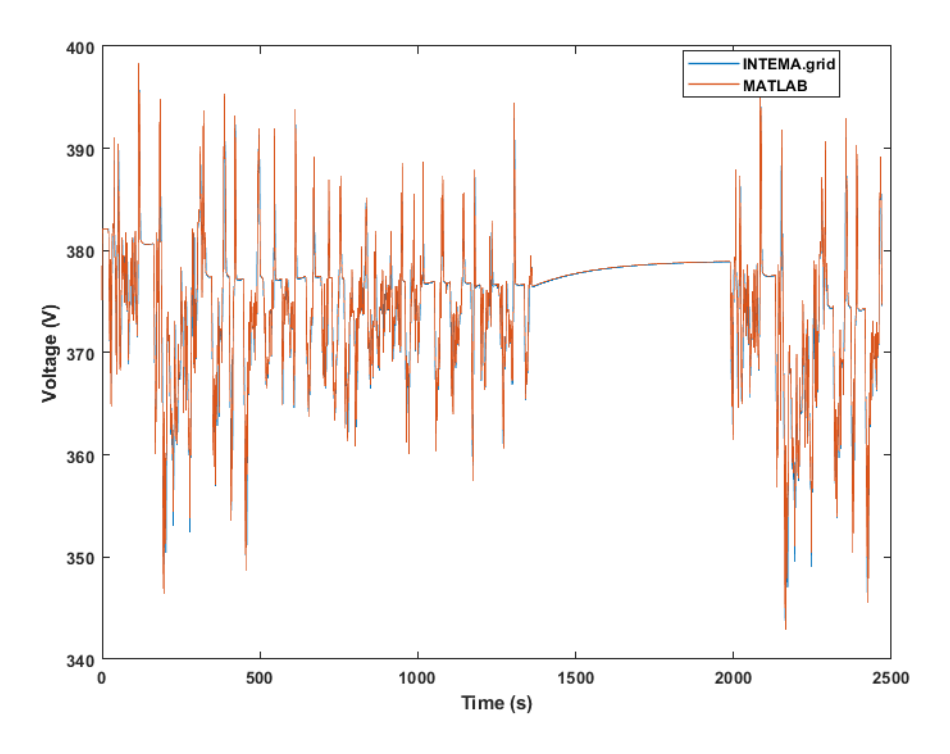


Figure 58: Comparison of battery pack voltage results between MATLAB and Modelica.

In the next paragraphs, the verification results of the following powertrain components, which are not directly related to the EV battery, are presented:

- the torque applied by the motor,
- the motor rotational speed,
- the fuel economy, given in miles per gallon gasoline equivalent (MPGge)[37]
- the brake, drag and friction forces applied to the vehicle

In Figure 59, the results of the torque provided by the EV motor show an accurate match of the solutions of the two software. This is a key result to come to the conclusion of accurate estimations of power transactions throughout the EV powertrain.



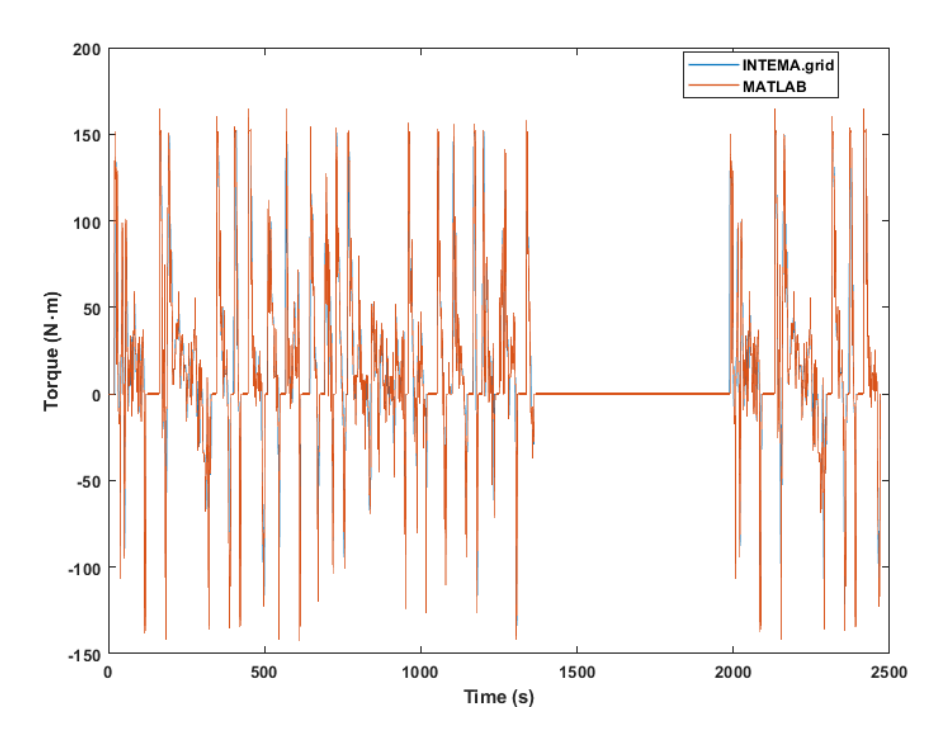


Figure 59: Comparison of output results between MATLAB and Modelica. Torque supplied by the EV motor in both software

Similarity in rotational speed results in Figure 60 is also anticipated based on the vehicle and torque results presented up to this point. The evolution of the MPG $_{ge}$  index, introduced by the US Environmental Protection Agency in 2010, is compared in Figure 61. As can be seen a slight divergence is carried throughout the simulation. This index evolves cumulatively in time so an instant error value during peak discharge currents leads to a relatively constant error until the end of the time considered. However, the error's latest value is equal to 2.2 MPG $_{ge}$  or 1.4%.

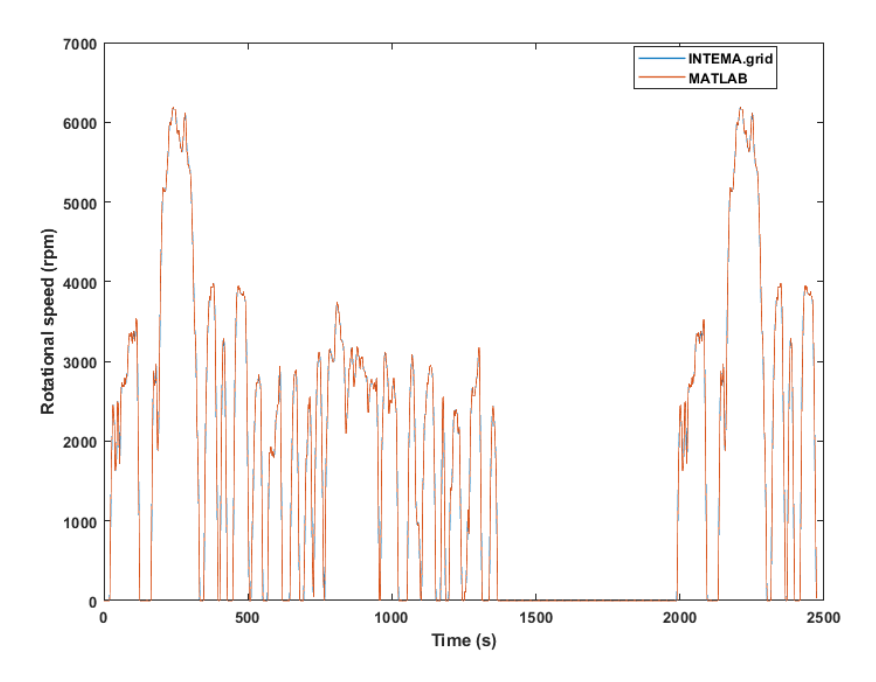


Figure 60: Comparison of EV motor rotational speed results between MATLAB and Modelica.



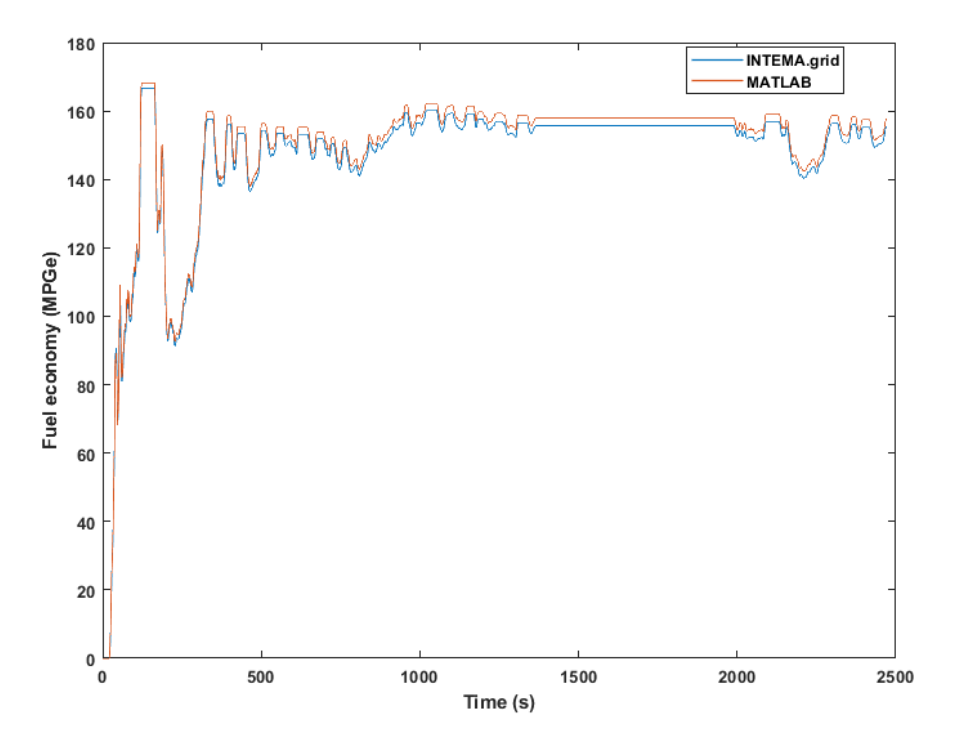


Figure 61: Comparison of EV fuel economy results between MATLAB and Modelica.

Results in Figure 62 and Figure 63 are also necessary to verify the simplifications made in the applied forces of the drivetrain. Results show that the applied forces of aerodynamic drag, friction and EV brake are estimated in the same way in both software.

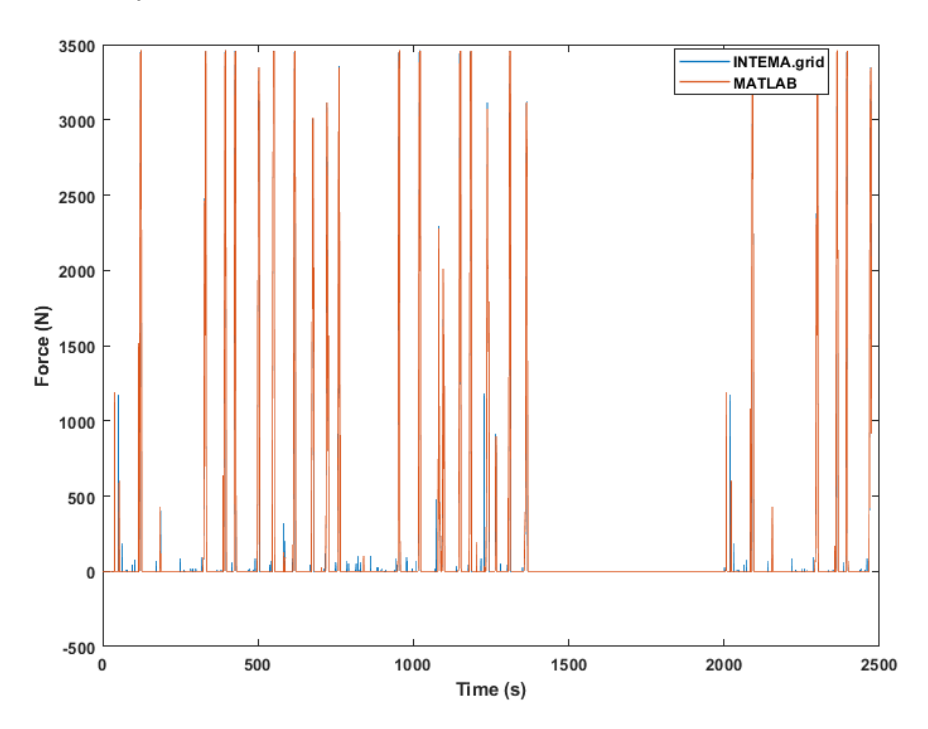


Figure 62: Comparison of EV brake force results between MATLAB and Modelica.



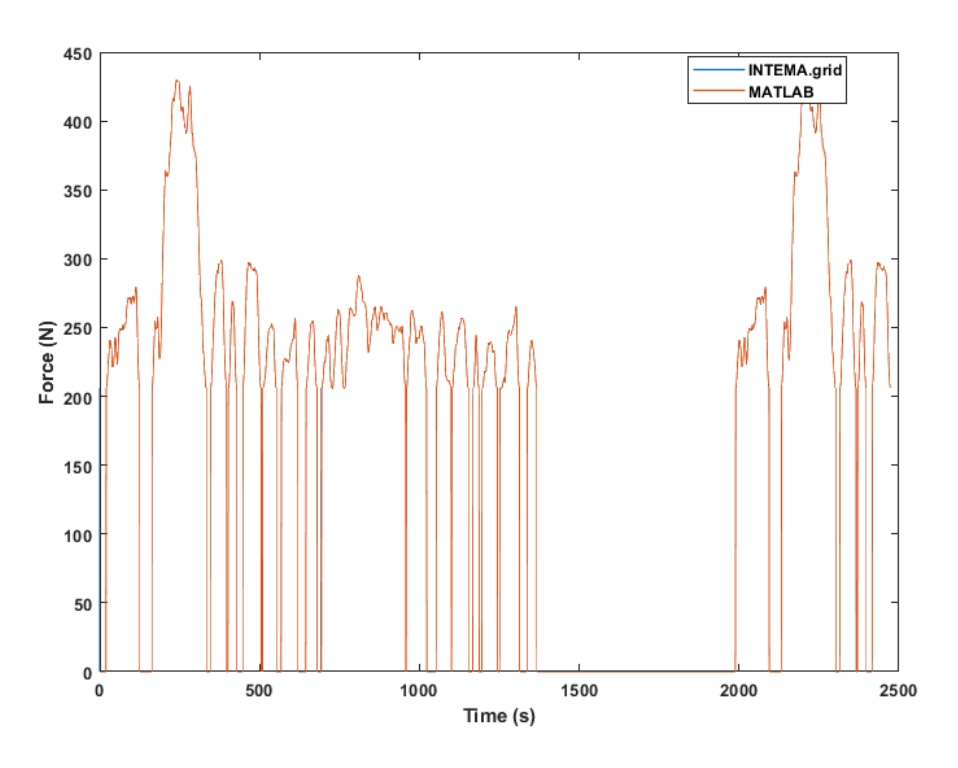


Figure 63: Comparison of the sum of drag and friction forces applied to the EV results between MATLAB and Modelica.

# 12.6 User Manual CERTH Tool for Bus and Line Visualisation Application

### 12.6.1 Overview

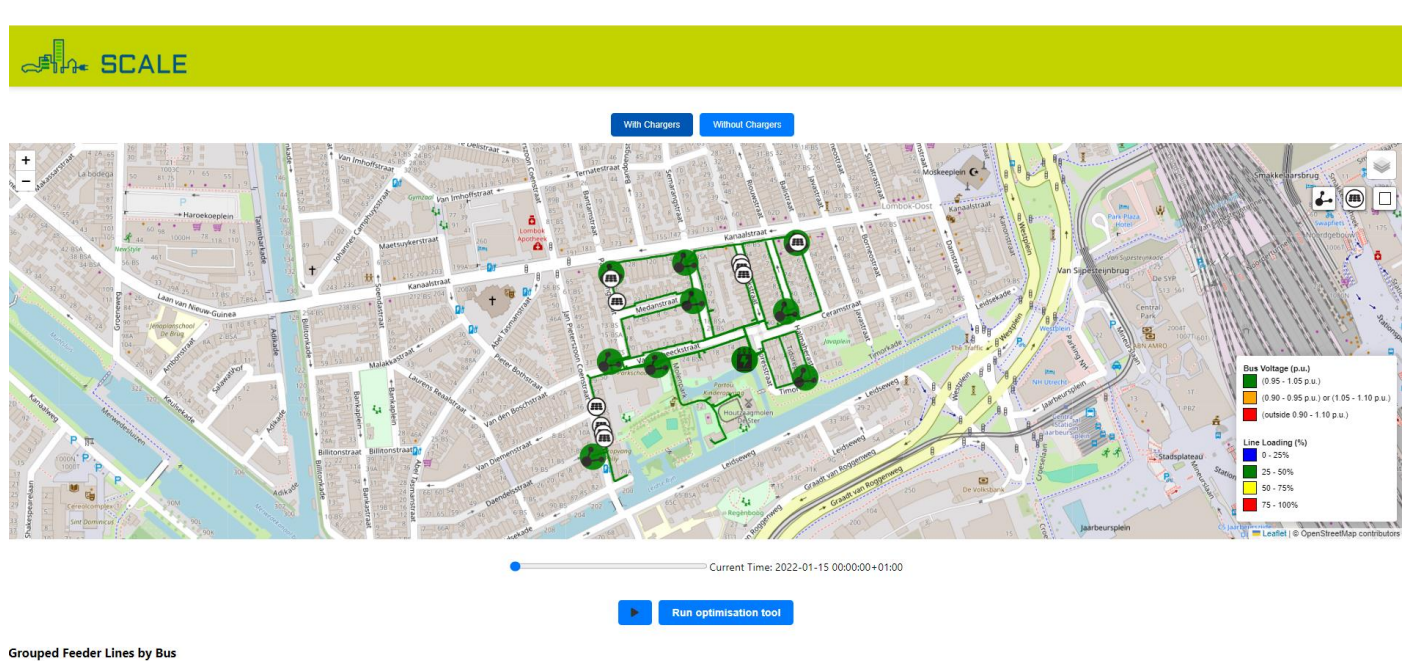


Figure 64: Overview of the visualization tool

This application provides an interactive map-based visualization of buses, prosumers, and feeder lines using the Leaflet library. Users can view, highlight, and interact with various elements on the map, including buses,



lines, and prosumers (solar panels). The application includes additional features such as a lasso tool for selecting multiple map elements and an optimization tool for dynamically modifying bus data.

#### 12.6.2 Main Features

- 1. Interactive Map: Displays buses, lines, and prosumers on an OpenStreetMap or Satellite map.
- 2. **Time-Series Visualization**: Allows users to scroll through time to see how bus and line properties (voltage, angle, and loading) change over time.
- 3. Lasso Selection Tool: Enables users to select multiple buses and lines for detailed information.
- 4. **Optimization Tool**: Allows users to simulate optimization, changing the map dynamically.
- 5. **Highlighting**: Users can highlight all the lines associated with a selected bus or use the chart's "Highlight Lines" button to show relevant lines.
- 6. **Download Data**: Users can download bus and line data in CSV format for further analysis.

#### 12.6.3 How to Use the Application

#### 12.6.3.1 1. Initial Setup and View

When the map first loads, it displays buses, lines, and prosumers on the map based on a specific dataset for the current time index.

- Buses are represented with icons based on their types (standard bus, charger, or transformer).
- Lines connecting buses represent feeders between the buses, with color-coded loading levels.
- **Solar panels** are also displayed with their corresponding icons.

### 12.6.3.2 2. Layer Visibility Controls



Figure 65: Visibility control button, toggle buses, PVs and lasso tool.

In the top-right corner of the map, there are control buttons to toggle the visibility of buses, prosumers, and lines.

- Bus Visibility: Show or hide buses on the map.
- PV Visibility: Show or hide prosumers (solar panels).
- Lasso Tool: Activate or deactivate the lasso tool for selecting multiple buses and lines.



### 12.6.3.3 3. Time-Series Playback



Figure 66: Playback and Optimisation tool buttons.

Below the map, there is a control panel for interacting with time-series data.

- **Slider**: Scroll through the time index to update the displayed buses and lines based on data at different time steps.
- Play/Pause Button: Play the time series to animate the bus and line data over time.

### 12.6.3.4 4. Optimization Tool

- Run Optimization Tool Button: When clicked, the button triggers an optimization process (simulated by a delay), which changes the icons of specific buses (chargers and transformers).
  - After running the optimization tool, buses like 1\_31170 and 1\_31167 will display charger icons, while 1\_31306(1) will display a transformer icon.



### 12.6.3.5 5. Highlighting Lines and Buses

### 12.6.3.5.1 From the Map

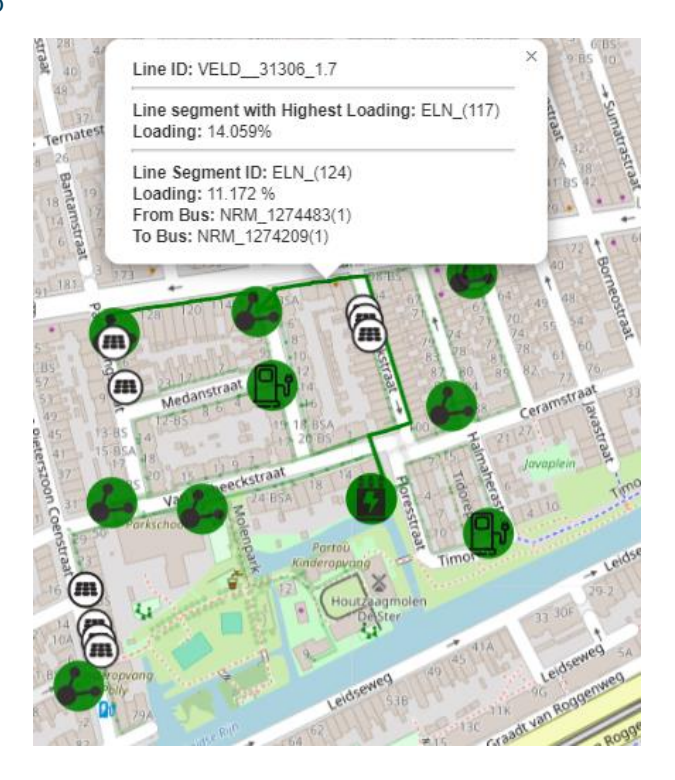


Figure 67: Line highlight using the map selection.

• When you **click on a line**, the entire group of lines associated with the same bus will be highlighted, while all other lines will become opaque for better visibility.

### 12.6.3.5.2 From the Feeder Lines Chart



Figure 68: Line highlight using the table button.

• The **Highlight Lines** button in the Feeder Lines Chart allows you to highlight all the lines associated with the selected bus group, dimming the other lines on the map.



#### 12.6.3.6 6. Lasso Tool for Multi-Select



Figure 69: Lasso tool utilization.

The **lasso tool** can be used to select multiple buses and lines on the map:

- Activate: Click the Lasso Tool button in the control panel to activate the tool.
- Select: Click and drag on the map to create a lasso around the buses and lines you want to select.
- **Popup**: After selection, a popup will show detailed information about the selected buses (voltage, angle, type) and the selected lines (highest loading values).

#### 12.6.3.7 7. Legend

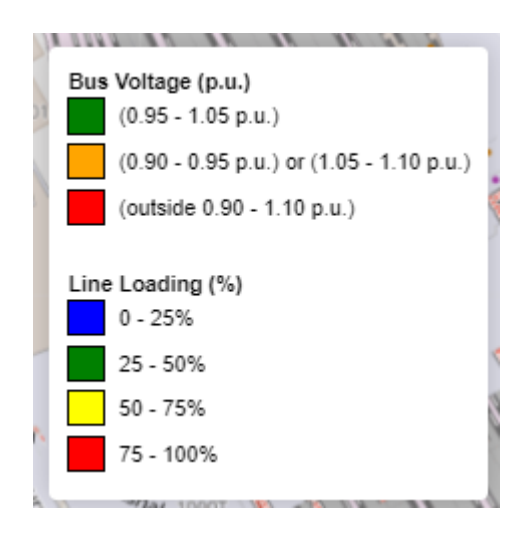


Figure 70: Map legend showing for the line loading and bus voltage.

In the bottom-right corner of the map, a legend provides the color code information:

- Bus Voltage (p.u.):
  - o Green: Between 0.95 and 1.05
  - o **Orange**: Between 0.90–0.95 or 1.05–1.10
  - o Red: Outside the 0.90–1.10 range
- Line Loading (%):
  - Blue: 0–25%Green: 25–50%
  - Yellow: 50–75%



o Red: 75–100%

### 12.6.3.8 8. Downloading Data



Figure 71: Download CSV button utilization.

Each bus group has a **Download CSV** button that allows users to download detailed bus and line data for the current time step.

 The downloaded CSV will include columns for timestamp, bus ID, line ID, loading percentage, and line coordinates.

#### 12.6.4 Additional Information

#### 12.6.4.1 Popup Information

The popups that appear when clicking on buses or lines show relevant details:

- For Lines: Displays the line ID, the loading percentage, and information on the bus that the line connects to.
- **For Buses**: Shows the bus ID, voltage (in p.u.), angle (in degrees), and bus type (standard bus, charger, or transformer).

#### 12.6.4.2 Custom Control Buttons

- 1. Bus Toggle: Turns bus visibility on/off.
- 2. Prosumer Toggle: Turns prosumer visibility on/off.
- 3. Lasso Tool: Activates or deactivates the lasso tool for multi-selection